Individuality of glioma cell responses to hypoxia; roles of metformin as a regulator

Calvo Tardon, Marta

UNIVERSITÉ DE GENÈVE
FACULTÉ DE MÉDECINE

Section de médecine clinique
Département de médecine

Dr. Paul R. Walker, MER

INDIVIDUALITY OF GLIOMA CELL RESPONSES TO HYPOXIA; ROLES OF METFORMIN AS A REGULATOR

THÈSE

présentée aux Facultés de médecine et des sciences de l'Université de Genève
pour obtenir le grade de Docteur ès sciences en sciences de la vie,
mention Sciences biomédicales

par

Marta CALVO TARDÓN

de

Mollet del Vallès (Spain)

Thèse N° 22

GENÈVE

2019

LIFE SCIENCES PhD SCHOOL GENEVA

DOCTORAT ÈS SCIENCES EN SCIENCES DE LA VIE DES FACULTÉS DE MÉDECINE ET DES SCIENCES MENTION SCIENCES BIOMÉDICALES

Thèse de Madame Marta CALVO TARDON

intitulée:

«Individuality of glioma responses to hypoxia; roles of metformin as a modulator»

Les Facultés de Médecine et des Sciences, sur le préavis de Monsieur Paul WALKER, Docteur et directeur de thèse (Département de Médecine), Madame Patrycja NOWAK-SLIWINSKA, Professeure assistante (Département des Sciences Pharmaceutiques), Madame Marie COHEN, Professeure assistante (Département de Pédiatrie, Gynécologie et Obstétrique), Madame Monika HEGI, Professeure ordinaire (Service de Neurologie et Centre de Recherche en Neurosciences), Hôpital Universitaire de Lausanne et Université de Lausanne, autorisent l'impression de la présente thèse, sans exprimer d'opinion sur les propositions qui y sont énoncées.

Genève, le 20 juin 2019

Thèse - 22 -

Le Doyen
Faculté de médecine

Le Doyen
Faculté des sciences

N.B. - La thèse doit porter la déclaration précédente et remplir les conditions énumérées dans les "Informations relatives aux thèses de doctorat à l'Université de Genève".

RÉSUMÉ

Le glioblastome multiforme (GBM) est la forme la plus commune et la plus agressive des tumeurs primaires du cerveau comme en témoigne les faibles succès des thérapies actuelles, avec un taux de survie d'approximativement 15 mois. Le GBM est hautement hétérogène, que ce soit entre les patients (hétérogénéité intertumorale), ainsi que dans la tumeur elle-même (hétérogénéité intratumoral). Cependant, l'hypoxie tumorale est une caractéristique partagée par la majorité des GBM. L'hypoxie tumorale stimule l'immunosuppression, des propriétés propres aux cellules souche, ainsi que des résistances à la radio- et la chimiothérapie. Cette étude avait pour but d'examiner comment les cellules du GBM *in vitro* répondent à l'hypoxie et s'il était possible de moduler cette réponse *in vivo*.

Nous avons utilisé une approche exploratoire non-biaisée afin d'étudier *in vitro* les adaptations des cellules du GBM à un environnement pauvre en oxygène. Nous avons réalisé une analyse complète du transcriptome sur plusieurs lignées cellulaires de souris et humaine, préalablement exposées à différents niveaux d'oxygénation : l'hypoxie (1% O_2), la physioxie (5% O_2) et la condition standard de culture (21% O_2). Nous avons observé de nombreuses réponses spécifiques à l'hypoxie, ce qui témoigne de la grande hétérogénéité intertumorale. Néanmoins, nous avons pu identifier une signature génétique commune à toutes les lignées cellulaires. Cette signature était corrélée aux réponses glycolytiques, inflammatoires et plus singulièrement à la survie des patients GBM. Nous avons modulé les caractéristiques principales de cette signature génétique à l'aide d'une drogue réassignée, la metformin, originalement utilisée dans le diabète sucré de type II. Cette drogue réduit la viabilité et la consommation d'oxygène *in vitro*. Nous avons évalué de façon orthotopique et syngenéique, les effets de la metformin *in vivo,* dans deux

modèles de GBM de souris, en utilisant deux combinaisons thérapeutiques différentes. Toutefois, nous n'avons pas réussi à augmenter la survie globale des souris. Nous avons cependant observé des différences notoires au niveau de la vascularisation des tumeurs chez les souris traitées avec la metformin. En effet, les régions hypoxiques de la tumeur étaient plus vascularisées et elles avaient plus de péricytes, ce qui indique une normalisation de la vascularisation de la tumeur. Ces observations nous encouragent à tester la metformin en combinaison avec d'autres approches thérapeutiques.

Nous avons aussi étudié les deux seuls gènes qui étaient modulés de manière homogène dans toutes les lignées cellulaires entre hypoxie et conditions de culture standard : *ATF3* et *ZFP36*. Nous avons analysé le rôle de ces gènes dans plusieurs lignées de gliome humain après avoir diminué leurs expressions. Nous avons observé une diminution de la viabilité cellulaire, de la capacité de former des clones et de la capacité de migration *in vitro*, plus spécialement lorsque l'expression de *ZFP36* était diminuée. Nos résultats indiquent que ATF3 et ZFP36 ont des rôles indépendants par rapport à la biologie des cellules de GBM.

L'hétérogénéité de GBM, au niveau moléculaire ainsi qu'au niveau de son histopathologie, est bien connue. En revanche, les adaptations du GBM à son microenvironnement hypoxique ont été plutôt décrites comme des adaptations communes à toutes les cellules, comme par exemple la modification du métabolisme pour faciliter la survie cellulaire. Dans cette étude, nous avons trouvé que les lignés cellulaires de GBM s'adaptent au stress hypoxique de manière individuelles au niveau transcriptionel. Cependant, même parmis cette hétérogénéité, nous avons identifié une réponse commune à l'hypoxie qui pouvait être régulé par une drogue d'intérêt clinique, la metfomin.

En conclusion, nous avons identifié des caractéristiques communes et particulières du GBM qui peuvent nous guider vers de futures combinaisons thérapeutiques personnalisées en incluant des propriétés du gliome telles que l'hypoxie, et l'adapter à des groupes de patients spécifiques suivant leurs caractéristiques individuelles.

ABSTRACT

Glioblastoma multiforme (GBM) is the most common and aggressive form of primary brain tumor, and limited success of current therapies results in median overall survival of approximately 15 months. GBM is highly heterogeneous, both between patients (intertumoral heterogeneity), and within the same tumor (intratumoral heterogeneity). However, tumor hypoxia is a shared feature. Tumor hypoxia promotes immunosuppression, angiogenesis, stemness properties on stem-like cells, and resistance to radio- and chemotherapy. The aim of this study was to examine how glioma cells *in vitro* respond to hypoxia, and whether we can modulate these responses *in vivo*.

We followed an exploratory unbiased approach to investigate the adaptations of glioma cells *in vitro* to low oxygen levels. We performed whole transcriptome analysis on several human and mouse glioma cell lines that were exposed to several levels of oxygenation, namely hypoxia (1% O_2), physioxia (5% O_2), and standard culture conditions (21% O_2). We observed many unique responses to hypoxia, indicating a high degree of intertumoral heterogeneity. However, we identified a hypoxia gene-signature that was common to all cell lines. This signature was correlated with glycolytic and inflammatory responses, and importantly, with survival of GBM patients. We modulated key features of this signature with the use of a repurposed drug, metformin, originally used for type II diabetes mellitus. This drug reduced viability and oxygen consumption rate *in vitro*. We evaluated the effects of metformin *in vivo* in two orthotopic syngeneic mouse glioma models, and using two different therapeutic combinations. However, we did not achieve an increase in overall survival. We did observe differences on the tumor vasculature of metformin-treated mice—hypoxic areas were more vascularized and

contained more pericytes, indicating normalization of the tumor vasculature. This provides rationale to test metformin in combination with other therapeutic modalities.

We also studied the only two genes that were commonly modulated in all cell lines between hypoxia and standard culture conditions: *ATF3* and *ZFP36*. We investigated the role of these genes in several human glioma cell lines by knocking-down their expression. We observed a decrease in cell viability, clonogenicity, and migration capacity, especially when *ZFP36* was knocked-down, although this was regardless of the oxygen they were exposed to. Our results suggest independent roles of ATF3 and ZFP36 in glioma cell biology.

The molecular and histopathological heterogeneity of GBM has been widely explored, but the adaptations of GBM to a hypoxic microenvironment have mostly been described in terms of common metabolic adaptions facilitating cancer cell survival. Here we discovered that individual GBM cell lines adapt in unique ways to hypoxic stress at the transcriptional level, highlighting intertumoral heterogeneity also in response to hypoxia. Nevertheless, within this heterogeneity, we identified a common response to low oxygenation that could be modulated by a clinically relevant drug, metformin.

Overall, we have defined common and individual features of GBM that may point towards future combination therapies that incorporate common targets (for example hypoxia), but which can be tailored to specific patient groups according to their individual characteristics.

ACKNOWLEDGEMENTS

Thank you, **Paul**, for this opportunity, for teaching me during these years. Science does not always work as we expect, but I have learned that perseverance and hard work can make up for it.

I would like to express my gratitude to the members of the committee, **Prof. Monika Hegi**, **Prof. Patrycja Nowak-Sliwinska**, and **Prof. Marie Cohen**, for your feedback, and your time to read this thesis and to evaluate my work.

Thank you, **Eliana**, for all your help with the bioinformatics analysis, for your input, and support during presentations and the writing process. Thank you, **Erika**, for helping me so much with the project, for the brainstorming sessions, and your constant big smile and encouragement.

Thank you, my colleagues from the lab who helped me in various ways, from brainstorming to performing experiments. Thank you, **Viviane** for your support, especially with *in vivo* experiments. Thank you, **Emily**, for your help with the crazy hypoxic Seahorse experiments. Thank you, **Vassilis**, especially for Friday's craziness. Thank you **Stoyan** and **Marc**, and thank you past members of the lab, especially **Laura**, for your endless enthusiasm.

Thank you, **Valérie Dutoit** and all her team **Francesca**, **Valérie**, **Géraldine**, **Mathilde**, and **Soline**, for all your support and advices during lab meetings and long hours in the P2 lab.

Thank you, **Pierre-Yves**, for the support these years, and your feedback on the review.

I want to thank several facilities at the Faculty of Medicine of the University of Geneva, for the advices and for making possible many experiments. **Genomics platform**, for the various experiments I have done from the beginning of my PhD, until almost the very last day. **Bioimaging facility**, both for the technical help and analysis. **Reads unit**, for making the seahorse experiments possible. Facs facility, animal house, and small animal preclinical imaging platform.

Thank you, *biogirls*, for your support, for your kind words, our spa weekends, and escape games, for the alcohol-free happiness. Thank you, **Cristina**, for your coaching in life (and

thesis), I have learned a lot from you. Thank you, **Leticia**, the time with you in the lab was priceless. Thank you, **Robin**, for all your support already from the masters and throughout the whole PhD.

Thank you, dear **friends** from CMU. You have been like my family since I started this PhD. We have shared a lot of special moments and we have gone through all our theses together. I will always remember this period of time with a big smile thanks to you.

Muchas gracias **Dani**, has sido una persona muy especial en estos últimos años de doctorado. Me has ayudado muchísimo, me has apoyado, y sobretodo has hecho mis días más llevaderos y desde luego más divertidos.

Moltes gràcies als meus **amics** de Barcelona, Anna, Cristina, Ariadna, Helena, Helena, Gemma, Christian i Marta. Gràcies per les vostres visites, per sempre trobar un moment per veure'm a cada tornada express a Mollet.

Moltes gràcies **Laia**, per sempre estar allà, per sempre veure'ns cada cop que vaig a Mollet, per compartir i crear juntes moments importants de les nostres vides. Gràcies pels teus consells, i per donar-me suport en moments de transició.

Moltes gràcies *poder de 3*, **Jonathan** i **Laura**, per tots els moments viscuts, i haver crescut junts. Especialment, gràcies J, pel recolzament impresionant que has suposat per mi. M'has ajudat un munt durant aquests anys, m'has escoltat, m'has aconsellat, i m'has ensenyat que aquest camí no només és aprendre ciència, sinó també aprendre d'un mateix.

Muchas gracias, a mi familia que siempre ha estado ahí en todo momento. Gracias **tita Nani** por tu tiempo, tus sonrisas y tu apoyo. Gracias a mis **abuelos** por siempre creer en mí, os lo agradezco de todo corazón.

Muchas gracias **papa** por tus mensajes diarios, por el apoyo incondicional que siempre me has dado, y por dejarme emprender este camino lejos de casa. Siempre has creído y confiado en mí, y eso me ha ayudado a crecer como persona.

Thank you, **Alex**, husband, love of my life. This adventure would have not been the same without you. You have helped me in ways only you could do. I will always be grateful for your patience, your infinite support, for always listening to me, for even coming with

me to the lab on weekends, for advising me on so many levels, for being who you are. Thank you from the bottom of my heart.

Mama, esta tesis doctoral te la dedico a ti. Muchas gracias por todo el amor que sé que tenías reservado para mí. Éste es mi granito de arena, mi contribución. Gracias por darme las fuerzas y la motivación para llegar hasta el final. Esto no hubiera sido posible sin ti, e, irónicamente, contigo tampoco.

TABLE OF CONTENTS

ABBREVIATIONS

ACT: adoptive cell transfer

AMPK: AMP-activated protein kinase

APC: antigen presenting cell

BBB: blood-brain barrier

bFGF: basic fibroblast growth factor

BILs: brain-infiltrating leukocytes

BMDM: bone marrow-derived macrophages

CAIX: carbonic anhydrase IX

CAR: Chimeric antigen receptor

CCL: C-C Motif Chemokine Ligand

CD: cluster of differentiation

CMV: cytomegalovirus

CNS: central nervous system

CSC: cancer stem cell

CSF-1: colony stimulating factor-1

CSF: cerebrospinal fluid

CTC: circulating tumor cells

CTL: cytotoxic T lymphocyte

CTLA-4: cytotoxic T-lymphocyte-associated protein 4

DDIT4: DNA-damage-inducible transcript 4

EGF: epidermal growth factor

EGFR: epidermal growth factor receptor

ETC: electron transport chain

FDA: Food and Drug administration

G-CIMP: glioma-CpG island methylator phenotype

GBM: Glioblastoma multiforme

GDC: glioma differentiated cell

GEMM: genetically engineered mouse model

GMFI: geometric mean fluorescent index

GSC: glioma stem-like cell

H&E: hematoxylin and eosin

HAP: hypoxia-activated prodrug

HBO: hyperbaric oxygen

HIF: Hypoxia-inducible factor

HPLC: high-performance liquid chromatography

HRE: hypoxia-responsive element

IDH: isocitrate dehydrogenase

IF: immunofluorescence

IP: intraperitoneal

Ivy GAP: Ivy glioblastoma atlas project

MGMT: O-6-methylguanine-DNA methyltransferase

MHC: major histocompatibility complex

MRI: magnetic resonance imaging

mTOR: mammalian target of rapamycin

OS: overall survival

OVA: ovalbumin

PBMC: peripheral blood mononuclear cell

PD-1: programmed death 1

PD-L1: programmed death-ligand 1

PET: positron emission tomography

PFA: paraformaldehyde

PFS: progression-free survival

PHD: prolyl hydroxylase

PIMO: pimonidazole

REDD1: regulated in development and DNA damage responses 1

RNA-seq: RNA sequencing

ROS: reactive oxygen species

TAM: tumor-associated macrophage

TCA: tricarboxylic acid

TCGA: the cancer genome atlas

TCR: T cell receptor

TGFb: transforming growth factor beta

TMZ: temozolomide

TNF: tumor necrosis factor

Treg: regulatory T cell

TSC: tuberous sclerosis

VEGF: vascular endothelial growth factor

WHO: World Health Organization

1 INTRODUCTION

1.1 Hypoxia

The main issue of this thesis is to understand how brain tumor cells adapt to low levels of oxygen, i.e. hypoxia. This section provides information about how cells sense and respond to hypoxia, how we define and work with physiologic and hypoxic conditions, and the implications of the presence of hypoxia in the context of a tumor.

1.1.1 Cellular responses to hypoxia

Hypoxia can be present in a physiological context, for instance while adapting to high altitudes or during embryonic development, and in various pathologies, such as stroke or cancer. Cells can sense differences in oxygen availability, and the best-characterized response to low levels of oxygen is that of hypoxia-inducible factors (HIFs). However, it is important to note that there are also oxygen-independent modulators of HIFs, and conversely, HIF-independent responses to the absence of oxygen.

1.1.1.1 HIF-dependent responses

One of the key sensors of oxygen changes in cells has been known about since 1992, thanks to the elegant work of Semenza and Wang, who identified the hypoxia-responsive element (HRE) in the erythropoietin gene that is present in liver cells after hypoxic treatment [1]. A few years later the same group characterized the star of the pathway, Hypoxia-Inducible Factor-1α (HIF-1α) [2], which heterodimerizes with HIF-1β (also known as aryl hydro-carbon receptor nuclear translocator [ARNT]) forming a transcription factor that is able to bind HRE and unravel a plethora of downstream signaling cascades.

The oxygen-dependent regulation of these factors was described during the following years by three independent groups, led by Semenza, Ratcliffe, and Kaelin, respectively. While HIF-1β is constitutively expressed, levels of HIF-1α change according to the availability of oxygen. The modulation of HIF-1α levels occurs at a post-translational level through the oxygen-dependent action of prolyl hydroxylases (PHDs) [3-5]. Hydroxylated HIF-1α can then be targeted by von Hippel-Lindau (VHL), an E3 ubiquitin ligase protein, for proteasomal degradation [6, 7], as represented in Figure 1. Similarly, another hydroxylation of HIF-1α can occur. Factor Inhibiting HIF (FIH) can hydroxylate HIF-1α at asparagine residues, which interferes with the binding of the transcriptional coactivators p300 and CREB-binding protein (p300/CBP), thus inhibiting HIF activity, the function from which the protein's name was derived [8-10].

There are other isoforms of HIF: HIF-2α and HIF-3α. HIF-2α (also termed EPAS1) was perhaps at first eclipsed by the essential role played by HIF-1α in the hypoxic stress response, but it was described as an important factor regulating vascular remodeling during the early 2000s [11, 12]. There is no overlap between the downstream genes of HIF-1α and HIF-2α, despite having the same HRE core sequence. For many years, how cells could discriminate between these factors remained unknown, but subsequent studies have shown the involvement of coactivators, cooperation with other transcription factors, and differential tissue-dependent expression of HIFs [13]. The timing of the action of these two factors is also different: HIF-1α regulates acute hypoxic responses, whereas HIF-2α modulates more prolonged hypoxic exposures [14]. On the other hand, the HIF-3α isoform (also known as IPAS) is far less explored. It has been described as a negative regulator of HIF-1α and HIF-2α, by binding and inactivating

them, for example in tissues with physiological low oxygenation such as the cornea [15, 16].

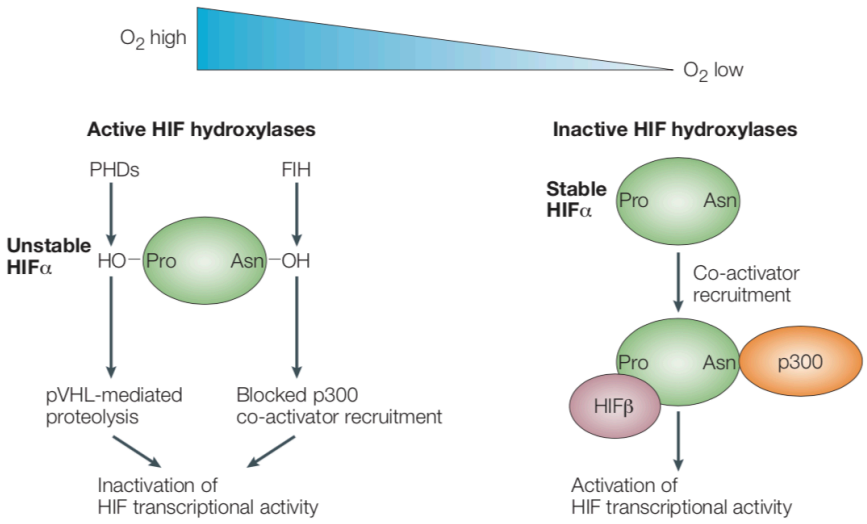

Figure 1: A schematic representation of HIF-1α regulation depending on oxygen availability (Adapted from [17]).

In the absence of oxygen, hydroxylation of HIF-1α no longer occurs, meaning that it is able to bind to HIF-1β and its coactivators, forming a complex that translocates to the nucleus and has transcriptional activity on the genes containing HRE. Using DNA sequencing, the HRE sequence 5'-RCGTG-3' (where R is A or G) has been identified in close vicinity to the promoters of over 200 genes [13]. More recently, coupling chromatin immunoprecipitation with next-generation sequencing has allowed screening of genes containing this HRE sequence (regardless of distance from their promoters), thus identifying several hundreds of genes that are downstream of HIF [18].

Generally, HIF stabilization and activation after HRE binding orchestrates processes that either increase oxygen delivery or reduce cellular oxygen consumption, a phenomenon known as oxygen conformance. Some examples of this are the induction of angiogenesis through VEGF upregulation, first described by Ratcliffe's group [19]; the upregulation of erythropoietin, promoting the production of red blood cells [1]; and the

upregulation of glycolytic enzymes, thus stimulating glycolysis over oxidative phosphorylation [20]. In order to prevent persistent stabilization of HIFs, negative feedback mechanisms exist, such as microRNA-210 and the regulation of PHD activity [21, 22]. These regulations occur very fast, HIF-1α stabilizes and translocates to the nucleus in less than 2 min of hypoxic exposure, and can get degraded in less than 16 min after reoxygenation [23].

Importantly, oxygen is not the only modulator of HIFs; HIF can be stabilized even in the presence of enough oxygen. For example, myeloid cells stabilize HIF-1α protein to maintain a high glycolytic rate during inflammation [24], and similarly, T cells upon TCR activation [25, 26]. Moreover, lack of the PHD cofactors Fe^{2+} and ascorbate, prevents the hydroxylation of HIF, allowing its activation [27].

1.1.1.2 HIF-independent responses

Cellular responses to low levels of oxygen do not occur exclusively through the HIF pathway. In addition, several HIF-independent mechanisms have been described, whereby hypoxia triggers mechanisms that alert the cell to environmental stress, leading to energy-saving strategies.

Some examples of this response are the hypophosphorylation of mammalian target of rapamycin (mTOR) and its downstream signaling targets through HIF-independent mechanisms, leading to a reduction in protein synthesis [28]; or the internalization of neuronal glutamate receptors through the modulation of EGL-9, one of the PHD proteins that senses O_2, without involving HIF, resulting in a reservoir of glutamate receptors for when oxygen becomes abundant again [29].

Hypoxia can also increase the mitochondrial production of reactive oxygen species (ROS), which activate Nuclear Factor Of Kappa Light Polypeptide Gene

Enhancer In B-Cells (NF-kB) and promote cell survival [30]. However, ROS can also cause the destabilization of PHD proteins, leading to the final stabilization of HIF [31]. This suggests that even when hypoxia initially induces HIF-independent mechanisms, there is interaction between these and the HIF pathways.

In conclusion, hypoxia is mainly sensed via the HIF pathway, but cells do not always detect low oxygen levels in this way. Therefore, when studying hypoxia, it is more relevant to modify oxygen availability, rather than just changing HIF stabilization and/or activity, as when using the PHD inhibitors cobalt chloride ($CoCl_2$) and deferoxamine (DFX), which are often used as hypoxia mimetics [32, 33].

1.1.2 Hypoxia and physioxia: definitions

What do we mean by hypoxic and physiologic oxygen conditions? It turns out that what seems to be a simple question is actually an important debate in the field of hypoxia research. The first challenge when studying hypoxia is to determine the actual level of tissue oxygenation *in vivo* (both physiologic and hypoxic) and to define the amount of oxygen to work with in *in vitro* cultures.

1.1.2.1 In vivo

It is important to consider the physiological levels of oxygen available in healthy tissues, i.e. physioxia, which is known to be tissue-dependent. Hypoxia, on the other hand, is defined as inadequate oxygen supply, implying as well its tissue-dependency. The term normoxia has been generally misinterpreted as reflecting physiological levels of oxygen in a given tissue, but it is often applied to atmospheric levels of oxygen (21% O_2).

We refer to the levels of oxygen in partial pressures (pO_2), measured in kPa or mmHg (oxygen tension). However, due to the frequent inability to measure partial

pressures, many studies refer to oxygen levels in percentages (oxygen fraction). Levels of oxygen can be measured using various techniques, such as polarographic electrodes with capacity to quantify pO_2 of small sized samples, or imaging techniques that can provide a large sample area but do not quantify pO_2 unless combined with tracers, often used for cancer diagnosis. Recently, these two approaches are being combined, offering the best of both worlds [34].

Polarographic electrodes, based on the original Clark's electrodes from 1958, are metals able to reduce oxygen, thus consuming oxygen for the measurement, making them less reliable [35]. Moreover, their big size disrupts the tissue as they penetrate it. Alternatives to these first probes are microelectrodes with fluorescent- or phosphorescent-quenching by molecular O_2 [36], and to more recent coupling with microscopy techniques, such as two-photon imaging [37]. In recent years, these microelectrodes have been optimized into optical sensors, in formats suitable for both tissue and *in vitro* settings.

Immunohistochemical (IHC) methods are used to visualize hypoxic regions within a tissue. Derivates of 2-nitroimidazole like pimonidazole or EF5 get reduced at pO_2 lower than 3-10 mmHg (0.4-1.3 kPa) and can bind irreversibly nucleophilic groups on surrounding macromolecules [38, 39]. These compounds need to be injected in living organisms or cells, and stained using antibodies, restricting its use in the clinics but very practical for animal studies. Another IHC approach for hypoxia detection is by staining HIF-1α or downstream regulated proteins such as carbonic anhydrase (CAIX) [40, 41], although they are indirect measurements and do not always show a sustained expression [42].

In the clinics, imaging techniques are used to detect hypoxic areas, such as positron emission tomography (PET) following injectable 2-nitroimidazole tracers like ^{18}F-labeled fluoromisonidazole (^{18}F-MISO) [43], or using several variants of magnetic resonance imaging (MRI): with injectable perfluorocarbon (^{19}F-MRI) to measure pO_2, or with blood oxygen level-dependent MRI (BOLD-MRI) to detect changes in blood oxygenation (reviewed in [34]), or using a more recent quantitative variant qBOLD-MRI [44, 45]. Other imaging approaches to detect hypoxia, though less frequently used, are near-infrared spectroscopy (NIRS) that can measure real-time oxygen saturation but has lower resolution [46]; and electron paramagnetic resonance (EPR) that is less developed for clinical applications [47].

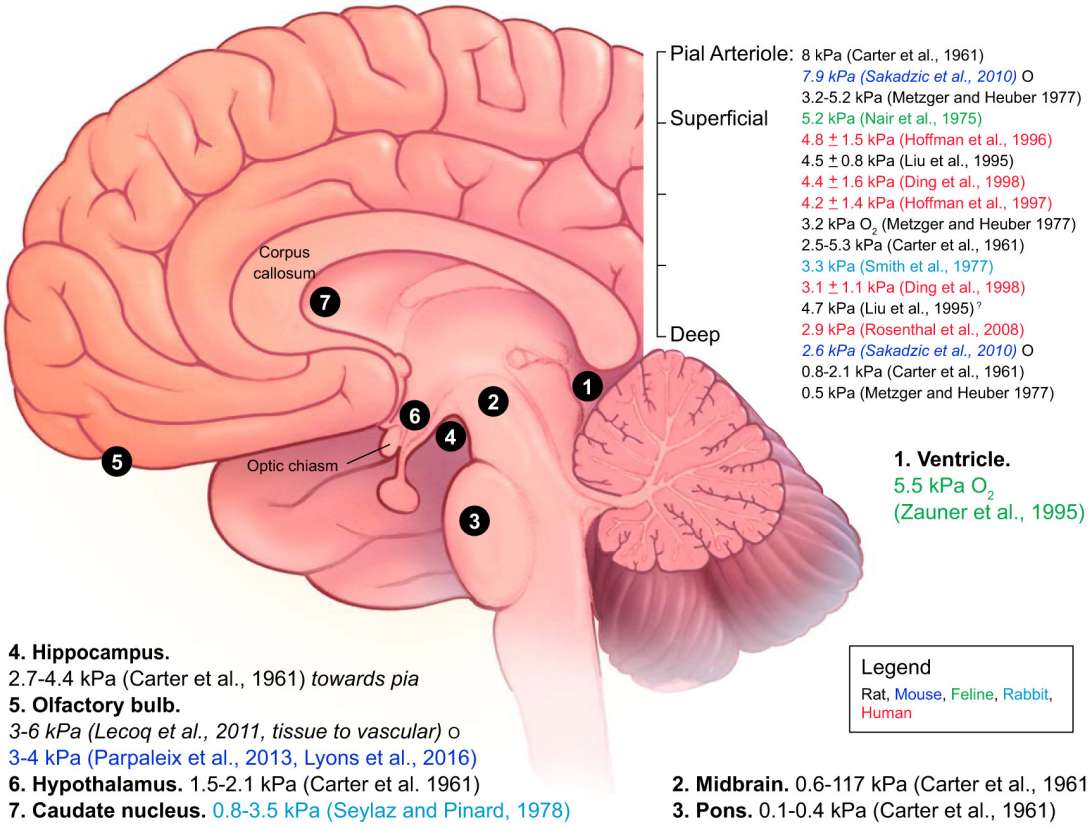

Figure 2. Scheme with annotated physiologic partial pressures of oxygen at different regions of the human brain, according to the indicated studies (Taken from [48]) References in the image: Lecoq et al., 2011 [37]; Cater et al., 1961 [49]; Sakadzic et al., 2010 [50]; Metzger and Heuber 1977 [51]; Nair et al., 1975 [52]; Hoffman et al., 1997 [53]; Liu et al., 1995 [54]; Dings et al., 1998 [55]; Smith et al., 1977 [56]; Rosenthal et al., 2008 [57]; Parpaleix et al., 2013 [58]; Lyons et al., 2016 [59]; Seylaz and Pinard, 1978 [60]; Zauner et al., 1995 [61].

In the brain, the main organ of interest in this thesis, pO_2 range from 5 kPa at the superficial cortex to 3 kPa in the deep inner white matter, and even to 0.5 kPa in some inner regions like the midbrain (Figure 2). As an average value, some studies consider that the brain is exposed to 4.4% O_2 [62]. All these recorded values are physiologic, suggesting that even within the same organ there is a gradient of oxygen availability.

1.1.2.2 In vitro

In vitro cultures should mimic the real physiologic and hypoxic oxygen values in the different tissues, known either from *in vivo* measurements (as summarized in figure 2), or experimentally identifying the oxygen condition for optimal cellular performance, as approached by Timpano and colleagues [63]. In this study, the authors empirically identified a window of oxygen in which cells produced less ROS and DNA damage, were more viable, and had proper functional and normal shaped mitochondria – window that the authors termed "goldiloxygen" zone (figure 3).

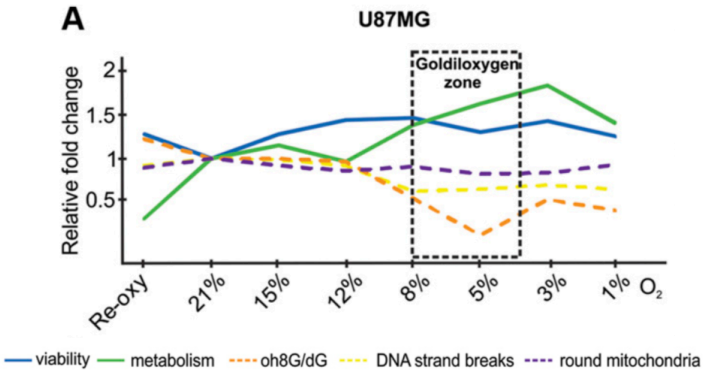

Figure 3. Oxygen-dependent cellular performance of U87 glioma cell line regarding cell viability, metabolism, DNA damage and mitochondrial shape (adapted from [63]).

From this and other studies we understand the impact oxygen has in *in vitro* cultures, suggesting that working at real physiological oxygen tensions could help translating research to *in vivo* observations [64, 65]. In any case, atmospheric conditions (21% O_2) do not represent any tissue *in vivo* – atmospheric conditions are hyperoxic.

Regular incubators are exposed to ambient air, with additional 5% CO_2 and 100% humidity, leaving 18.5% (18.8 kPa) O_2, which it still is hyperoxic. Despite the growing evidence proving that atmospheric conditions do not recapitulate physiologic features, most of the studies on hypoxia still use hyperoxic exposures as their control to their hypoxic cultures [48].

It is possible to maintain oxygen conditions lower than atmospheric in the laboratory. Incubators that can regulate oxygen content and chambers fluxed with desired gas mixes exist, although in these systems cells will get re-oxygenated from the moment they are exposed to ambient air again, and will require hours to reach the desired conditions. The best alternative is using oxygen-regulated workstations, which can serve both as a working hood and an incubator, ensuring a total exposure to the desired oxygen throughout the experiment, although they are more expensive.

1.1.3 Tumor hypoxia

Cancer cells rapidly replicate, forming a tumor mass with reduced O_2 diffusion and increased O_2 consumption, promoting formation of hypoxic areas spread heterogeneously in the tumor mass. Hypoxia is a hallmark of cancer, and is found in many solid tumors [66, 67]. From Vaupel's extensive work on detecting and studying hypoxia, we know that tumor hypoxia is associated with poor prognosis and increased metastasis [68, 69]. Indeed, low oxygen availability provides pro-tumoral signals to the tumor and its microenvironment affecting angiogenesis, promoting an aggressive phenotype, promoting radio- and chemo-resistance, and stemness properties.

1.1.3.1 Vasculature and neoangiogenesis

The vasculature is an important component of the tumor microenvironment and one of the key factors contributing to tumor hypoxia. Cancer cells will increase the distance from vessels as they divide reducing the diffusion of oxygen, a phenomenon referred as diffusion-limited or chronic hypoxia, when distances between cancer cells and vessels are larger than 70 μm. Simultaneously, tumor cells exert mechanical compression on microvessels leading to less perfused zones, which are often transient, producing perfusion-limited or acute hypoxia [70].

Normal vasculature is formed by endothelial cells, but it is immature unless vascular support cells are recruited, such as pericytes and smooth muscle cells, forming a basement membrane with tight junctions to maintain a controlled permeability of the vessels. On the other hand, tumor-associated vasculature is highly irregular and poorly functioning, as already described in 1945 by Algire and Chalkley, who quantified morphologic changes of vasculature following transplantation of tumors in mice [71]. Hypoxic exposure is the main factor that will trigger angiogenesis in the tumor; cancer cells will excessively produce signals to augment the vascular network, which will rapidly form at the expense of abnormal construction without proper pericyte coverage, and being loose and leaky. At least 6 different types of tumor-associated vessels exist, classified according to their shape and size, as well as their pericyte coverage, responding differently to stimuli in the microenvironment (reviewed in [72]).

Vascular endothelial growth factor A (VEGF-A) is one of the key factors promoting angiogenesis [73]. The amounts being produced, as well as the isoform, and the distribution of this crucial growth factor impacts on the formation of the new vessels [72]. Other described ways to promote neoangiogenesis and vasodilatation are production of Angiopoietin-1 and -2 and their receptor (Tie-2), adrenomedullin (ADM) or other

growth factors, such as fibroblast growth factor (FGF) and platelet-derived growth factor subunit B (PDGF-β), amongst other factors [74].

The state of the vasculature is generally assessed by staining sections from tumors with the markers CD31, CD34 and von Willebrand factor (vWF), or *in vivo* using windows in animal models to image subcutaneous tumors. Additionally, staining of pericytes and tight junctions are used to determine the functionality of the vessels.

1.1.3.2 Promoting an aggressive phenotype

Tumor hypoxia produces a selective pressure on cancer cells with the ability to adapt to low oxygen environment. It promotes an aggressive tumor phenotype through several ways: promoting metastasis and genomic instability, and inhibiting apoptosis.

Hypoxia, and mostly acute hypoxia, is associated with increased metastasis, and therefore with poor prognosis [75, 76]. Indeed, hypoxia induces invasiveness of cancer cells by upregulating proteins such as metalloproteases (MMP-9) that can degrade proteins of the extracellular matrix, or VEGF that can also promote perivascular invasiveness [77, 78].

Hypoxia promotes genomic instability, by supporting DNA replication errors as a result of the induction of DNA brakes at fragile sites and defective DNA damage repair mechanisms [79, 80]. Some examples leading to increased mutagenesis and genomic instability are downregulation of mismatch repair (MMR) genes such as MLH-1 and -2, and MSH-2 and -6 [81, 82]. Moreover, when DNA breaks are not repaired oncogenes like MYC activate or tumor suppressor genes like Phosphatase And Tensin Homolog (PTEN) inactivate, leading to clones with increased growth and metastatic potential [66].

Low oxygen supply induces apoptosis, even in malignant cells. However, some hypoxic cancer cells can survive it, depending on the severity of hypoxia and the fact that

some cancer cells can be inherently resistant to hypoxia-induced apoptosis [83]. For instance, cancer cells can activate anti-apoptotic pathways by overexpressing B-Cell CLL/Lymphoma 2 (Bcl-2), or prevent transcription of pro-apoptotic genes by losing p53 function or expression by upregulating the gene Mouse Double Minute 2 (Mdm2) [84-86].

1.1.3.3 Radio- and chemo-resistance

Tumor hypoxia is associated with resistance to conventional anticancer treatments: radiotherapy and chemotherapy. Resistance to radiotherapy in the context of tumor hypoxia was described as early as 1909 by Schwartz [87]. In the presence of oxygen, irradiation produces DNA damage due to formation of toxic free radicals, whereas in the absence of oxygen irradiation produces less free radicals, and therefore less toxicity [88, 89].

Hypoxia can also promote chemotherapy-resistance. The irregular tumor vasculature limits drug delivery, especially in chronic hypoxic regions distant from blood vessels [90, 91]. Ineffective chemotherapy also occurs because most agents are not designed to target hypoxic cells; they generally proliferate at a lower rate than oxygenated cancer cells, and they overexpress ATP-dependent drug efflux pumps, ATP-binding cassette (ABC) transporters, chemical transporters that can actively expel the compounds intended to kill them [92].

1.1.3.4 Metabolic switch

In1956, Otto Warburg already described the metabolic switch cancer cells undergo to cope with rapid proliferation needs, a phenomenon now known as the Warburg effect [93]. This metabolic adjustment consists of substituting the tricarboxylic acid (TCA) cycle by glycolysis as the means to produce ATP. Although the latter produces

less ATP per mole of glucose (2 ATP molecules/ glucose molecule) than the TCA cycle (38 ATP molecules/glucose molecule), glycolysis is much faster and globally can produce more ATP. Of note, this change in metabolism is defined as aerobic glycolysis, since this switch occurs in the presence of sufficient oxygen [94].

Hypoxia will emphasize this glycolytic dependence, mainly because the TCA cycle requires oxygen as a substrate for the oxidative phosphorylation step. Hypoxic cancer cells increase expression of glycolytic enzymes (e.g. aldolase A (ALDO-A), lactate dehydrogenase A (LDHA), and phosphoglycerate kinase 1 (PGK1)), and glucose transporters (e.g. GLUT1 and GLUT3) to support the metabolic switch [95, 96]. As a consequence of this increase in glycolysis, lactic acid is generated, decreasing the extracellular pH [97]. However, hypoxia also strongly upregulates expression of CAIX that can regulate pH, providing pro-survival help to cancer cells [98, 99].

1.1.3.5 Immunosuppressive features

The immune cells within the tumor microenvironment are influenced by low levels of oxygen directly impacting their functioning, or indirectly through changes in cancer cells that will in turn affect immune cells. Hypoxia inhibits infiltration and function of immune cells that could potentially recognize and kill tumor cells. For example, the excessive production of extracellular adenosine increases expression of immunosuppressive molecules, such as transforming growth factor beta (TGF-β), programmed cell death 1 (PD-1), and Cytotoxic T-Lymphocyte Associated Protein 4 (CTLA-4), on T cells [100]. Hypoxia promotes a reduction of proliferation and increased IL-10 production of cytotoxic CD8 T cells (CTLs) [101]. The activation of Signal Transducer And Activator Of Transcription 3 (pSTAT3) signaling, or upregulation of programmed-death ligand 1 (PD-L1) expression on cell lines from breast cancer, prostate cancer, and melanoma has been demonstrated to impair CTL-mediated killing [102, 103].

Simultaneously, hypoxic cancer cells will promote infiltration and function of inhibitory immune cells, which in turn will inhibit CTL function. Some reported examples are the increased expression of PD-L1 on myeloid-derived suppressor cells [104], or the secretion of chemoattractants, such as C-C Motif Chemokine Ligand 2 (CCL2) and CCL5, which induce the recruitment of monocytes into hypoxic areas [105]. Hypoxic cancer cells promote regulatory T cell (Treg) infiltration by secreting CCL28, and function by enhancing pSTAT3 activity, skewing macrophages towards a pro-tumoral phenotype with decreased phagocytic capacity [106, 107].

1.1.3.6 Promoting stemness

Tumor hypoxia impacts cancer stem cells (CSC); further described and referred to as glioma stem-like cells (GSC) in the next chapter of this thesis. Briefly, CSC have a de-differentiated phenotype, a slow proliferation rate, and can self-renew and differentiate into rapidly dividing cancer cells. CSC are therefore less targeted by conventional therapies acting on rapidly dividing cells, and can potentially repopulate the tumor after such treatments. Importantly, hypoxia promotes all these stemness properties, maintaining this population of cells and promoting their invasiveness and tumorigenicity [108, 109].

1.1.3.7 Hypoxia signatures

As discussed, the presence of hypoxia is a sign for poor prognosis and failure of many current therapies, due to changes on cancer cells and its tumor microenvironment. It is therefore of importance to identify biomarkers and/or signatures generated by hypoxia that could indicate low oxygen supply, allowing segregation of patients accordingly, to potentially follow differential treatment regimens if they exist. Therapies targeting hypoxia and brain tumors are further detailed in section 1.3.

In recent years, advances in technologies have allowed generation of genetic and transcriptional data from tumor cells, either from the tumor bulk, but also from specific regions (e.g. hypoxic) and even at the single cell level. Examples of such signatures are the 15-gene hypoxia signature from hypoxic areas of histology sections from human head and neck cancer, which was associated with clinical outcome and further validated for clinical trial [110, 111]; or the hypoxia-associated antigen repertoire being presented, changing the visibility towards the immune system, as described by Ge and colleagues in the context of glioma [112].

Very recently, Bhandari and colleagues quantified hypoxia scores in 19 tumor types, associated with a signature of mutations, oncogene expression, loss of tumor suppressor genes, and microRNA abundance profiles, helping identify tumor types that could benefit from therapies targeting hypoxia [66].

In conclusion, these advances provide a lot of information about tumor hypoxia, but the field remains full of unanswered questions. Hypoxia, through several mechanisms either HIF-dependent or independent, is associated with poor prognosis in many cancer types. This is why scientists and clinicians are still searching for ways to target hypoxic cancer cells (treatments discussed in section 1.3). Misleading results obtained from *in vitro* studies using inadequate physiologic controls will not help to produce results that are readily translatable to an *in vivo* setting.

1.2 Glioblastoma multiforme

In this project, we explore the effect of hypoxia on a particular tumor type: glioblastoma multiforme (GBM). In the following pages, I will describe the origin and characteristics of these particularly aggressive tumors, emphasizing the high degree of heterogeneity and the importance of the tumor microenvironment.

1.2.1 Astrocytomas

Cancer is defined as the malignant transformation of cells, resulting in their uncontrolled proliferation and the invasion of healthy tissue. Malignant tumors growing in different organs of the body have particularities that make almost every type of cancer unique. In the case of the central nervous system, tumors are classified according to the type of the transformed cell. Gliomas develop from glial cells, which are part of the neuroepithelial tissue that supports neuronal circuitry. Different glial cells give rise to different types of tumor: astrocytoma, oligodendroglioma, ependymoma, and mixed glioma. Gliomas have a relatively low incidence in the general population—among adults in the US, there were, on average, 9 cases per 100,000 person-years between the years 2011 and 2015 [113]. The 3-year and 10-year survival rates are 2–5% and 0.71%, respectively [114].

Astrocytoma is the most common type of glioma [115]. The World Health Organization (WHO) classifies astrocytomas according to their malignant features and level of aggressiveness (from grades I to IV) based on histopathological observations and genetic profiles [116, 117]. Grades I and II are considered to be low-grade gliomas, whereas III and IV are defined as high-grade gliomas. Low-grade gliomas are characterized by slow cancer cell proliferation but may eventually evolve into higher-

grade gliomas, resulting in a 42.6% 5-year relative survival rate [116]. Low-grade gliomas are associated with the isocitrate dehydrogenase (IDH) 1/2 gene and the α-Thalassemia/mental Retardation syndrome X-linked (ATRX) gene mutations [118].

Grade III gliomas are termed anaplastic astrocytomas. They are generally observed in relatively young patients (with a median age of onset of 41–50 years) and are defined by nuclear atypia, increased cellularity, and high proliferative activity [119]. The average 5-year relative survival rate for patients with anaplastic astrocytoma is 28% and the median overall survival is 3 years [120]. They can be subclassified according to the mutation status of IDH1/2, which has an impact on survival [121].

1.2.1.1 Glioblastoma multiforme

Grade IV gliomas are known as GBM, and these are the most aggressive and lethal form of glioma. Unfortunately, GBM is the most common type of primary brain tumor, accounting for 65% of all gliomas, and a total of 3–7 cases per 100,000 person-years in Europe and North America [122]. GBM has a 5-year survival rate of <3%, and the average age of incidence age is 62 years. The survival rate decreases with increasing age, i.e. children and young adults will survive longer than adults and those from the elderly population [119].

The vast majority of newly diagnosed GBM are sporadic; the only known causes of glioma are exposure to high doses of irradiation and very rare familial syndromes (involving mutations to TP53, Neurofibromin 1 (NF1), and retinoblastoma 1 (RB1), among others) [123]. It is believed that gliomas originate from the accumulation of oncogenic mutations, either in a somatic cell (the stochastic model) or in a stem cell (the hierarchical model), in both cases giving rise to a heterogeneous tumor [124, 125]. A recent study has provided evidence supporting the second hypothesis, demonstrating that

astrocyte-like neural stem cells from the subventricular zone containing driver mutations can migrate to distant regions of the brain and develop into malignant tumors [126].

Common symptoms presented by GBM patients include headaches, double or blurred vision, vomiting, seizures, and/or focal neurologic deficits (depending on the tumor location). Moreover, peritumoral edema and intracranial hypertension are frequently observed. The preferred techniques for the diagnosis of GBM are gadolinium contrast-enhanced magnetic resonance imaging (MRI) and computerized tomography (CT). The imaging of hypoxia and other functional aspects of GBM biology is performed using positron emission tomography (PET), or MRI combined with PET, and quantifying the intensity of the injectable tracer ^{18}F-FMISO [127]. However, the uptake and clearance of this molecule are slow, resulting in a high background signal. Therefore, other compounds, such as ^{18}F-EF5, ^{18}F-FAZA, ^{18}F-FRF170 and Cu-ATSM, are being used or developed to overcome its limitations (reviewed in [128, 129]).

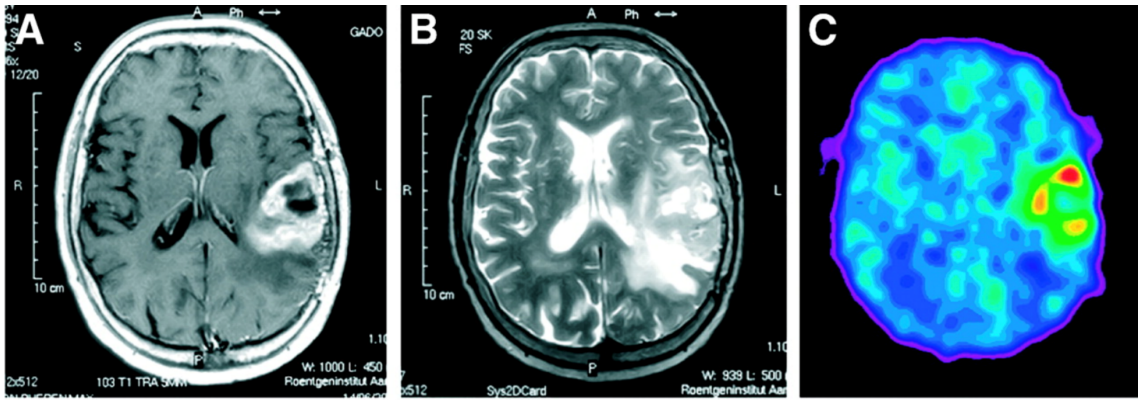

Figure 1.2.1: Images of a brain with GBM obtained using different techniques. (A) and (B) Gadolinium contrast-enhanced MRI images: T1 (A) and T2 (B). (C) PET scan with ^{18}F-FMISO tracer to visualize hypoxia 150-170 min after injection (normalized to its maximum value). (Adapted from [43])

Neuropathologists then examine a surgical biopsy at the histological and molecular level to specify grade and potentially give a prognosis. GBM is characterized by the same histopathological criteria as anaplastic astrocytoma, with the additional

presence of necrotic areas and microvascular proliferation. The zones surrounding necrosis, known as pseudopalisading areas, are hypoxic and hypercellular; tumor cells actively migrate away from the necrotic zone, whose vessels are absent or highly defective [130, 131]. The presence of hypoxia in gliomas is correlated with aggressiveness and more rapid tumor recurrence [132].

An important property of GBM is its infiltrative mode of growth, as described in 1940 by Scherer, who observed cancer cells infiltrating the brain parenchyma. These patterns of growth are now known as the *secondary structures of Scherer* [133]. GBM cells migrate through the extracellular space of healthy brain tissue forming multiple distant tumor foci [134]. Given the invasive nature of GBM, it should not be surprising to observe circulating tumor cells (CTCs) in the peripheral blood. GBM CTC have been reported in 21–40% of GBM patients, presenting an aggressive phenotype [135, 136]. However, CTCs are generally not able to establish tumors in other organs—GBM rarely produces metastasis (the estimated rate is <2%) [137, 138]. The almost complete absence of glioma metastasis might be explained by the fact that brain CTCs require neural growth factors only found in the brain, as well as the lack of communication between the intra- and extra-cerebral perivascular spaces. In fact, the majority of reported metastases originating from the brain occur after surgical intervention, which could create communication between tumor cells and extra-cerebral vessels [137].

The standard-of-care for GBM, together with a few other therapeutic approaches, are described in section 1.3.

1.2.2 Heterogeneity

One of the most important characteristics of GBM biology is its high degree of heterogeneity. This has huge clinical implications, since different patients are likely to respond differently to similar therapeutic approaches. Several classifications of these tumors have been proposed according to histological, genetic, transcriptional, epigenetic, and imaging features, aiming to stratify patients according to common features with predictive value for clinical outcome, and to find specific treatments accordingly.

We can describe two levels of heterogeneity: inter- and intratumoral. Intertumoral heterogeneity refers to the differences observed between patients, whereas intratumoral heterogeneity indicates differences within the same tumor of a single patient.

1.2.2.1 Sources of intertumoral heterogeneity

Origin

The first classification subdivides GBM patients into two groups according to the origin of the tumor: primary or secondary. Primary or *de novo* GBM is the most common type of GBM (85% of all cases) and develops very rapidly without clinical evidence of a lower-grade precursor. Secondary GBM progresses from lower-grade gliomas, hence they are associated with IDH1/2 mutations [121, 139]. It also has a better prognosis and generally manifests in younger patients [140]. Although primary and secondary GBM are indistinguishable at the histological level, they show differential gene expression profiles [141].

Genetic and transcriptional features

Although GBM is not one of the most highly mutated types of tumor [142, 143], there are two mutations that are frequently observed in GBM patients: amplification of epidermal growth factor receptor (EGFR) (36%), and mutated TP53 (15-28%) [144]. And

despite the high level of heterogeneity, there are three core pathways that are commonly altered in GBM: tyrosine kinase signaling (*88%)*, TP53 (87%), and the retinoblastoma tumor suppressor pathway (77%) [144, 145]. Over the past few decades, great advances in the technologies producing and analyzing genomic and transcriptional data have allowed GBM to be studied beyond its histological features. This has helped to unravel the genetic profiles of GBM patients, demonstrating their informative potential to predict survival [146].

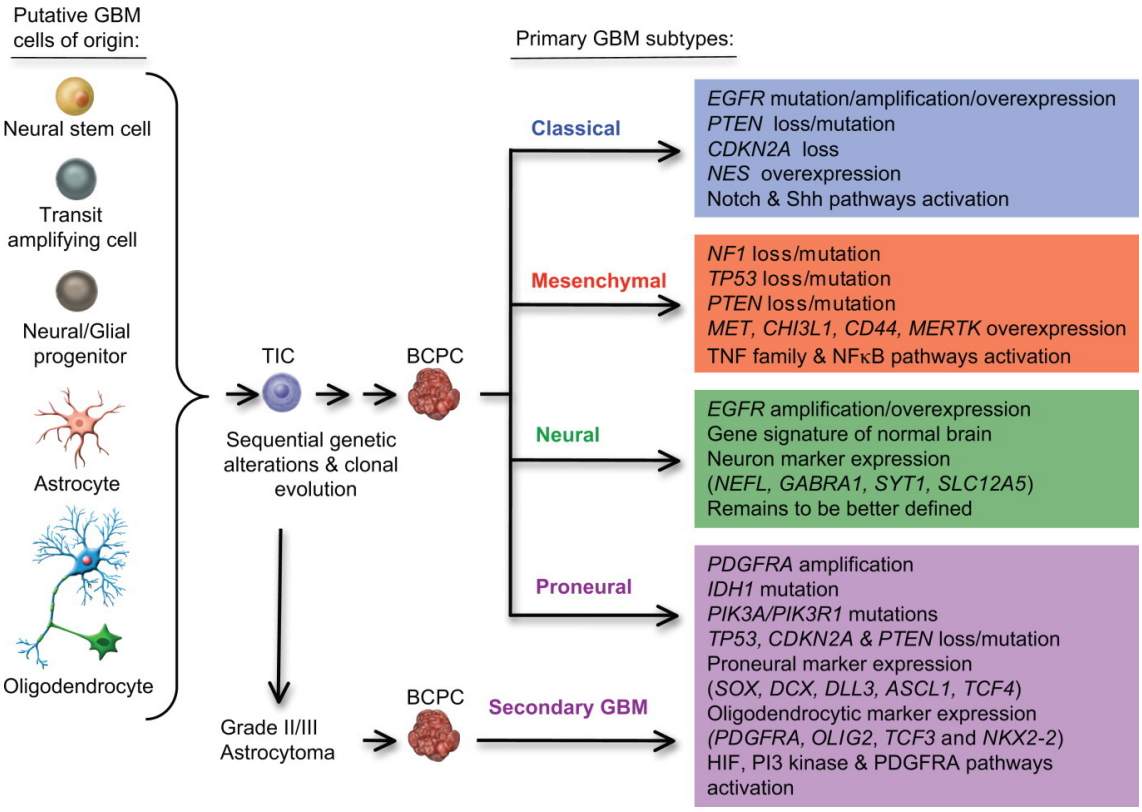

Figure 1.2.2. A schematic representation of the origin of GBM cells and the classification of primary and secondary GBM using molecular subtypes based on Verhaak's classification [147]. Abbreviations: TIC=tumor-initiating cell; BCPC=brain cancer-progenitor cell. (Taken from [148])

Molecular subclasses were first proposed by Phillips and colleagues, who classified GBM into three groups according to their mutations: mesenchymal, proliferative and proneural [149]. A few years later, in the first study on cancer by the cancer genome atlas (TCGA) research network, the genomic and core pathways

alterations in GBM were described [144]. The authors later on suggested a similar subclassification for primary GBM, known as the *GBM molecular subtypes* (Figure 1.2.2) [147]. The authors segregated GBM tumors into four groups characterized by key mutations: classical (EGFR amplification or EGFRvIII mutation, loss of PTEN), mesenchymal (NF1 mutation, loss of TP53 and CDKN2A), neural (overexpressed NEFL and neuron markers), and proneural (mutated IDH1/2 and TP53, amplification of PDGFRa, CDK6, CDK4 and MET) [147]. The same group described differential radio- and chemotherapy responses among these subtypes, which are associated with distinctive immune infiltrate within the tumor, changing as the tumor recurs [147, 150].

Epigenetic features

One very important epigenetic change in GBM is the methylation of the O-6-methylguanine-DNA methyltransferase (MGMT) promoter, which has an impact on the response to temozolomide (TMZ), the chemotherapeutic agent used in the standard treatment for GBM [151]. TMZ is an alkylating agent that methylates O6-guanine residues on DNA, producing DNA mismatch. These modifications can be restored by the action of MGMT, but not when the gene is silenced due to the methylation of its promoter [152]. Methylation of the MGMT gene promoter, therefore, confers sensitivity to TMZ.

Another epigenetic modification noted in glioma is hypermethylation, known as the glioma-CpG island methylator phenotype (G-CIMP), which is observed more frequently in low-grade gliomas and associated with IDH1 mutations, and therefore with better prognosis [153, 154]. Several studies have demonstrated the feasibility and potential of DNA methylation as a biomarker with clinical applications [155]. For example, one recent study was able to report the DNA methylation landscape of GBM by mapping the DNA methylation of paired primary and recurrent glioblastomas (which were matched with MRI and histology), providing information about immune infiltration,

the extent of necrosis, and the percentage of proliferating cells, all of which were correlated with progression-free survival [156].

Other features

Alternative approaches have been used to classify GBM tumors, for example, the use of imaging techniques. In one MRI-based study, the authors stratified their 121-patient GBM cohort into three clusters (pre-multifocal, spherical, and rim-enhancing) that were associated with differences in survival and molecular signaling pathways. This approach could potentially help identify patients who might benefit from particular targeted therapies [157].

Another approach has been the observation of phenotypic features such as tumor-growth kinetics [158]. This study produced the unexpected result that tumors that were larger and had faster growth kinetics at diagnosis showed a better response to the standard treatment, and therefore significantly better survival rates. Consequently, patients with slow-growing, small tumors are less likely to benefit from this treatment and should be considered for alternative therapies.

More recently, microRNA signatures have been explored. The classification of GBM into five groups according to microRNA expression has been proposed. These groups are associated with the Verhaak subtyping (with an additional subdivision of the proneural group according to G-CIMP status) [159]. Moreover, microRNA can be found in the peripheral blood, providing a noninvasively-obtained biomarker for clinical purposes – its feasibility was demonstrated in a study for lung cancer [160], and multiple circulating microRNAs have been already described in GBM [161].

Although all these classifications may help segregate patients, identify their potential responses to specific treatments, and determine their prognoses, it is also the

case that different molecular subtypes have been described within the same patient, i.e. GBM shows intratumoral heterogeneity [162].

1.2.2.2 Intratumoral heterogeneity

Intratumoral heterogeneity is defined as differences within the same tumor on several levels, e.g. cellular, genetic, and transcriptional, as described in the extensive work done by the Ivy Glioblastoma Atlas Project (Ivy GAP) [163]. In this publicly available atlas, the authors analyzed tumors originating from 41 GBM patients using *in situ* hybridization and laser microdissection on histological sections to define different anatomical regions within each tumor, and applied RNA sequencing (RNA-seq) to evaluate their transcriptional profiles. Focusing on mutations, such as point mutations and gene amplifications, has also allowed the identification of differences between regions within the same GBM tumor [164].

We could consider the evolution of GBM tumors over time to be another level of intratumoral heterogeneity, since differential responses to the microenvironment and to potential drugs have been described, mainly at the transcriptional level. For instance, it has been shown that recurrent GBM tends to show an aggressive mesenchymal profile [149, 165-167]. Others have evaluated epigenetic profiles as GBM evolves, which provided comparable results interpretation as genetic-originated data [168].

Another source of intratumoral heterogeneity is associated with the presence of cells with different differentiation statuses, namely differentiated cancer cells and cancer stem cells, here referred to as *glioma stem-like cells*.

Glioma stem-like cells

Over the years, the existence of a population of cells within the tumor mass with stem-like characteristics has become evident. These cells can give rise to heterogeneous

tumors, are very plastic, are resistant to therapies, and are responsible for tumor recurrence. In the human brain, glioma stem-like cells (GSCs) were first described by two independent groups: Singh and Galli, both in 2004 [169, 170]. There is lack of consensus regarding the definition of GSCs. Scientists generally use one marker to identify this cellular subpopulation, usually CD133 (Prom-1, Prominin-1). Singh and colleagues have shown that human GSCs defined as CD133 can generate a heterogeneous tumor population *in vitro*, and are tumorigenic in immunodeficient mice *in vivo* [169]. However, recent studies have demonstrated $CD133^{+}$ cells that have failed to generate tumors *in vivo*, and on the other hand, $CD133^{-}$ cells that are able to do, suggesting that CD133 is not an exclusive stem cell marker [171]. Another marker frequently used to identify GSCs is MET, but this is only expressed on mesenchymal and proneural subtypes [172].

In GBM, the tumor mass is formed by both glioma stem-like cells, which account for a small proportion of the tumor, and by glioma differentiated cells (GDCs), which form the bulk of the tumor and are characterized by rapid proliferation [173]. This definition is based on two extreme positions regarding cellular differentiation status. In reality, however, as revealed by the elegant work of Patel and colleagues using single-cell RNA-seq, there is actually a gradient of stemness gene expression within these tumors [174]. Another study has shown similar results using clonal genomic and functional assays [175].

However, to simplify routine *in vitro* work, researchers use the two extremes for their studies, which are achieved by changing the composition of the culture media. Adding epidermal growth factor (EGF) and basic fibroblast growth factor (β-FGF), as opposed to using media containing serum that supports a differentiated phenotype, allows GSC these cells to be maintained in culture, producing a phenotype akin to the one observed in the original tumors [176]. Another way to increase heterogeneity, while at

the same time conserving the oxygen gradient within the culture of cells, is to use 3D organoids [177]. Recent studies have implemented these organoids to provide a phenotype that is very close to reality, as shown in metastatic gastrointestinal tumors [178].

The GSC population *in vivo* is maintained in niches, described as both perivascular niches [179, 180] and hypoxic niches [181], the latter being observed, for example, at hypoxic pseudopalisades [182]. In the context of GBM, stemness properties are also potentiated by hypoxia [108]. Various mechanisms for this have been proposed, most of them involving HIF-1α and HIF-2α [183, 184]. An often-described pathway that could explain the increased aggressiveness of GBM caused by GSCs is through the activation of the CXCL12/CXCR4 axis, whereby CXCR4 is overexpressed in the GSC population, which can decrease tumor size *in vivo* when blocked [185].

The elegant work of Suvà and coworkers focused on the plasticity of cancer cells, deciphering the mechanisms by which GDCs can reprogram to GSCs. Four specific transcription factors were needed for such reprogramming: Sex Determining Region Y-Box 2 (SOX2), Oligodendrocyte Transcription Factor 2 (OLIG2), POU Class 3 Homeobox 2 (POU3F2) and Spalt Like Transcription Factor 2 (SALL2) [186]. Some years later, the same group demonstrated epigenetic modifications (chromatin remodeling) that drive GSC plasticity [187].

GSCs are resistant to conventional therapies such as chemotherapy and radiotherapy. These treatments generally target GDCs, which divide rapidly, but not the GSC population, which have a slow proliferation rate. Moreover, GSC express ABC transporters, for instance potentiated by hypoxia. As a result, many clinical readouts show tumor regression after conventional treatment, since the bulk of the tumor has responded

to therapy, but the few live GSCs remain virtually undetected and have the capacity to repopulate the tumor thanks to their ability to self-renew and differentiate. Consequently, GSCs are considered to be the cause of recurrence after treatment [188, 189].

1.2.3 The glioblastoma microenvironment

Cancer research has evolved from being very tumor-centric to appreciating the value of the tumor microenvironment. I have already described the importance of hypoxia, but it is also necessary to understand other components in this microenvironment that contribute to the formation and maintenance of the GBM mass, such as immune cells and brain-specific cells.

The brain has historically been believed to be immune privileged due to its controlled inflammatory responses, its distinctive cellular composition, and its anatomical location. Although we now know that immune responses can occur in the brain (through both peripheral and brain-resident mediators), several features make brain-immune crosstalk unique (reviewed in [190]). For instance, the presence of the blood-brain barrier (described below), the low expression of major histocompatibility complex (MHC) molecules, and the lymphatic vessels present at the meninges, which are slightly different from those in the rest of the organism, and allow exchange between the lymphatic system and the cerebrospinal fluid (CSF) while maintaining tolerance of potentially central nervous system (CNS)-reactive T cells [191]. Moreover, the brain is equipped with unique cellular components: astrocytes, neurons, oligodendrocytes and microglia (brain-resident macrophages).

In the context of glioma, both brain-specific cells and immune-system components are found within the tumor microenvironment. As illustrated in Figure 1.2.3,

the tumor mass is formed by glioma cells but also contains many non-cancerous cell types: blood vessels, macrophages and microglia, dendritic cells, neutrophils, lymphocytes and astrocytes. While microglia and astrocytes are cell types resident in the brain, the rest need to reach the brain through the blood circulation. Glioma cells provide pro-tumoral cues to all of these cell types that ensure the survival of cancer cells, creating a generally immunosuppressive microenvironment, i.e. they carry out tumor immunoediting [192].

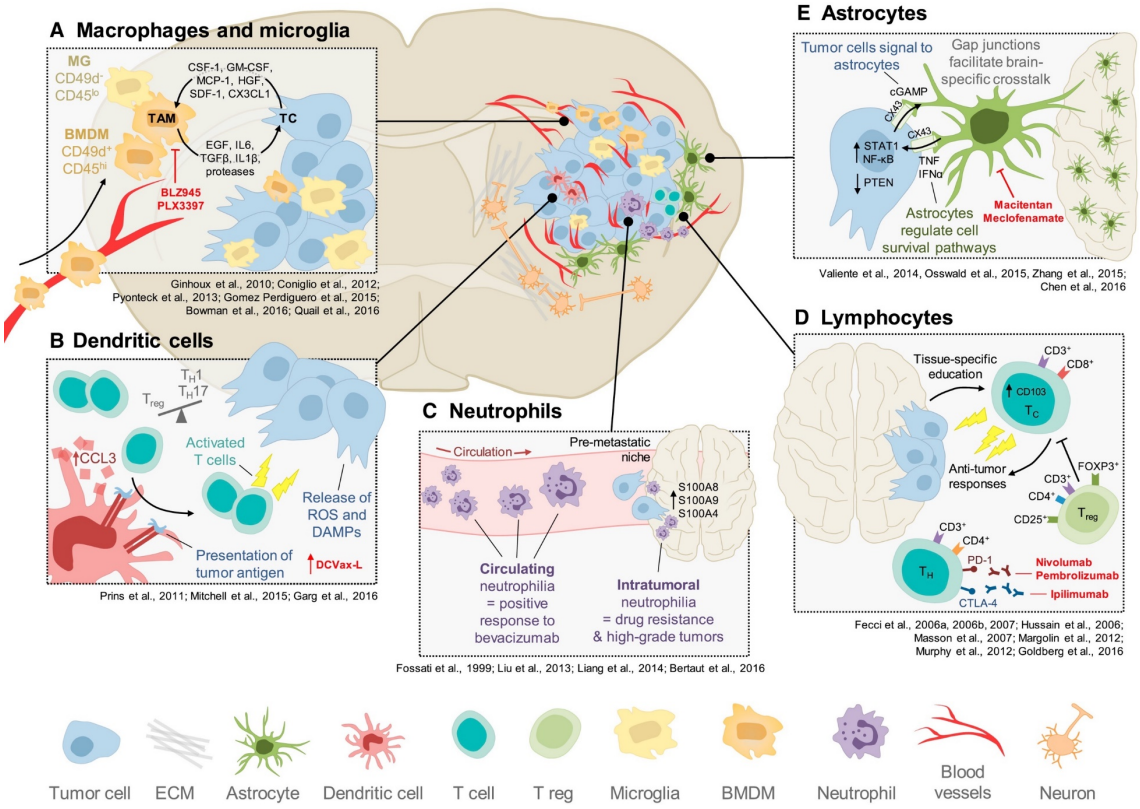

Figure 1.2.3. A schematic representation of the cellular components of the brain tumor microenvironment, with a focus on immune infiltrate. (Taken from [193])

Tumor-associated macrophages (TAMs) account for the largest population of infiltrating immune cells in the GBM microenvironment, and are correlated with poor prognosis in GBM [194]. TAMs can be polarized towards either a pro-tumoral or an anti-tumoral phenotype, depending on microenvironmental cues. GBM will cause them to be skewed towards the pro-tumoral phenotype, but with appropriate treatments, re-

polarization towards the anti-tumoral phenotype has been achieved in mouse models [195, 196]. Resident microglia also have an impact on GBM biology, for instance, by enhancing glioma cell invasiveness [197, 198].

The lymphocytic compartment, although less abundant, is potentially capable of identifying and killing glioma cells. However, the glioma microenvironment strongly inhibits CTLs) by inducing anergy, exhaustion, etc. and promotes inhibitory Tregs [199]. This is why many immunotherapies have been developed focusing on this immune-cell type (see the chapter on immunotherapies).

Communication between cells in the tumor microenvironment is not exclusively through direct cell–cell contact [200]. Recently, extracellular vesicles produced by cancer cells have come under the spotlight. For example, extracellular vesicles from apoptotic GBM cells containing factors, such as RNA Binding Motif 11 (RBM11), can promote gene-expression changes, driving surviving GBM cells towards a malignant (mesenchymal) phenotype [201].

1.2.3.1 The blood–brain barrier

The blood–brain barrier (BBB) constitutes an important biological barrier for the brain and also has impact on GBM biology and, notably, treatments aimed at killing cancer cells. It is comprised of astrocytes, pericytes, and endothelial cells, which have tight junctions that will allow only certain molecules to pass. The BBB also helps control ion homeostasis, maintains a low-protein milieu for optimal neural activity, and allows immune surveillance while ensuring minimal inflammation (reviewed in [202]).

Importantly, drugs in general will be denied entry to the brain tissue by this controlled highway; it is estimated that around 98% of molecules have their transport blocked [202]. However, in the context of brain tumors and other brain pathologies, the

BBB loses its integrity and becomes leaky [203, 204]. This might increase the likelihood of drug delivery into the brain, but it is not guaranteed. Of note, the BBB integrity loss is heterogeneous, as demonstrated in a rat glioma model [205], or in humans, using contrast-enhanced MRI (reviewed in [206]). Several strategies are being developed to help compounds pass through the BBB, such the use of focused ultrasound and nanoparticles (reviewed in [207]).

1.2.4 Animal models

Many properties of GBM biology can be studied in *ex vivo* tissues originating from human GBM patients. However, to fully understand tumor formation and maintenance, the interactions of glioma cells with other cell types in the tumor microenvironment, and the response to treatments, it is necessary to use *in vitro* and *in vivo* models. *In vitro* settings allow the control of parameters, and importantly, multiple drug combinations. Nevertheless, this approach cannot provide extensive information regarding the interactions between several cell types. The use of animal models can. However, we have to be cautious about the choice of animal model—many treatments that have been successful in mouse models have failed to translate into success in human clinical trials. This could be partially due to the use of non-optimal pre-clinical models, which may be based on xenografts or syngeneic implants.

1.2.4.1 Xenografts

Most of the xenograft studies consist of mouse models, although xenografts on zebrafish, which allow visualization *in vivo* of tumor progression and invasion, are also used [208, 209].

Implanted glioma xenografts can be derived from commercially available established cell lines (such as the classical U87 and U251) or from primary tumors from GBM patients. Generally, tumors grown following this approach do not recapitulate the invasive nature of human GBM. The implantation of GSCs has improved xenografts in animals by achieving intratumoral heterogeneity [210]. Using *in vivo* models not only allows the testing of multiple therapeutic approaches, but also enables the identification of key molecules in GBM biology. For instance, Miller and colleagues performed direct phenotypic screening of pooled RNA interference in patient-derived xenograft models allowing them to identify a crucial factor (JMJD6) for GBM growth [211].

However, one major disadvantage of using xenografts of human origin in animal models is the obligatory use of immunodeficient animals to avoid rejection of the implanted graft by the host adaptive immune system (T and B lymphocytes). This restricts any studies aiming to assess the interaction of cancer with adaptive immune cells. To overcome this limitation, syngeneic models have been established.

1.2.4.2 Syngeneic models

Syngeneic models for GBM are frequently based on a mouse glioma cell line that originates from the same genetic background as the mouse being implanted, meaning that the graft can be tolerated. GL261 is a classic mouse glioma model which originates from carcinogenic exposure and is able to recapitulate several characteristics of human GBM [212], including hypoxia formation and HIF-1α expression patterns [213]. Another carcinogen-induced model is the rat C6 glioma model [214]. Genetically engineered models have been developed to express similar genetic lesions as in human GBM. For example, the SB28 model targets p53, PDGF, and RAS on mouse astrocytes, recapitulates a proneural GBM subtype, and shows similar responses to immune checkpoint blockade as predicted in human primary GBM patients [215].

An alternative to the use of rodents is the chorioallantoic membrane assay on chicken embryos [216]. This model is particularly useful for angiogenesis after graft insertion [217]. Knowing the advantages of each model, as well as their limitations, means that we now have multiple tools with which to study the biology of GBM cells and their interaction with the tumor microenvironment.

Considering that GBM is characterized by a high level of heterogeneity, the aim is to either find common aspects between patients, or to stratify them according to differential features in order to improve treatments for this aggressive and lethal tumor type.

1.3 Therapies

Different therapeutic approaches currently exist to reverse hypoxia and to treat GBM; however, the options are still limited and, so far, not totally successful. There is an urgent need to find new therapies, including, for instance, the repurposing of existing drugs such as metformin. This section provides information on these approaches, focusing on therapies for GBM.

1.3.1 Hypoxia

The reversion of tumor hypoxia became an obvious aim for clinicians and researchers after inadequate oxygenation was observed in almost all solid tumors, and after many negative consequences of its presence were defined [68]. Indeed, reducing hypoxia improves anti-tumor immunity, by enhancing CTL infiltration, recognition of cancer cells, and killing function [218, 219]. The following approaches have been mainly studied in the field: targeting HIFs directly, HIF downstream cascades, drugs that are activated under hypoxic conditions, and hyperbaric oxygen breathing.

1.3.1.1 Targeting HIFs

Due to the central role of HIFs in the response to hypoxia, and the fact that HIF-1α expression is correlated with higher tumor aggressiveness and poor prognosis, it is clear that HIF as a therapeutic target, using inhibitors and genetic modifications of HIFs [213], should be considered.

Genetic approaches using animal models have demonstrated the importance of HIFs during both physiology and pathology; HIF-1α or HIF-2α mutants are lethal during embryonic development, mainly due to abnormal vascular development, and HIFs are essential for tumor formation and maintenance [11, 220]. Indeed, in a tumoral context,

lack of HIFs (including HIF-1β) shows reduced tumor size, aggressiveness, and angiogenesis [220, 221].

Chemical HIF-1α inhibition has been studied extensively using multiple methods (reviewed in [222, 223]), by affecting either HIF levels or activity. Some examples of modulating HIF levels are: reducing HIF-1α at mRNA levels using aminoflavones, and at protein levels by reducing protein translation with mTOR inhibitors such as temsirolimus; and decreasing HIF stability with histone deacetylase (HDAC) inhibitors such as LAQ824 or vorinostat. Examples of reducing HIF activity are: inhibiting HIF-1α and HIF-1β dimerization, using acriflavine; reducing HIF DNA-binding activity with anthracyclines such as adriamycin; and inhibiting the interaction of HIF with coactivators, such as the proteasome inhibitor bortezomib. Some of these compounds are now in the long process of clinical trial development (including for GBM), though they have shown limited efficacy so far. A phase II trial using the HDAC inhibitor vorinostat on GBM showed that the drug was well tolerated, but showed only a modest clinical benefit [224]. Consequently, it was dropped as a monotherapy and combined in a phase II trial for GBM with the proteasome inhibitor bortezomib, though it did not provide a positive clinical outcome [225].

1.3.1.2 Targeting downstream of HIF

There are many downstream signaling cascades of HIF; however, in a therapeutic context, targeting those leading to angiogenesis have been prioritized. Blocking the VEGF/VEGFR pathway has seen modest objective responses in some cancer types, but it is still a long way from being able to clear a tumor, or to stop it growing entirely—in the best cases, it increases survival slightly (reviewed in [226]). However, it has been also

observed that, when treating tumors with anti-angiogenic drugs, cancer cells become more hypoxic and can even antagonize chemo- and radiotherapies (e.g. [227]).

Jain hypothesized the theory of tumor vasculature normalization, in which optimal dosing (dose and timing) of anti-angiogenic therapies can not only stop the formation of new vessels that could support tumor growth, but also normalize the tumor's vasculature, which otherwise is chaotic and leaky, i.e. abnormal [228]. Normalizing the vessels increases tumor perfusion, providing oxygen and potential drugs to cancer cells. Some drugs used for this purpose are the previously mentioned anti-VEGF therapy, or the VEGFR tyrosine kinase inhibitors sunitinib and cediranib [229, 230]. Tumors with hyperpermeable but largely uncompressed vessels, such as those found in GBM, could benefit from anti-angiogenic therapies as they normalize the vasculature, as suggested by mathematical models [231].

1.3.1.3 Others

Hypoxia-activated prodrugs (HAPs) are an appealing alternative. The normally inactive pro-drug becomes enzymatically reduced when oxygen is scarce, releasing a cytotoxic ligand. This allows specificity of the compound under hypoxia, reducing the toxicity of the drug to normal tissues. Class I HAPs, such as tirapazamide, are activated under mild hypoxia [232]. Class II HAPs, such as evofosfamide (TH-302) are activated under severe hypoxia. HAPs are expected to work on a large spectrum of cancers, including GBM. So far, there are no FDA-approved HAPs and, although some pre-clinical studies and clinical trials have shown promising results [219, 233], phase III trials have failed to show beneficial effects [234, 235]. It is possible that a pre-selection of patients with significant hypoxia presence will help to clarify the heterogeneous results obtained in such trials. Optimal combination(s) of HAPs with other drugs are still to be found.

Another approach, and perhaps the most straightforward, to potentially reverse tumor hypoxia consists of breathing carbogen, a mixture of 95% O_2 and 5% CO_2, which, when administered in combination with oral nicotinamide, could increase tumor oxygenation [236]. However, a phase III trial failed to control tumor growth in advanced laryngeal cancer [237]. Breathing hyperbaric oxygen (HBO), with either 100% O_2 or a carbogen mixture, increments the levels of oxygen compared to normobaric administration [238]. HBO has been tested in GBM, and the levels of oxygen increased in the intratumoral and peritumoral regions, though the benefit was of very short duration [239]. Fluorocarbons are also used to increase delivery of oxygen, and these are being investigated in clinical trials [240].

1.3.2 Glioblastoma multiforme

As described in the previous section, GBM is highly heterogeneous. Consequently, no universal treatment exists from which all GBM patients can benefit. The reality is that there are few treatment options with proven efficacy available, and the treatment for GBM has essentially remained the same for decades. Current therapies only extend the life of the patient, but the cancer remains fatal. The heterogeneity, the anatomical location, and the invasive nature of GBM pose further challenges.

1.3.2.1 Surgery

The first action after high-grade glioma diagnosis consists of maximal surgical resection. Total resection is not always an option due to the potential location of the tumor affecting a vital region in the brain. Moreover, the invasive nature of GBM makes it impossible to totally eliminate all tumor cells.

Even when total gross resection is achieved, GBM invariably recurs, and is observed at the margin of the resection or within 4 cm of the original tumor [241]. This means that the cells responsible for the recurrence are left in the brain and do not respond to subsequent treatments [242]; typically this is attributed to GSC [243]. Moreover, in some patients, new tumor foci far from the original surgery site are found at recurrence, which could be because of a new invasion at recurrence, or they could already have existed but been undetectable at the time of diagnosis.

1.3.2.2 Radio- and chemotherapy

The standard of care treatment for GBM is radiotherapy with concomitant chemotherapy. Radiotherapy is directed at the tumor site, including the margins so as to target migrating cells. Chemotherapy consists of the imidazotetrazine alkylating agent temozolomide (TMZ), which can cross the BBB [244]. TMZ methylates DNA O^6-guanine residues, producing mismatch errors in DNA and eventually killing those cells that fail to repair such errors. The landmark phase III clinical trial led by Stupp evaluated 573 primary GBM patients receiving radiotherapy alone or radiotherapy plus concomitant TMZ followed by six cycles of TMZ, resulting in a median survival of 12.1 and 14.6 months, respectively (Figure 1.3.1) [245]. Thereafter, the first-line treatment for GBM consists of radiotherapy with concomitant and adjuvant TMZ.

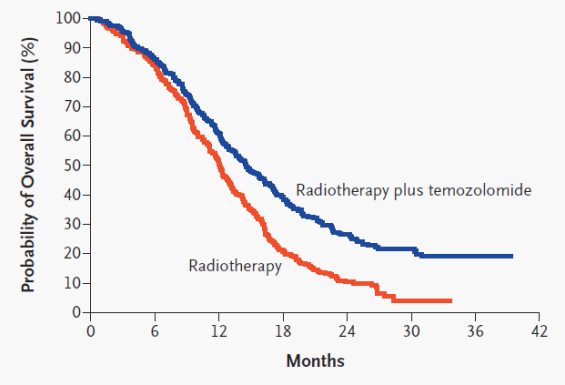

Figure 1.3.1. Results from the landmark phase III trial for GBM patients following radiotherapy only or radiotherapy with concomitant and adjuvant TMZ. (Taken from [245])

As mentioned earlier, methylation of the MGMT promoter confers an advantage to respond to alkylating agents. The first indications came from Esteller's work, which showed a correlation between the methylation of the MGMT promoter and the response to the alkylating agent carmustine [246]. The MGMT promoter status was assessed in patients from the Stupp trial, and it was confirmed that patients with methylated MGMT promoter benefited from TMZ therapy (21.7 months) compared to patients with unmethylated MGMT (15.3 months) [151]. Around 45% of GBM patients show methylated MGMT promoter [247]. Once the MGMT promoter is methylated, it provides a better response to TMZ, and distinct levels of methylation are not correlated with better prognosis—low levels of methylation already confer a survival benefit [248]. Although they do not benefit from TMZ, patients with unmethylated MGMT still receive such treatment.

Despite this treatment regimen, GBM always recurs. There is a selective pressure for those clones that are resistant to the treatments; the tumor evolves and the genetic and transcriptional profiles are different at recurrence [249, 250]. Therefore, it is important to choose second-line treatments carefully to target the cells that overcome the first therapeutic approach.

1.3.2.3 Second-line treatments

Reoperation is not performed systematically, although it is not clear whether repeated surgeries is beneficial for many GBM patients—it is dependent on the preoperative neurological status, or unless specified for clinical trial purposes [251, 252]. There are limited therapeutic options for recurrent GBM, but amongst them, four FDA-approved approaches are: carmustine wafer, lomustine, bevacizumab, and tumor-treating fields.

Carmustine wafer, under the name gliadel, are biodegradable implantable wafers loaded with carmustine, which is an alkylating agent [253]. It is the first approved brain cancer drug to be delivered directly into the brain, and it has also been approved for anaplastic astrocytoma. Gliadel combined with radiotherapy and TMZ provides additive survival benefits, without increasing toxicity profiles [254].

Lomustine is another an alkylating agent that also induces DNA interstrand crosslinks, which can lead to cell cycle arrest. In a recent phase III clinical trial for methylated MGMT promoter GBM patients, treatment with lomustine and TMZ combination increased median survival (48.1 months) compared to TMZ only (31.4 months) [255]. Although the results were impressive, the relatively small sample size (n=141) makes this trial relatively inconclusive; however, it does provide hope in relation to the use of combined lomustine and TMZ for GBM patients with methylated MGMT promoter.

A frequent treatment for recurrent GBM is to use bevacizumab (avastin), an anti-VEGF antibody. This was approved by the FDA for recurrent GBM in 2009 [256]. A phase III trial (avaglio) assessed the potential use of bevacizumab as a first-line treatment for GBM patients; it failed to extend overall survival when added to radiotherapy and TMZ therapy, but increased progression-free survival [257]. The failure to extend survival after this treatment could be because of resistant cells that are positively selected [258]; alternatively, some evidence suggests that GBM cells become more motile and invasive [259]. As a monotherapy, anti-angiogenic therapy has provided underwhelming results. The combination of lomustine with bevacizumab has also been tested in patients with progressive GBM, after radio-chemotherapy, reporting an increase in progression-free survival (PFS) but not in overall survival (OS) [260].

Tumor-treating fields consist of directed low-intensity alternating electric fields, which have an antimitotic effect on rapidly dividing cells. They have been shown to increase OS and PFS of GBM patients in a randomized clinical trial [261].

1.3.2.4 Targeted therapies

Other therapeutic options like targeted therapies are being explored, such as EGFR, integrin, or mTOR. Targeting of mTOR will be further described in section 1.3.3.

EGFR, which is amplified or mutated in a high percentage of GBM patients [262], has tyrosine kinase activity, initiating signaling cascades such as the phoshoinositide 3-kinse (PI3k)/Akt pathway [263]. EGFR can be targeted using small molecules such as erlotinib or gefitinib [264, 265], or with monoclonal antibodies such as cetuximab or nimotuzumab; however, these have not managed to extent GBM patient survival [266, 267].

The targeting of integrins has been tested in cancer, affecting angiogenesis and the invasiveness of cancer cells due to its role in cell–cell and cell–extracellular matrix interactions. An example of this type of drug is cilengitide, a selective inhibitor for integrins $\alpha v\beta 3$ and $\alpha v\beta 5$. However, in a phase III trial, cilengitide failed to improve survival for GBM patients with methylated or unmethylated MGMT [268, 269].

1.3.2.5 Immunotherapies

Immunotherapies aim to act on the host immune system to trigger a response against the tumor. The immune system has the potential capacity to detect and kill neoplastic cells, but the tumor microenvironment is highly immunosuppressive. In general, tumors with an immune infiltrate are correlated with a better prognosis, but the composition of this infiltrate is a determinant of the clinical outcome [270]. In previous years, several modalities of anti-cancer (including GBM) immunotherapies have been

developed, aiming to target several aspects of the "cancer-immunity cycle" (Figure 1.3.2) [271]. Few GBM immunotherapies have been tested in randomized trials to date, and success is expected to be limited as monotherapies, because GBM form "cold" tumors that are poorly immunogenic, and contain immunosuppressive cells.

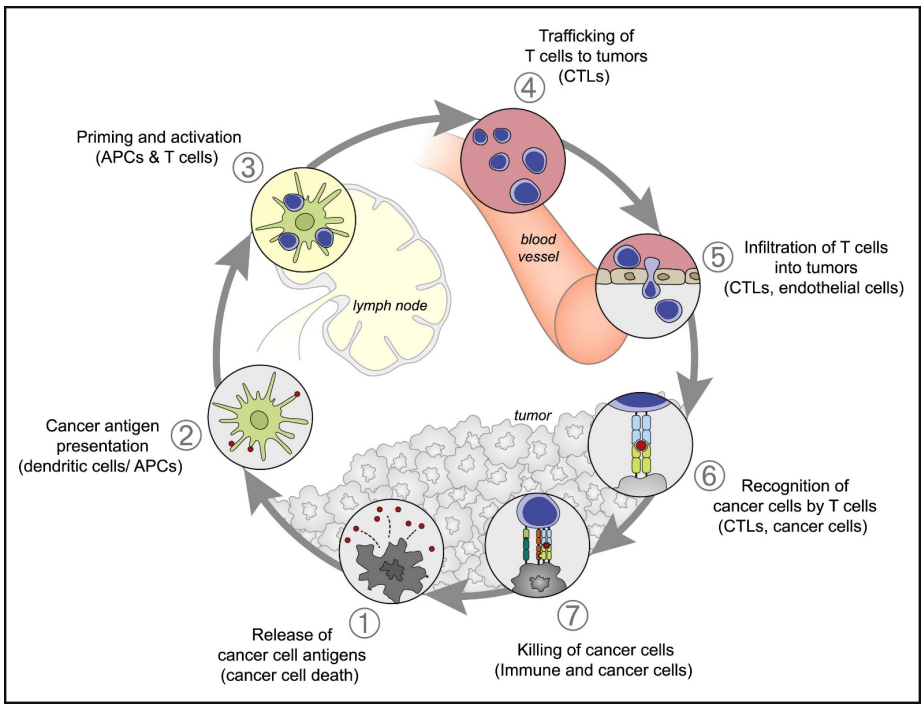

Figure 1.3.2. The cancer-immunity cycle. (Taken from [271])

It is worth noting that, not only is GBM immunosuppressive by nature, but many of the therapeutic approaches for GBM are also immunosuppressive, such as chemotherapy. Moreover, during the course of the therapy, patients frequently experience brain edema and hypertension. Consequently, they receive corticosteroids (e.g. dexamethasone) that reduce the edema, but are highly immunosuppressive. However, optimizing chemo- and immunotherapies can have additive or synergistic effects. For example, the chemotherapeutic agent decitabine could increase the response to adoptive cell transfer in a glioma mouse model [272], and sensitize glioma cells *in vitro* to immune attack [273].

Immune checkpoint blockade has become a significant breakthrough in the field of onco-immunology, achieving long-term survival in melanoma by blocking the axis PD-1/PD-L1 or CTLA-4 [274]. Although, to date, immune checkpoint blockade in GBM has shown limited efficacy, recent studies have demonstrated that anti-PD-1 administration before and after surgery (neoadjuvant regimen) was associated with an anti-tumor immune response, better survival, and even long-term survival [275, 276]. Recent studies have begun to explore which patients, with specific gene signatures and immune infiltration, can benefit from such therapy [277].

Another strategy has been to administer agonistic anti-CD40 monoclonal antibody. CD40 is a member of the tumor necrosis factor (TNF) receptor family, expressed by professional antigen presenting cells (APC) such as B cells and dendritic cells, but also by non-immune cells and cancer cells. CD40 binds to CD40L expressed by activated T cells, and induces antigen presentation functions in APCs (reviewed in [278]). In a preclinical glioma model, the agonistic CD40 monoclonal antibody was able to potentiate an anti-tumor immune response, and induce apoptosis in several solid tumor cell lines *in vitro* [279, 280].

Vaccination against cancer can be based on direct administration of tumor antigens, for instance, using peptides (see our review in the results section [281]), or on antigen-loaded cells, such as dendritic cells (reviewed in [282]).

Adoptive cell transfer of autologous T cells is possible, but isolating specific anti-tumor lymphocytes is a limiting factor. Chimeric antigen receptor (CAR) T cells are being developed to overcome this problem, since they originate from peripheral blood mononuclear cells (PBMCs). CAR T cells are genetically modified T cells to express an improved T cell receptor (TCR) with specificity for a given tumor-specific antigen, while

maintaining the killing machinery of a CTL. Safety, feasibility, and capacity to kill GBM cells by IL13Rα2 or EGFRvIII targeting CAR T cells have been proven [283-285]. Due to GBM heterogeneity of antigen expression and potential antigen loss in response to these therapies, it is necessary to target additional antigens, and this is being envisioned [286].

Outstanding results have been obtained from cytomegalovirus (CMV) antigen targeting, though few patients have been involved in studies so far, and this evidence lacks clinical and accurate scientific validation. Approximately 50–90% of humans are infected with CMV, and GBM cells, though not normal brain cells, contain CMV products [287]. A randomized phase II trial reported negative results of the antiviral valganciclovir in GBM [288]. But a retrospective analysis of these data showed an increased survival (56.4 months) when this antiviral medication was administered continuously [289]. Targeting of the CMV epitope pp65 using dendritic cells also increased OS and PFS in patients in a pilot trial, and polyfunctional CD8 T cells, including CMV-specific cells, were detected [290, 291].

1.3.2.6 Targeting glioma stem-like cells

Because GSC are responsible for tumor recurrence, this cell population represents a very attractive target for cancer therapies. However, as described earlier, GSC are particularly resistant to many therapies. A strategy is to induce terminal differentiation of GSC, which can be further killed by radio- and/or chemotherapy. For instance, increasing the levels of Achaete-scute homolog 1 (ASCL1) on GSC induces neuronal differentiation and renders these cells sensitive to inhibitors of the Notch pathway [292]. However, another study showed that terminal differentiation is unachievable on GSC using Bone Morphogenetic Protein (BMP), probably because these cells retain specific stemness transcription factors, and they perform incomplete epigenetic changes [293].

As there is intertumoral heterogeneity, combinations of several drugs targeting the different GSC niches have also been suggested, such as the simultaneous inhibition of EZH2 and BMI1, which can target perivascular GSC and hypoxic GSCs, respectively [294]. An innovative approach suggests gene therapy delivered by encapsulated siRNA in nanoparticles to remove key genes in GSC, resulting in a survival benefit in a GBM xenograft mouse model [295].

1.3.2.7 Alternative medicine

The reality of treating this particular cancer is that many patients, and their family members, do not agree with or do not want to follow full treatment protocols, or do not wish to participate in clinical trials, which is understandable in view of the poor efficacy and significant side effects of the treatments offered. It is not surprising that many GBM patients decide to follow a "less chemical" approach and choose natural products (reviewed in [296]).

Some examples of such alternative therapies are phytotherapy, which uses natural plants [297], or fasting approaches, which aim to reduce the caloric intake to starve the tumor, such as ketogenic metabolic therapy or short-term starvation [298]. The latter was shown to enhance the efficacy of radio- and chemotherapy in a glioma mouse model [299]. No evidence exists for clinical benefit of these approaches, although multiple clinical trials are assessing complementary medicine, i.e. combining standard treatment with alternative medicine (clinicatrials.gov).

In conclusion, there is an urgent need to find new therapeutic approaches for GBM, especially for those with an unmethylated MGMT promoter. Immunotherapies and targeted therapies have been studied for years, but with modest success so far. Many phase III trials have failed to extend the overall survival of GBM patients, probably

because of the significant heterogeneity within groups, the low numbers of enrolling patients, and suboptimal phase II-generated information [300]. New or optimized approaches are needed. Some repurposed drugs are being proposed for GBM treatment, such as the combination of tricyclic antidepressants and the anticoagulant ticlopidine, which could induce glioma cell lethal autophagy in a glioma mouse model [301]. Here, we have evaluated the repurposing of metformin for GBM treatment *in vitro* and *in vivo*.

1.3.3 Metformin

Metformin is an FDA-approved biguanide indicated for the treatment of type 2 diabetes mellitus. Diabetic patients show increased incidence of cancer, such as liver and colorectal [302]. In 2005, Evans and colleagues described a decreased risk of developing cancer in type 2 diabetic patients treated with metformin compared to other anti-diabetic medications [303], validated by Bowker and colleagues in a retrospective study [304]. Metformin is used for diabetes because of its reduction of glucose levels through the inhibition of gluconeogenesis. However, the effects of metformin as an anti-cancer drug have been studied over the past decade, and it involves more pathways than those described for diabetes [305]. It has been used as anti-cancer drug in two ways: as a prophylactic setting or as a curative approach.

Prophylactic use of metformin was proposed from the initial observations of this drug lowering the risk of developing cancer. Many studies have then investigated the capacity of metformin to prevent or slow down tumor growth. The main focus of such studies is to examine the effect of metformin in the progression of tumors that evolve from benign tumors, before malignant tumor formation [306]. These include a phase III trial showing that metformin reduced the formation of metachronous colorectal adenomas or polyps [307].

As a curative therapy, to treat already established tumors, metformin was studied first in diabetes-related tumors, such as in the liver and pancreas [308, 309]; research on the subject then rapidly expanded to other types of cancer. Positive results have been obtained from colorectal cancer as an adjuvant therapy, but no beneficial effect was observed in breast and urothelial cancers [310], or in a phase II trial for pancreatic cancer [311]. Metformin appears to affect cancers differently depending on the type, timing, and combination with other treatments.

In GBM, *in vitro* use of metformin has provided promising results, such as an increased response to TMZ treatment and overcoming TMZ resistance [312]; such a combination was well tolerated in a phase I study for newly diagnosed GBM [313]. It impacted on the proliferation, viability, and also the motility and invasion of glioma cells *in vitro* [314]. Metformin can also target the GSC population; *in vitro* evidence has shown a reduction in the stemness and aggressiveness of GSC after combining metformin and 2-deoxyglucose [315]. Preclinical models based on human subcutaneous xenografts in immunodeficient mice have shown a reduction in tumor volume following metformin treatment [316].

The low price and long history of metformin in the market are great advantages of this drug. Research has provided abundant information about its toxicity, pharmacodynamics, etc. It is also known to have a low toxicity profile, unless the patient is suffering from renal deficiency [317].

1.3.3.1 Mechanisms

Metformin impacts several signaling pathways that could impact cancer biology and its surrounding microenvironment, though some of these are still uncharacterized. Many mechanisms have been described, mainly through AMP-activated protein kinase

(AMPK) signaling, but AMPK-independent mechanisms and others have also been described [318]. Moreover, metformin reduces the levels of insulin in the blood, which is a growth factor that promotes the division of cancer cells through the PI3K/Akt pathway [319, 320]. Because metformin impacts cancer cell growth and oxygen consumption (providing a link to tumor hypoxia), I will focus mainly on two cellular effects of this drug: the inhibition of the mTOR, and the inhibition of the electron transport chain (ETC), outlined in Figure 1.3.3.

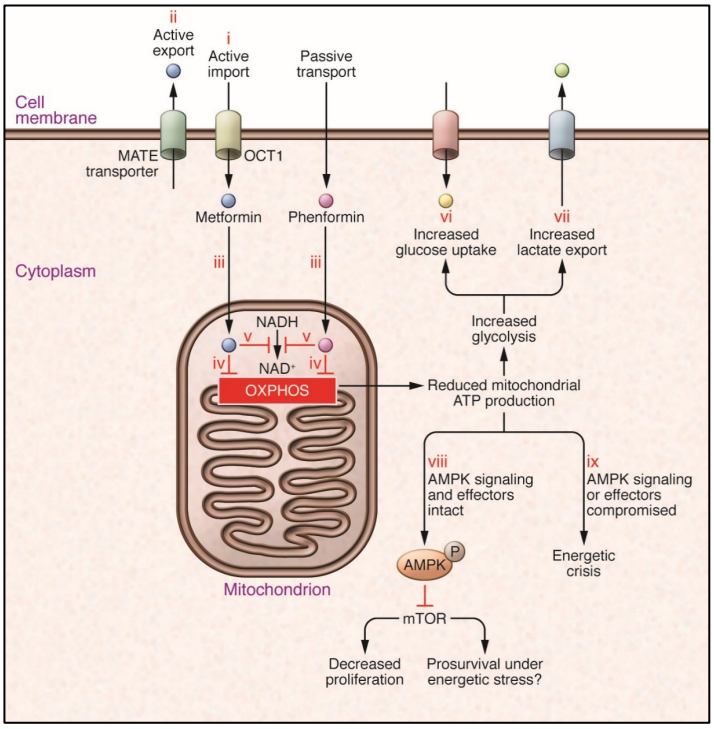

Figure 1.3.3 Schematic of the effect of metformin (and other biguanides) at the cellular level. (Taken from [321])

mTOR inhibition

Metformin inhibits mTOR, thus reducing protein translation initiation [322] and, consequently, cancer cell proliferation [323]. mTOR is also inhibited under hypoxic conditions, mainly through the activation of AMPK, or via an increase in REgulated in Development and DNA damage responses 1 (REDD1), also known as DNA-Damage-Inducible Transcript 4 (DDIT4) or RTP801 [324]. REDD1, a HIF-1α target gene,

activates the tuberous sclerosis 1 (TSC1)–TSC2 complex, resulting in the suppression of the mTOR complex [325, 326]. Therefore, both hypoxia and metformin inhibit mTOR. However, further inhibition of mTOR, for example, using rapamycin or metformin, on hypoxic cells reduces tumor growth *in vitro* and *in vivo* [327].

mTOR inhibitors in GBM have been tested. A phase II trial showed no survival benefit from adding everolimus to the standard of care [328], and a phase II trial testing temsirolimus combined with radiotherapy on GBM patients without MGMT promoter methylation showed no survival benefits compared to radio-chemotherapy [329]. However, GBM patients with phosphorylated mTOR at Ser2448 could benefit from this therapy, which suggests that $mTOR^{Ser2448}$ could be used as a biomarker for GBM patients that could benefit from mTOR inhibitor.

ETC inhibition

Metformin is also used as a means to reduce cellular oxygen consumption. Metformin can translocate into the mitochondria and inhibit the complex I of the electron transport chain [330]. Consequently, mitochondrial respiration is inhibited and ATP cannot be produced by oxidative phosphorylation, forcing the use of alternative metabolic pathways, mainly glycolysis. ETC inhibition reduces tumor growth both *in vitro* and *in vivo* [331].

As a consequence of ETC inhibition, less oxygen is consumed. Therefore, it is concluded that metformin can also affect hypoxia. Metformin decreases the stabilization of HIF under hypoxic conditions [331]. Indeed, some studies have demonstrated that metformin can improve reoxygenation of tumors *in vivo*, and thus influence a better response to radiotherapy, for example, in colorectal cancer [332]. Metformin also affects

the tumor vasculature, by targeting the HIF pathway, and VEGF secretion, affecting the angiogenesis response [333].

All of the *in vitro* studies and GBM xenograft *in vivo* data mentioned have shown promising results; however, whether metformin improves tumor vasculature and anti-tumor immunity has not been addressed in orthotopic immunocompetent mouse models.

1.3.3.2 Combinations

Throughout this chapter, it has been evident that many therapeutic approaches used as a monotherapy to treat GBM and/or to reduce hypoxia fail to control such an aggressive type of tumor. Instead, drug combinations are an alternative that allow several pathways to be targeted, reducing the concentration of each individual drug, overcoming resistance to one drug, and potentially providing synergistic effects [334]. Realistically, targeting hypoxic cancer cells or glioma stem-like cells with a single agent is unlikely to provide good clinical outcomes since these account for a small proportion of cells in the whole tumor mass. It is therefore important to find combination therapies that could target several cell populations from these heterogeneous tumors.

Understanding better how metformin affects glioma cell biology, as well as the impact on other cell types in the tumor microenvironment, could help to find a suitable drug combination to extend the OS or PFS of preclinical glioma models and, ultimately, GBM patients.

1.4 Aims of the study

Tumor hypoxia in the context of GBM exists and induces an immunosuppressive microenvironment and significant angiogenesis. GBM is highly heterogeneous, but common adaptations to hypoxia have been described. The aim of this study was to investigate how glioma cells adapt *in vitro* to low levels of oxygen. We sought to unravel common and unique mechanisms, which can be potentially targetable, while estimating both intratumoral and intertumoral heterogeneity, with the use of both glioma differentiated cells and glioma stem-like cells. To do so, we investigated the adaptations to hypoxia using a relevant physiologic control for oxygen availability in the brain. With the use of metformin, we intended to target some of the responses of glioma cells to low levels of oxygen *in vitro* and *in vivo.*

Precisely, we asked the following questions:

1. What mechanisms, common and unique, do glioma cells use to adapt to hypoxia?

   This point is addressed in results sections 2.1 and 2.2.

2. Does metformin affect glioma cells *in vitro,* and the glioma microenvironment *in vivo* (immune cells and vasculature) in a syngeneic GBM mouse model?

   This question is addressed in section 2.1 regarding some *in vitro* effects of metformin on glioma cells, and extensively in section 2.2 focusing on the *in vivo* effects of metformin in syngeneic GBM mouse models.

2 RESULTS

In order to address the first question of this study of how glioma cells respond to low oxygenation levels, we followed an unbiased approach. We cultured 5 glioma cells lines under different oxygen conditions: hypoxia (1% O_2), physioxia (5% O_2), and standard culture conditions (21% O_2), and we analyzed their transcriptional profiles. We compared hypoxia to the other two oxygen conditions, and we observed that most of the differentially expressed genes were unique to each cell lines. However, in both comparisons we could detect some common genes between all cell lines used:

- Identification of a common hypoxia signature in glioma cell lines using the physiological oxygen control; use of metformin to modulate this response (CHAPTER I)
    - We continued to address the questions of how glioma cells (both differentiated and stem-like cells) adapt to hypoxia, and how metformin impacts glioma cells *in vitro* and *in vivo*, and its tumor microenvironment in two glioma mouse models (CHAPTER II: sections 2.2.1-5)
- Identification of two hypoxia-regulated genes that were upregulated under hypoxia (*ATF3* and *ZFP36*) using the standard oxygen culture conditions (CHAPTER II: section 2.2.6)

2.1 CHAPTER I: An experimentally defined hypoxia gene signature and its modulation by metformin

This is a manuscript in preparation, from the following authors:

Calvo Tardón, Marta; Marinari, Eliana; Migliorini, Denis; Bes, Viviane; McKee, Thomas A.; Dutoit, Valérie; Dietrich, Pierre-Yves; Cosset, Erika; and Walker, Paul R.

Summary:

In this study, we addressed how glioma cells adapt to low oxygenation levels, i.e. hypoxia. GBM is a very aggressive tumor type, and is highly heterogeneous. Tumor hypoxia is an important feature found in most solid tumors, including GBM. We compared the transcriptional profiling of 5 human glioma cell lines exposed to hypoxia (1% O_2) and to physiologic oxygen conditions, physioxia (5% O_2). We focused on the adaptations that were common, despite the high degree of heterogeneity of GBM. We identified a hypoxia gene signature composed of 36 genes that was common between all cell lines tested. This signature correlated with hypoxic, glycolytic, and inflammatory responses. Importantly, high expression of the hypoxia signature was associated with poor prognosis of GBM patients. Using metformin, we modulated the expression of some genes from the hypoxia signature, partially reversing the hypoxia effect on glioma cells.

My contribution to this manuscript has been developing the project, performing all experiments, analyzing the *in vitro* assays, and writing the manuscript.

An experimentally defined hypoxia gene signature and its modulation by metformin

Calvo Tardón, Marta; Marinari, Eliana; Migliorini, Denis; Bes, Viviane; McKee, Thomas A.; Dutoit, Valérie; Dietrich, Pierre-Yves; Cosset, Erika; and Walker, Paul R.

Abstract

Glioblastoma multiforme (GBM) is the most common and aggressive primary brain tumor, characterized by a high degree of intertumoral heterogeneity. However, a common feature of the GBM microenvironment is hypoxia, which can promote radio- and chemotherapy resistance, immunosuppression, angiogenesis, and stemness. We experimentally defined common GBM adaptation mechanisms to hypoxia that occur under physiologically relevant oxygen gradients, and we assessed the impact of the metabolic drug metformin to modulate such mechanisms. We directly exposed human GBM cell lines to low oxygenation levels (hypoxia, 1% O_2) and to relevant physiological oxygen conditions (physioxia, 5% O_2), and performed transcriptional profiling, and compared findings to predicted hypoxic areas *in vivo* using *in silico* analyses. We observed a heterogenous response to hypoxia, but also a common gene signature of 36 genes that was modulated under hypoxia and that was induced by a physiologically relevant change in oxygenation from 5% O_2 to 1% O_2. *In silico* analyses showed that this hypoxia signature was highly correlated with perinecrotic localization in GBM tumors, inflammation, glycolysis, and poor prognosis of GBM patients. Metformin treatment of GBM cell lines under hypoxia and physioxia reduced cell viability, oxygen consumption rate, and partially reversed the hypoxia gene signature. We identified a common gene signature in GBM cell lines exposed to hypoxia and validated *in silico*. Metformin partially reversed GBM adaptation to hypoxia, supporting further exploration of this drug as a treatment component for hypoxic GBM.

Introduction

Glioblastoma multiforme (GBM), grade IV astrocytoma, is the most common and aggressive primary tumor in the central nervous system [1] and median survival of GBM patients is only 12-15 months [2], despite standard of care, consisting in surgical resection and radio- and chemotherapy. An important characteristic of these tumors is the high level of heterogeneity, both intertumoral [3, 4] and intratumoral [5, 6].

A common feature found in most solid tumors is the presence of hypoxia as a result of rapid cancer cell proliferation and aberrant vasculature that is unable to maintain oxygen supply [7]. Tumor hypoxia drives malignancy by promoting chemo- and radiotherapy resistance, an immunosuppressive microenvironment, cancer cell stemness, angiogenesis, and a glycolytic metabolic switch [8-10]. The study of tumor hypoxia *in vitro* frequently uses cell cultures exposed to atmospheric conditions (21% O_2) as a control, although this does not represent any physiological oxygen fraction found *in vivo* [11] and does not always recapitulate cellular functions under physioxia [12]. Physiologic oxygen availability is tissue-dependent, with 2-9% O_2 (10-40 mmHg) being reported for the healthy brain [13]. Oxygen fractions used to refer to tumor hypoxia vary between studies, but 0.5-2% O_2 (i.e., less than physiologic values, and thereby inadequate oxygenation) are observed *in vivo* in the tumor bed and are used experimentally *in vitro* [14, 15]. One of the key regulators of the hypoxia response is hypoxia-inducible factor 1α (HIF-1α) [16], but HIF-independent cellular pathways have also been reported [17, 18].

Aberrant signaling pathways such as mTOR, or pro-tumoral functions such as VEGF release have been individually targeted in GBM therapy, using rapamycin (or its derivatives) or bevacizumab, respectively, but with limited success on overall survival of

GBM patients so far [19, 20]. Metformin, a type 2 diabetes drug, has been shown to decrease risk of developing certain types of cancer [21], and can potentially both target mTOR signaling and reprogram oxygen metabolism, thereby reducing hypoxia in the tumor microenvironment. Metformin has been shown to improve the anti-tumor immune response in several tumor mouse models [22-24]. In the context of GBM, metformin can inhibit cell growth through mTOR inhibition, and has been observed to enhance the therapeutic effect of temozolomide in human xenografts [25].

In the treatment of GBM, a better understanding of its genetic, epigenetic, and/or transcriptional characteristics could help identify markers or signatures that predict outcome or response to specific therapies, as exemplified by MGMT promoter methylation status that predicts response to temozolomide [26]. More recently, gene mutations and expression profiles are being studied to associate specific gene signatures with clinical outcome [27, 28], including hypoxia-induced gene signatures in multiple cancer types [7, 29]. Here we evaluated the GBM response to low levels of oxygen and, despite GBM heterogeneity, we identified a common hypoxia gene signature that was determined experimentally and was associated with pseudopalisading and necrotic areas of GBM patients; the signature correlated with a glycolysis and inflammation gene clusters, and importantly, survival. We validated the use of metformin to modify the hypoxic response, to reduce tumor cell viability and oxygen consumption, due to a metabolic switch from oxidative phosphorylation towards glycolysis.

Material and methods

In vitro cultures

Human Ge904 (passage 11), Ge835 (p8), Ge898 (p10) were obtained in house from resection of primary GBM; LN18 (p560), LN229 (p209), U87 (px25), and U251

(p590) were obtained from ECACC or ATCC; mouse SB28 was kindly provided by H. Okada, UCSF, USA; and GL261-OVA was kindly provided by O. Grauer, University Hospital of Münster, UKM, Germany. All cell lines were cultured in serum-containing DMEM-based media, and passaged every 2-3 days. GBM cell lines were exposed to atmospheric O_2 conditions in a conventional hood and incubator, or to 1% O_2 or 5% O_2 using the Ruskinn 300 InVivO2 hypoxia workstation (Baker) for 48h. Media was pre-equilibrated to the desired oxygen level by flushing with the corresponding gas mix. All cell lines were tested as negative for mycoplasma.

Sequencing and polymerase chain reaction (PCR)

Total RNA was extracted using Qiagen RNeasy Kit following manufacturer's instructions. Gene expression was evaluated using Microarray PrimeView Human Gene Expression Array (Affymetrix).

qPCR of the hypoxia signature genes was performed to quantify mRNA levels of metformin or vehicle-treated cells exposed to hypoxia or physioxia. Briefly, DNase-treated RNA was used to synthesize cDNA (PrimerScript RT; Takara Bio Inc.) The following specificities and the corresponding primers were analyzed:

Gene ID	Forward primer	Reverse primer
ADM	TGCCCAGACCCTTATTCG	CCGGAGGCCCTGGAAGT
ALDOC	ATGCCTCACTCGTACCCAG	TTTCCACCCCAATTTGGCTCA
ANGPTL4	GGCTCAGTGGACTTCAACCG	CCGTGATGCTATGCACCTTCT
ANKRD37	TTAGGAGAAGCTCCACTACACAA	CACTGGCTACAAGCAGGCT
ARRDC3	TGTATTCTAGTGGGGATACCGTC	TCGCATGTCCTCTTGCATGAA
BHLHE40	ATCCAGCGGACTTTCGCTC	TAATTGCGCCGATCCTTTCTC
CA9	GGATCTACCTACTGTTGAGGCT	CATAGCGCCAATGACTCTGGT
DDIT4	TCCCTGGACAGCAGCAACA	AACGACACCCCATCCAGGTA
EGLN3	TCCTGCGGATATTTCCAGAGG	GGTTCCTACGATCTGACCAGAA
HAS2	CACTGGGACGAAGTGTGGATTA	GCATAGTGTCTGAATCACAAACCTG
HILPDA	GCGCTTTTGTCTCCGGGTC	GTAAGCCCTCTAGGGACTCCA
HK2	GAGCCACCACTCACCCTACT	CCAGGCATTCGGCAATGTG
PGK1	GAACAAGGTTAAAGCCGAGCC	GTGGCAGATTGACTCCTACCA
NDRG1	CTCCTGCAAGAGTTTGATGTCC	TCATGCCGATGTCATGGTAGG

PDK1	GGATTGCCCATATCACGTCTTT	TCCCGTAACCCTCTAGGGAATA
SLC2A3	TCCACGCTCATGACTGTTTC	GCCTGGTCCAATTTCAAAGA
STC1	AGGTGCAGGAAGAGTGCTACA	GACGACCTCAGTGATGGCTT
TMEM45A	GCATGGCTTTAACTGGCATGG	CAGCCCAGGAGTTGATTCCA
VEGFA	AGGGCAGAATCATCACGAAGT	AGGGTCTCGATTGGATGGCA

TP53 analysis

Ge898 and Ge904 cell lines *TP53* status were analyzed using Ion Ampliseq cancer hotspot panel v2 (ThermoFisher). The information regarding the *TP53* status of the others GBM cell lines was extracted from the literature for Ge835 [30], SB28 [31] and GL261 [32], or from available databases (p53.iarc.fr/CellLines.aspx; and ATCC).

Western blot

Fifteen µg of whole protein lysates (NP-40 based lysis buffer) or nuclear fractions (NE-PER™ Nuclear and Cytoplasmic Extraction Reagents, ThermoFisher) were loaded onto 12.5% SDS-PAGE gel and transferred onto nitrocellulose membranes. Membranes blocked with 5% non-fat dry milk were incubated with rabbit anti-HIF-1α (Bethyl), mouse anti-TBP (Novus Biologicals), followed by goat anti-rabbit IgG-HRP (Sigma) or goat anti-mouse IgG-HRP (Sigma). ECL detection (SuperSignal West Pico, ThermoFisher) was used to observe reactive bands.

In vitro assays

All assays were performed for 48h under the corresponding oxygenation conditions. Viability was assessed using CellTiter Glo (Promega), following manufacturer's protocol, with luminescence measured using a Cytation3 reader (BioTek). Oxygen consumption and extracellular acidification rates were measured using Cell Mito Stress kit in XF media containing 1 g/l glucose, 2 mM glutamine, and 1 mM sodium pyruvate measured in a Seahorse XFe96 Analyzer (Agilent) placed inside a hypoxia station.

Statistical analysis

The RMA normalized intensities from 3 independent biological replicates were analyzed for differential expression [33]. The following comparisons were done on each triplicate with a t-test and on all samples with a paired sample ANOVA (FC>1.3, $p<0.05$), using Partek® Genomics Suite® software, version 6.6.

In silico analysis included several datasets: TCGA (https://www.cancer.gov/tcga), Rembrandt [34], Phillips [3], Freije [35], IvyGAP [36], and were obtained using GlioVis data portal for visualization and analysis of brain tumor expression datasets [37]. Analysis was performed in R version 3.3.2 (https://www.R-project.org/) and figures were generated through Morpheus (https://software.broadinstitute.org/morpheus). Gene set enrichment analysis (GSEA) was performed as previously described [38].

Results

We exposed 5 human GBM lines to various oxygen conditions: inadequate oxygenation (hypoxia, 1% O_2), physiologic (physioxia, 5% O_2), and atmospheric (hyperoxia; 21% O_2) conditions, and performed transcriptional profiling using Affymetrix Microarray. Comparing 1% O_2 to 5% O_2 showed an enrichment in the hallmark hypoxia gene set after performing gene set enrichment analysis (GSEA) (**Fig 1a**). Our experimental approach consisted on directly modulating oxygenation levels reproducing *in vivo* attainable oxygen gradients. This allowed us to identify transcriptional changes reported in GSEA [38]. We confirmed hypoxia adaptation by quantifying nuclear stabilization of HIF-1α by western blot (**Supp. fig 1a**).

Comparing hypoxia (1% O_2) to hyperoxia (21% O_2), we identified 1040 common differentially expressed genes (ANOVA), whereas comparing hypoxia to physioxia (5% O_2) revealed only 36 differentially expressed genes. Twenty-five of these 36 genes (69%)

were common to the 21% to 1% O_2 comparison, but 11 genes were unique to the 5% to 1% O_2 comparison (Fig 1b). This suggests that using atmospheric conditions as a control not only leads to an overestimation of the adaptation of GBM cells to hypoxia, but might also obscure important biological processes taking place under physiologic conditions.

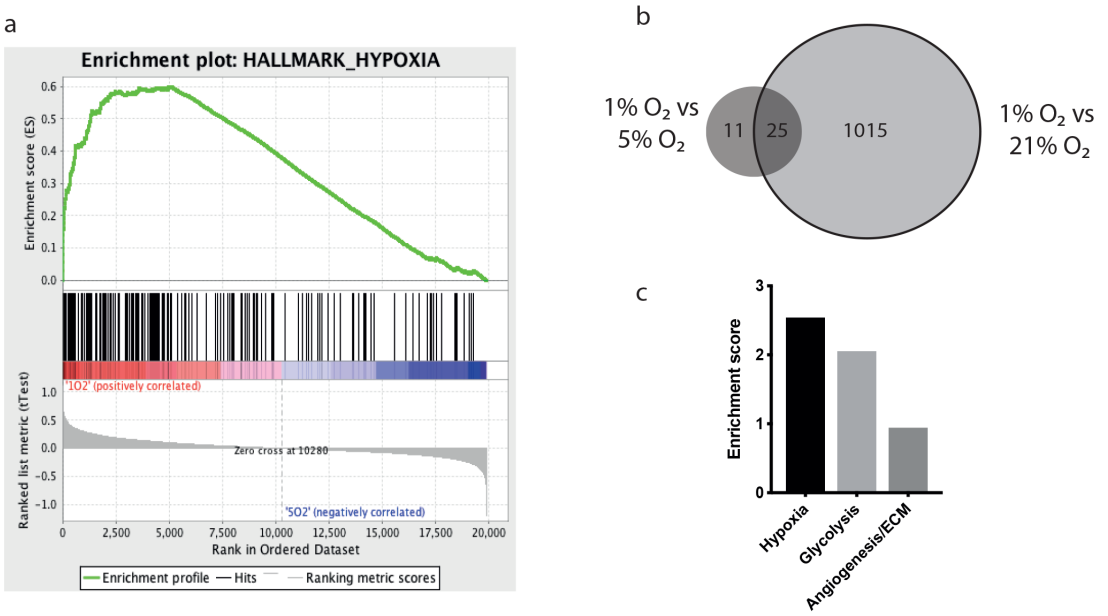

Fig. 1 Whole transcriptome analysis of five human GBM cell lines exposed to hypoxia, physioxia, or hyperoxia. (a) Gene set enrichment analysis for hypoxia geneset comparing transcriptional profiles of hypoxia versus physioxia. (b) Venn diagram of comparisons between hypoxia and physioxia, and hypoxia and hyperoxia. (c) Enrichment scores of gene families from DAVID analysis

Unsupervised clustering of the transcriptional data grouped the samples by cell line rather than by the effect of hypoxia, indicating a significant level of heterogeneity of GBM lines (Supp. fig 1b,c). Despite this high heterogeneity, we could build a hypoxia gene signature based on the 36 common differentially expressed genes between hypoxia and physioxia (Supp. fig 1d). Performing DAVID analysis [39], we determined that this experimentally defined signature was significantly enriched for hypoxia, glycolysis, and angiogenesis and extracellular matrix gene clusters (Fig. 1c). Of note, half of the genes in the signature (18/36 genes) are not reported to have a hypoxia-responsive element

(HRE) sequence [40, 41], and therefore may represent HIF-independent hypoxia-regulated responses (Supp. fig 1e).

Fig. 2 Expression and correlation of the hypoxia gene signature with Gliovis and Ivygap databases. (a) Expression of 33 genes from the 36-hypoxia gene signature in different areas of human GBM biopsies. (b,c) Correlation matrix of the hypoxia signature with (b) immune-associated genes or (c) three metabolic pathways gene lists

We validated the hypoxia signature with human GBM datasets originating from biopsies and microdissection, using the GlioVis and Ivy-GAP platforms [37, 36], on 33 genes from our signature, which excluded three non-coding genes (*C10orf10*, *C5orf46*, and *LOC154761*). The hypoxia signature was highly expressed within perinecrotic and pseudopalisading areas of tumors (hypoxic zones) confirming that our signature reflects

in vivo observed features (Fig. 2a). Our signature was strongly correlated with an inflammatory phenotype that included expression of genes encoding IL-1β, IL-6, and IL-8 (Fig 2b), and with the glycolytic pathway (Fig. 2c). High-grade glioma patients from Rembrandt, TCGA, Phillips, and Freije databases [35, 3, 34] were clustered according to signature expression, based on k-means cluster analysis (k=2). Importantly, high expression of our signature correlated with poor survival (Fig. 3).

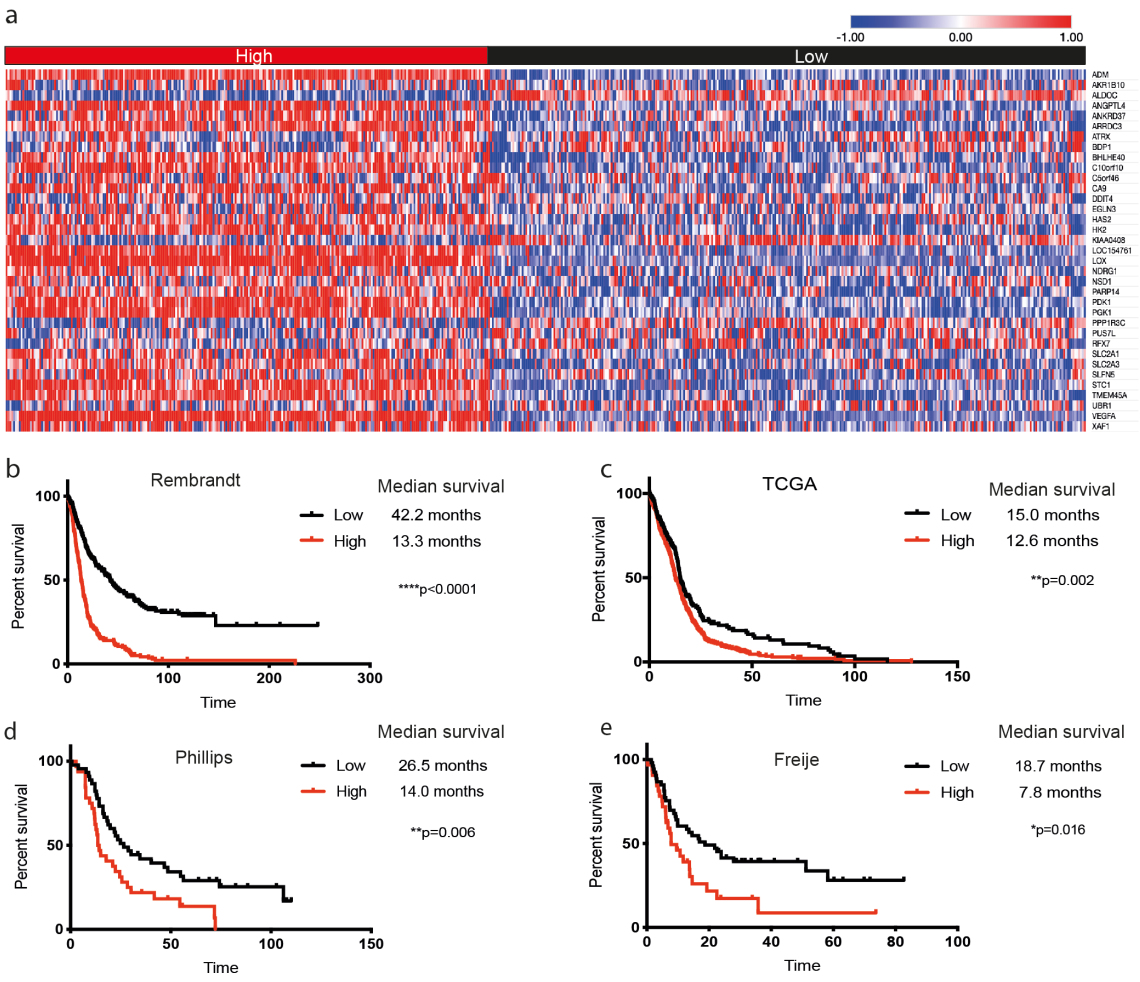

Fig. 3 Correlation of the hypoxia signature to survival of GBM patients. (a) Expression of the hypoxia gene signature (z-score) across patients from the Rembrandt database, segregated by high and low expression of the signature. (b-e) Kaplan-Meier survival curves corresponding to high (red) or low (black) expression of the hypoxia signature in (b) Rembrandt (n=580), (c) TCGA (n=538), (d) Phillips (n=100), and (e) Freije (n=85) databases

Tumor hypoxia could potentially be modulated by the metabolic drug metformin; we therefore investigated its effects on GBM cell viability and oxygen consumption rate, which were previously only described using non-physiologic oxygen conditions. In these *in vitro* assays, we used several human GBM cell lines, and two mouse glioma models. As expected, metformin reduced cell viability under hyperoxia (not shown), and we confirmed that this tendency was maintained under physioxia (Fig. 4a). Since mutational status can impact on metabolism [42], we assessed several mutations including *TP53*. We observed that those cell lines (U251, SB28, GL261 OVA, and LN18) that had a statistically significant reduction in viability in response to metformin ($p<0.001$) were all *TP53* mutant. Indeed, response to metformin was associated with the *TP53* mutation status (Fischer's exact test, $p<0.05$) (Fig 4b).

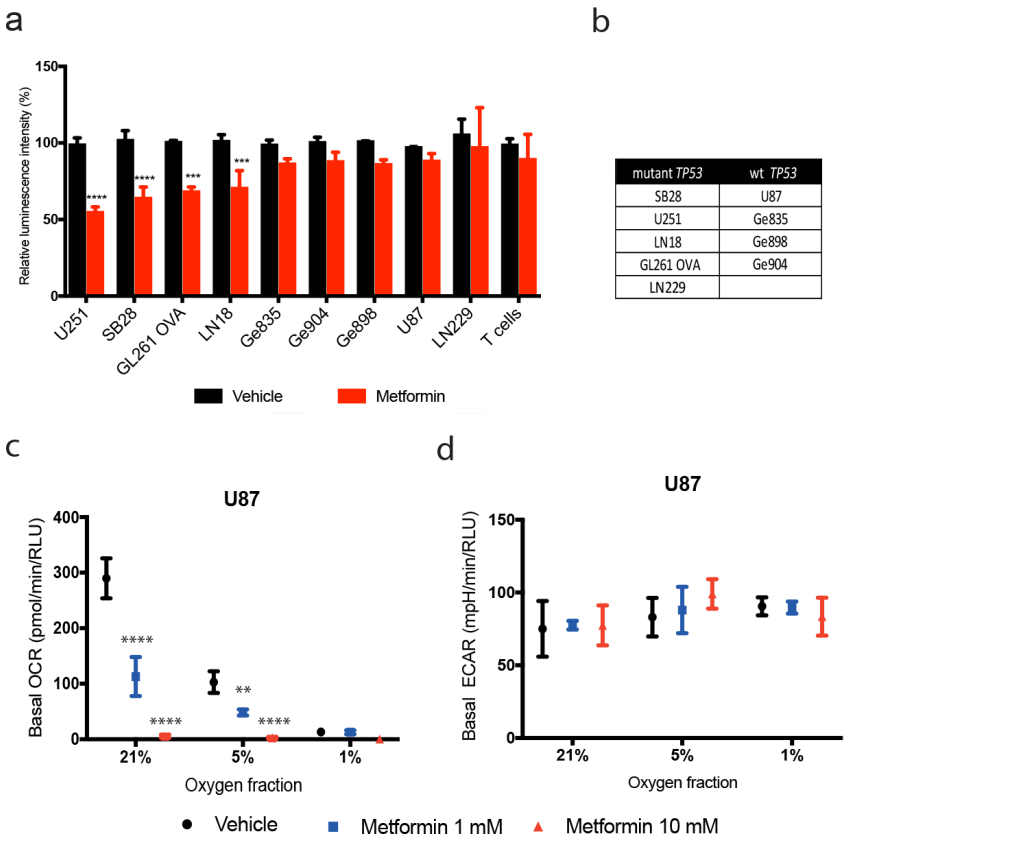

Fig. 4 Functional assays of GBM cell lines exposed to metformin. (a) Effect of metformin on cell viability under physioxia. (b) Table describing *TP53* mutation status of all GBM cell lines used; mutant or *wild type* (wt). (c) Basal OCR and (d) basal ECAR of U87 GBM cell line *in vitro* at 21%, 5%, and 1% O_2 (n=3; 2-way ANOVA, Sidak's adjusted p-value. ***p<0.001, ****p<0.0001)

We evaluated oxygen consumption rate (OCR) and extracellular acidification rate (ECAR) on metformin treated GBM cell lines under hypoxia, physioxia, or hyperoxia. We first validated the reduction on OCR induced by metformin at hyperoxic conditions (Fig 4c; Supp. fig 2a,b). Metformin reduced OCR under physioxia in human GBM cell lines *in vitro* (Fig. 4c; Supp. fig 2a,b). Under hypoxic conditions, the availability of oxygen was clearly a limiting factor in these measurements, indicated by the lower OCR (Fig. 4c). By inhibiting mitochondrial oxidative respiration, metformin potentiates the glycolytic pathway [43]. Consequently, there was a modest trend towards an increased ECAR, but only with high dose metformin in LN18, Ge904, U251, SB28, and GL261 OVA cell lines (Fig. 4d, Supp. fig 2c).

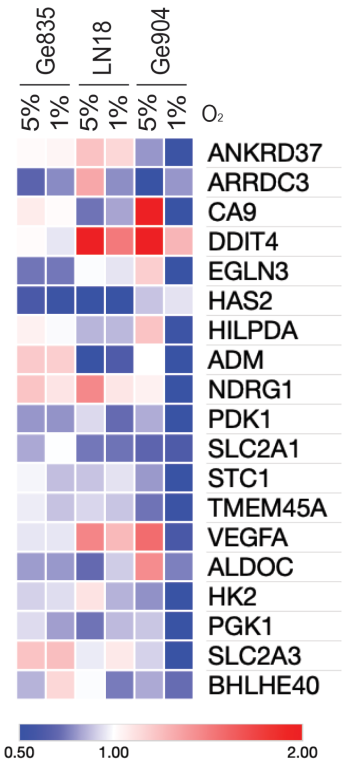

Fig. 5 Metformin modulation of the hypoxia gene signature. Represented fold-changes of expression between metformin-treated versus vehicle-treated cells (red, FC>2; blue, FC<0.5). mRNA expression measured by qPCR of upregulated genes from the hypoxia gene signature on Ge835, LN18, and Ge904 treated with metformin or vehicle and exposed to physioxia or hypoxia

A further consequence of metformin treatment was a downregulation of most genes of our hypoxia gene signature after exposure of different human GBM lines to hypoxia or physioxia, although there was a certain level of heterogeneity (Fig 5). This effect was more pronounced under hypoxia, compared to physioxia. Some genes, such as *DDIT4* and *VEGFA*, showed instead upregulation by metformin treatment, although this was mostly cell line-specific.

Discussion

Intertumoral heterogeneity of GBM is a known and expected feature. Here we provide detailed evidence of intertumoral heterogeneity at the transcriptional level by performing in vitro hypoxia studies using several human-derived cell lines, which allowed us to identify a robust common hypoxia signature, despite the heterogeneity. Importantly, we used 5% O_2 as physiological oxygen control, which more accurately represents the oxygenation levels within the brain and brain tumor tissues. This oxygen fraction has been proven to impact on cell viability, metabolism, and mitochondrial function [12]. Indeed, we have demonstrated that our gene signature correlated with in vivo generated data, supporting the use of physioxia as a biologically relevant oxygen condition.

The experimentally identified hypoxia signature was found in predicted hypoxic regions from human biopsies documented in databases. High expression of the signature was correlated with a pro-inflammatory profile, the glycolytic pathway; and was enriched for gene clusters of hypoxia, glycolysis, and angiogenesis, consistent with previous studies showing angiogenic and immunologic responses to hypoxia in GBM patients [44]. Furthermore, expression of the signature was highly correlated with poor survival in GBM patients, confirming the importance and robustness of this signature.

In our study, we directly modulated oxygen availability in our cell cultures, rather than directly modulating the transcription factor HIF-1α. This allowed us to study all potential adaptations of GBM cells to a lack of physiologic oxygenation, without limiting our findings to one transcription factor. Indeed, half of the genes in our signature are not reported to be HIF-dependent [40, 41]. Several HIF-independent mechanisms have been described, such as the mTOR inactivation [17], or the activation of NF-kB through ROS production [45].

Metformin is a well characterized inhibitor of gluconeogenesis, but in the past decade, there has been accumulating evidence of its anti-cancer effects [46], mainly through the reduction of cancer cell growth, consistent with our in vitro results showing a reduced viability of GBM cells after treatment. Metformin is currently in clinical trial for many cancer types (330 registered in clinicaltrials.gov), including GBM. A retrospective study of high-grade glioma patients taking metformin medication (mainly because of previous diabetes diagnosis) indicated improved outcome of anaplastic astrocytomas (grade III gliomas), but not GBM [47]. Nevertheless, studies in xenografted mice suggested that when metformin is used at doses higher than those used for diabetes, there is a survival benefit, together with sensitization to concomitant radio-chemotherapy [25].

Metformin reduces oxygen consumption rate by inhibiting complex I of the electron transport chain in the mitochondria, as we have validated under hyperoxic conditions, and reported for the first time under physiologically relevant oxygenation. The OCR reduction induces the use of the glycolytic pathway instead of oxidative phosphorylation, and therefore reduces the overall oxygen consumption. As less oxygen is being consumed, more oxygen could be available in the tumor microenvironment and in the cell cytoplasm, thus reducing tumor hypoxia and hypoxia-associated responses. We

observed an effect on OCR at 5% O_2 but not at 1% O_2, probably because under hypoxia the OCR is already very low. Extrapolating to in vivo use of the compound, this could potentially limit expansion of hypoxic regions, encouraging the use of metformin at early stages where hypoxic regions are less extensive. A downside of an increased glycolytic rate is the consequent increase in lactate production, increasing the risk of acidosis. In our in vitro settings, metformin maintained the same ECAR, except at high concentration, in accordance with other studies reporting modest acidification [48].

One disadvantage of using metformin is that it affects many cellular pathways, some of them still unknown or uncharacterized [49]. Nevertheless, decades of clinical usage confirm its low toxicity, which we can now extend to T cells that we tested, suggesting compatibility with future immunotherapies.

We could segregate all GBM cell lines tested into two groups depending on the presence or absence of response to metformin, which correlated with the TP53 mutation status, mutated or wt, respectively. Indeed, *TP53* can affect the glycolytic pathway [50]. Since metformin forces cancer cells to use glycolysis as a main metabolic source of ATP production, cells with mutated or loss of *TP53* cannot adapt to this rapid glycolytic switch and are selectively inhibited or killed by metformin.

Using a gene signature instead of analyzing individual genes allowed us to identify a robust adaptation of GBM cells to hypoxia. This hypoxia gene signature, which strongly correlated with poor survival, could potentially identify patients most likely to benefit from metformin treatment if this compound could achieve similar reversal of the signature in vivo as we observed in vitro with GBM cell lines. Nevertheless, some of the changes we noted for expression of individual genes were not following the general trend of downregulation after metformin treatment, as for example, *DDIT4* and *VEGFA*.

DDIT4, which is involved in cellular stress response, has been reported to be upregulated in the presence of metformin [51], in accordance with our results. *VEGFA* was upregulated in some of the cell lines, although this was not uniform for the three GBM lines tested, nor for all oxygen conditions. Indeed, metformin is proposed to globally inhibit angiogenesis, despite a transient stimulation of pro-angiogenic factors [52]. Even with extensive testing of metformin in our experiments using different cell lines and multiple oxygen conditions, it is possible that different time-points, or analysis of protein in addition to mRNA would have given different results. Ultimately, only assessing the impact of metformin in vivo will resolve these issues.

Taken together, our direct manipulation of oxygenation in vitro, including use of physioxia, has revealed a hypoxia gene signature that recapitulates human GBM observations in vivo (hypoxic localization, and inflammatory and glycolytic responses). Moreover, this hypoxia signature is correlated with shorter survival of GBM patients. Using metformin, we reduced GBM cell growth and oxygen consumption, as well as expression of key genes of the hypoxia gene signature, supporting further investigation of this drug in the context of GBM therapy.

Supplementary figures:

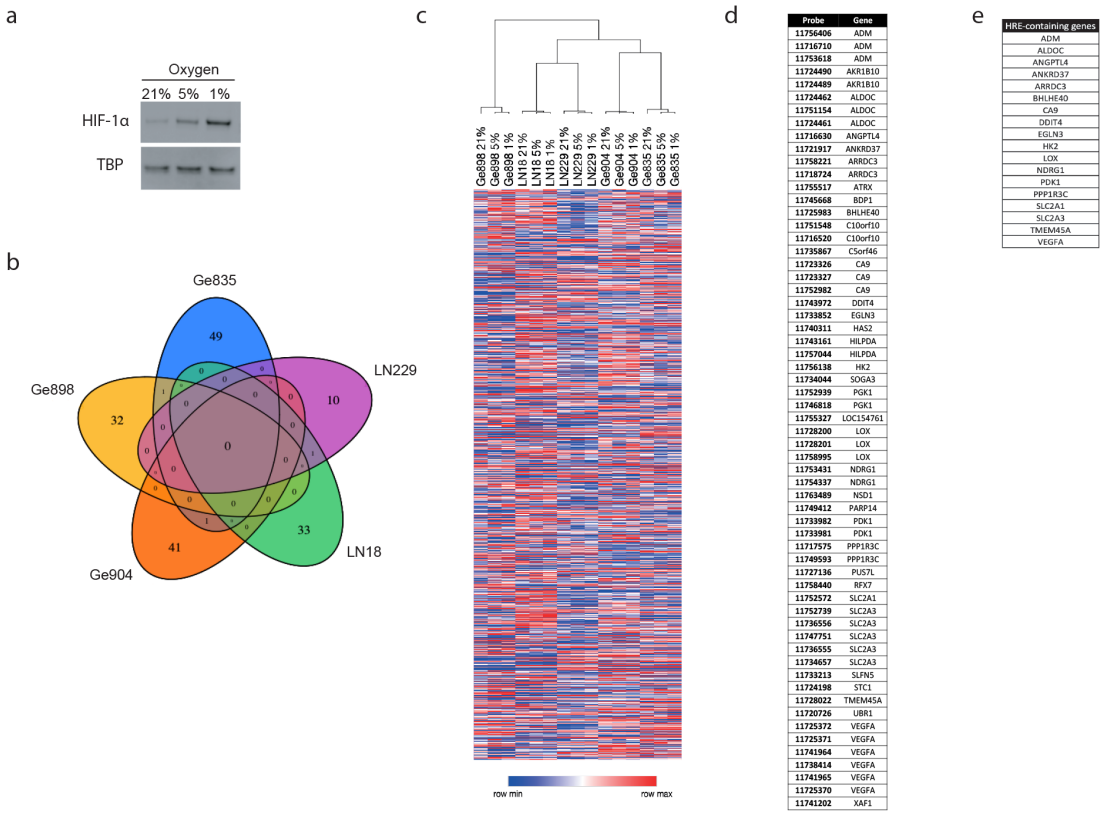

Probe	Gene
11756406	ADM
11716710	ADM
11753618	ADM
11724490	AKR1B10
11724489	AKR1B10
11724462	ALDOC
11751154	ALDOC
11724461	ALDOC
11716630	ANGPTL4
11721917	ANKRD37
11758221	ARRDC3
11718724	ARRDC3
11755517	ATRX
11745668	BDP1
11725983	BHLHE40
11751548	C10orf10
11716520	C10orf10
11735867	C5orf46
11723326	CA9
11723327	CA9
11752982	CA9
11743972	DDIT4
11733852	EGLN3
11740311	HAS2
11743161	HILPDA
11757044	HILPDA
11756138	HK2
11734044	SOGA3
11752939	PGK1
11746818	PGK1
11755327	LOC154761
11728200	LOX
11728201	LOX
11758995	LOX
11753431	NDRG1
11754337	NDRG1
11763489	NSD1
11749412	PARP14
11733982	PDK1
11733981	PDK1
11717575	PPP1R3C
11749593	PPP1R3C
11727136	PUS7L
11758440	RFX7
11752572	SLC2A1
11752739	SLC2A3
11736556	SLC2A3
11747751	SLC2A3
11736555	SLC2A3
11734657	SLC2A3
11733213	SLFN5
11724198	STC1
11728022	TMEM45A
11720726	UBR1
11725372	VEGFA
11725371	VEGFA
11741964	VEGFA
11738414	VEGFA
11741965	VEGFA
11725370	VEGFA
11741202	XAF1

HRE-containing genes
ADM
ALDOC
ANGPTL4
ANKRD37
ARRDC3
BHLHE40
CA9
DDIT4
EGLN3
HK2
LOX
NDRG1
PDK1
PPP1R3C
SLC2A1
SLC2A3
TMEM45A
VEGFA

Supp. fig 1 Whole transcriptome analysis from human GBM cell lines exposed to different oxygen conditions. (a) Representative example of western blot of nuclear stabilization of HIF-1α and loading control TATA-binding protein (TBP) of human GBM cell line Ge835 at 21%, 5%, and 1% O_2. (b) Venn diagram of unique genes modulated under hypoxia compared to physioxia for each individual cell line. (c) Unsupervised clustering of all samples (five cell lines exposed to three oxygen conditions; mean of three biological replicates). (d) Affymetrix microarray probe and gene ID of the 36 genes of the hypoxia gene signature. (e) List of reported HRE-containing genes from our hypoxia signature

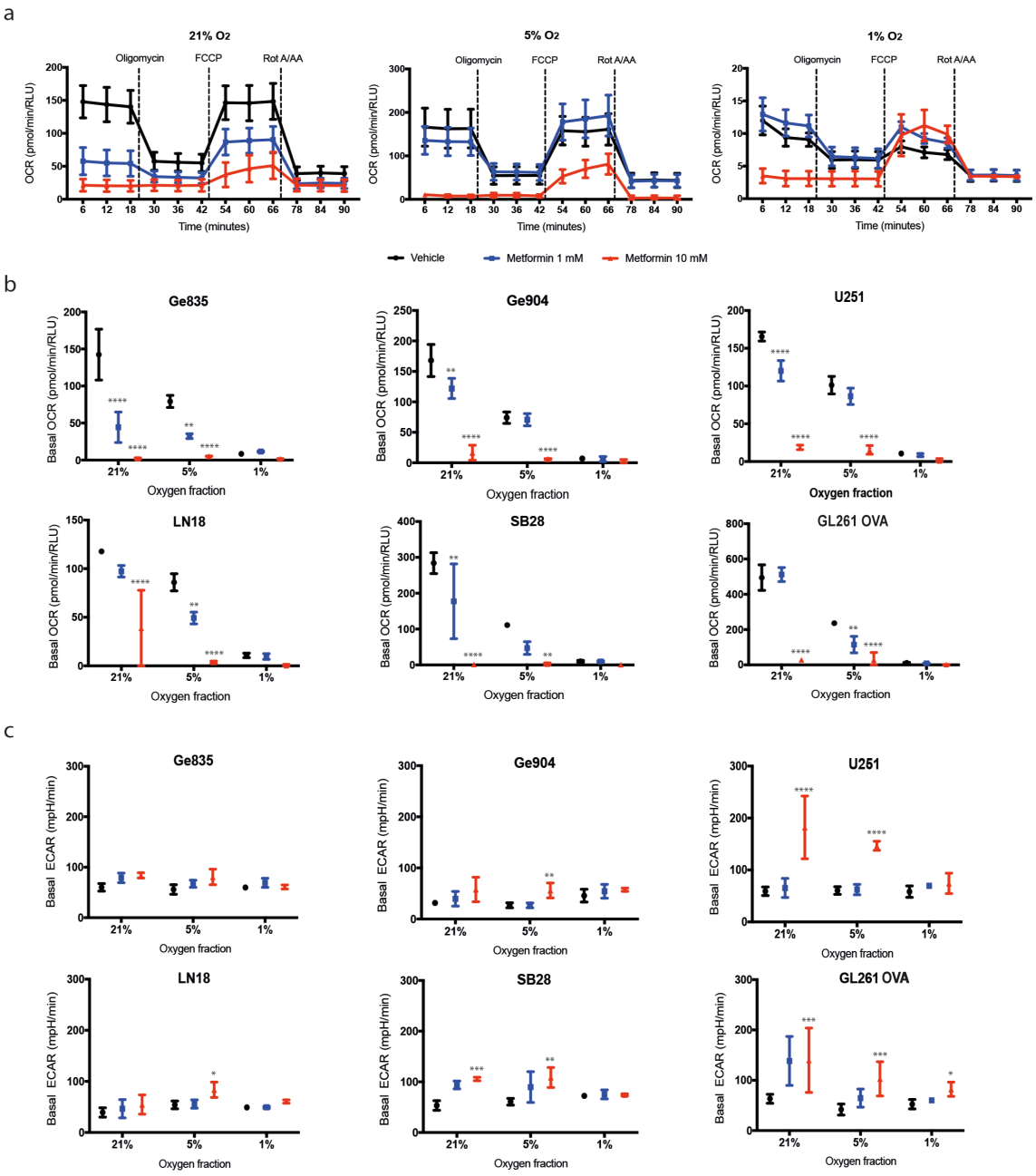

Supp. fig 2 Effect of differential oxygen availability and metformin on oxygen consumption rate (OCR) and extracellular acidification rate (ECAR) on human and mouse GBM cell lines. (a) Detailed Seahorse XF Cell Mito Stress test profiles on OCR data of Ge835 GBM cell line at 21%, 5%, and 1% O_2 following exposure to vehicle or different concentrations of metformin. (b) Basal OCR and (c) basal ECAR of all cell lines tested (n=3, 2-way ANOVA)

REFERENCES

1. Wen, P.Y. and S. Kesari, (2008) Malignant gliomas in adults. N Engl J Med 359(5):492-507.

2. Stupp, R., W.P. Mason, M.J. van den Bent, M. Weller, B. Fisher, M.J. Taphoorn, et al., (2005) Radiotherapy plus concomitant and adjuvant temozolomide for glioblastoma. N Engl J Med 352(10):987-96.

3. Phillips, H.S., S. Kharbanda, R. Chen, W.F. Forrest, R.H. Soriano, T.D. Wu, et al., (2006) Molecular subclasses of high-grade glioma predict prognosis, delineate a pattern of disease progression, and resemble stages in neurogenesis. Cancer Cell 9(3):157-73.

4. Verhaak, R.G., K.A. Hoadley, E. Purdom, V. Wang, Y. Qi, M.D. Wilkerson, et al., (2010) Integrated genomic analysis identifies clinically relevant subtypes of glioblastoma characterized by abnormalities in PDGFRA, IDH1, EGFR, and NF1. Cancer Cell 17(1):98-110.

5. Patel, A.P., I. Tirosh, J.J. Trombetta, A.K. Shalek, S.M. Gillespie, H. Wakimoto, et al., (2014) Single-cell RNA-seq highlights intratumoral heterogeneity in primary glioblastoma. Science 344(6190):1396-401.

6. Sottoriva, A., I. Spiteri, S.G. Piccirillo, A. Touloumis, V.P. Collins, J.C. Marioni, et al., (2013) Intratumor heterogeneity in human glioblastoma reflects cancer evolutionary dynamics. Proc Natl Acad Sci U S A 110(10):4009-14.

7. Bhandari, V., C. Hoey, L.Y. Liu, E. Lalonde, J. Ray, J. Livingstone, et al., (2019) Molecular landmarks of tumor hypoxia across cancer types. Nat Genet 51(2):308-318.

8. Tredan, O., C.M. Galmarini, K. Patel, and I.F. Tannock, (2007) Drug resistance and the solid tumor microenvironment. J Natl Cancer Inst 99(19):1441-54.

9. Vaupel, P., (2008) Hypoxia and aggressive tumor phenotype: implications for therapy and prognosis. Oncologist 13 Suppl 3:21-6.

10. Wei, J., A. Wu, L.Y. Kong, Y. Wang, G. Fuller, I. Fokt, et al., (2011) Hypoxia potentiates glioma-mediated immunosuppression. PLoS One 6(1):e16195.

11. Keeley, T.P. and G.E. Mann, (2019) Defining Physiological Normoxia for Improved Translation of Cell Physiology to Animal Models and Humans. Physiol Rev 99(1):161-234.

12. Timpano, S., B.D. Guild, E.J. Specker, G. Melanson, P.J. Medeiros, S.L.J. Sproul, et al., (2019) Physioxic human cell culture improves viability, metabolism, and mitochondrial morphology while reducing DNA damage. FASEB J:fj201802279R.

13. Erecinska, M. and I.A. Silver, (2001) Tissue oxygen tension and brain sensitivity to hypoxia. Respir Physiol 128(3):263-76.

14. Vaupel, P., M. Hockel, and A. Mayer, (2007) Detection and characterization of tumor hypoxia using pO2 histography. Antioxid Redox Signal 9(8):1221-35.

15. Vuillefroy de Silly, R., L. Ducimetiere, C. Yacoub Maroun, P.Y. Dietrich, M. Derouazi, and P.R. Walker, (2015) Phenotypic switch of CD8(+) T cells reactivated under

hypoxia toward IL-10 secreting, poorly proliferative effector cells. Eur J Immunol 45(8):2263-75.

16. Iyer, N.V., L.E. Kotch, F. Agani, S.W. Leung, E. Laughner, R.H. Wenger, et al., (1998) Cellular and developmental control of O2 homeostasis by hypoxia-inducible factor 1 alpha. Genes Dev 12(2):149-62.

17. Arsham, A.M., J.J. Howell, and M.C. Simon, (2003) A novel hypoxia-inducible factor-independent hypoxic response regulating mammalian target of rapamycin and its targets. J Biol Chem 278(32):29655-60.

18. Park, E.C., P. Ghose, Z. Shao, Q. Ye, L. Kang, X.Z. Xu, et al., (2012) Hypoxia regulates glutamate receptor trafficking through an HIF-independent mechanism. EMBO J 31(6):1379-93.

19. Akhavan, D., T.F. Cloughesy, and P.S. Mischel, (2010) mTOR signaling in glioblastoma: lessons learned from bench to bedside. Neuro Oncol 12(8):882-9.

20. Wick, W., T. Gorlia, M. Bendszus, M. Taphoorn, F. Sahm, I. Harting, et al., (2017) Lomustine and Bevacizumab in Progressive Glioblastoma. N Engl J Med 377(20):1954-1963.

21. Bowker, S.L., S.R. Majumdar, P. Veugelers, and J.A. Johnson, (2006) Increased cancer-related mortality for patients with type 2 diabetes who use sulfonylureas or insulin: Response to Farooki and Schneider. Diabetes Care 29(8):1990-1.

22. Ding, L., G. Liang, Z. Yao, J. Zhang, R. Liu, H. Chen, et al., (2015) Metformin prevents cancer metastasis by inhibiting M2-like polarization of tumor associated macrophages. Oncotarget 6(34):36441-55.

23. Eikawa, S., M. Nishida, S. Mizukami, C. Yamazaki, E. Nakayama, and H. Udono, (2015) Immune-mediated antitumor effect by type 2 diabetes drug, metformin. Proc Natl Acad Sci U S A 112(6):1809-14.

24. Scharping, N.E., A.V. Menk, R.D. Whetstone, X. Zeng, and G.M. Delgoffe, (2017) Efficacy of PD-1 Blockade Is Potentiated by Metformin-Induced Reduction of Tumor Hypoxia. Cancer Immunol Res 5(1):9-16.

25. Sesen, J., P. Dahan, S.J. Scotland, E. Saland, V.T. Dang, A. Lemarie, et al., (2015) Metformin inhibits growth of human glioblastoma cells and enhances therapeutic response. PLoS One 10(4):e0123721.

26. Hegi, M.E., A.C. Diserens, T. Gorlia, M.F. Hamou, N. de Tribolet, M. Weller, et al., (2005) MGMT gene silencing and benefit from temozolomide in glioblastoma. N Engl J Med 352(10):997-1003.

27. Ceccarelli, M., F.P. Barthel, T.M. Malta, T.S. Sabedot, S.R. Salama, B.A. Murray, et al., (2016) Molecular Profiling Reveals Biologically Discrete Subsets and Pathways of Progression in Diffuse Glioma. Cell 164(3):550-63.

28. Gravendeel, L.A., M.C. Kouwenhoven, O. Gevaert, J.J. de Rooi, A.P. Stubbs, J.E. Duijm, et al., (2009) Intrinsic gene expression profiles of gliomas are a better predictor of survival than histology. Cancer Res 69(23):9065-72.

29. Chang, W.H., D. Forde, and A.G. Lai, (2019) A novel signature derived from immunoregulatory and hypoxia genes predicts prognosis in liver and five other cancers. J Transl Med 17(1):14.

30. Cosset, E., S. Ilmjarv, V. Dutoit, K. Elliott, T. von Schalscha, M.F. Camargo, et al., (2017) Glut3 Addiction Is a Druggable Vulnerability for a Molecularly Defined Subpopulation of Glioblastoma. Cancer Cell 32(6):856-868 e5.

31. Kosaka, A., T. Ohkuri, and H. Okada, (2014) Combination of an agonistic anti-CD40 monoclonal antibody and the COX-2 inhibitor celecoxib induces anti-glioma effects by promotion of type-1 immunity in myeloid cells and T-cells. Cancer Immunol Immunother 63(8):847-57.

32. Szatmari, T., K. Lumniczky, S. Desaknai, S. Trajcevski, E.J. Hidvegi, H. Hamada, et al., (2006) Detailed characterization of the mouse glioma 261 tumor model for experimental glioblastoma therapy. Cancer Sci 97(6):546-53.

33. Irizarry, R.A., B.M. Bolstad, F. Collin, L.M. Cope, B. Hobbs, and T.P. Speed, (2003) Summaries of Affymetrix GeneChip probe level data. Nucleic Acids Res 31(4):e15.

34. Scarpace, L., A.E. Flanders, R. Jain, T. Mikkelsen, and D.W. Andrews, (2015) "Data from REMBRANDT". The Cancer Imaging Archive.

35. Freije, W.A., F.E. Castro-Vargas, Z. Fang, S. Horvath, T. Cloughesy, L.M. Liau, et al., (2004) Gene expression profiling of gliomas strongly predicts survival. Cancer Res 64(18):6503-10.

36. Puchalski, R.B., N. Shah, J. Miller, R. Dalley, S.R. Nomura, J.G. Yoon, et al., (2018) An anatomic transcriptional atlas of human glioblastoma. Science 360(6389):660-663.

37. Bowman, R.L., Q. Wang, A. Carro, R.G. Verhaak, and M. Squatrito, (2017) GlioVis data portal for visualization and analysis of brain tumor expression datasets. Neuro Oncol 19(1):139-141.

38. Subramanian, A., P. Tamayo, V.K. Mootha, S. Mukherjee, B.L. Ebert, M.A. Gillette, et al., (2005) Gene set enrichment analysis: a knowledge-based approach for interpreting genome-wide expression profiles. Proc Natl Acad Sci U S A 102(43):15545-50.

39. Huang da, W., B.T. Sherman, and R.A. Lempicki, (2009) Systematic and integrative analysis of large gene lists using DAVID bioinformatics resources. Nat Protoc 4(1):44-57.

40. Manalo, D.J., A. Rowan, T. Lavoie, L. Natarajan, B.D. Kelly, S.Q. Ye, et al., (2005) Transcriptional regulation of vascular endothelial cell responses to hypoxia by HIF-1. Blood 105(2):659-69.

41. Schodel, J., S. Oikonomopoulos, J. Ragoussis, C.W. Pugh, P.J. Ratcliffe, and D.R. Mole, (2011) High-resolution genome-wide mapping of HIF-binding sites by ChIP-seq. Blood 117(23):e207-17.

42. DeBerardinis, R.J. and N.S. Chandel, (2016) Fundamentals of cancer metabolism. Sci Adv 2(5):e1600200.

43. Andrzejewski, S., S.P. Gravel, M. Pollak, and J. St-Pierre, (2014) Metformin directly acts on mitochondria to alter cellular bioenergetics. Cancer Metab 2:12.

44. Murat, A., E. Migliavacca, S.F. Hussain, A.B. Heimberger, I. Desbaillets, M.F. Hamou, et al., (2009) Modulation of angiogenic and inflammatory response in glioblastoma by hypoxia. PLoS One 4(6):e5947.

45. Lluis, J.M., F. Buricchi, P. Chiarugi, A. Morales, and J.C. Fernandez-Checa, (2007) Dual role of mitochondrial reactive oxygen species in hypoxia signaling: activation of nuclear factor-{kappa}B via c-SRC and oxidant-dependent cell death. Cancer Res 67(15):7368-77.

46. Kasznicki, J., A. Sliwinska, and J. Drzewoski, (2014) Metformin in cancer prevention and therapy. Ann Transl Med 2(6):57.

47. Seliger, C., C. Luber, M. Gerken, J. Schaertl, M. Proescholdt, M.J. Riemenschneider, et al., (2019) Use of metformin and survival of patients with high-grade glioma. Int J Cancer 144(2):273-280.

48. Lalau, J.D. and J.M. Race, (2001) Lactic acidosis in metformin therapy: searching for a link with metformin in reports of 'metformin-associated lactic acidosis'. Diabetes Obes Metab 3(3):195-201.

49. Kheirandish, M., H. Mahboobi, M. Yazdanparast, W. Kamal, and M.A. Kamal, (2018) Anti-cancer Effects of Metformin: Recent Evidences for its Role in Prevention and Treatment of Cancer. Curr Drug Metab 19(9):793-797.

50. Liu, J., C. Zhang, W. Hu, and Z. Feng, (2015) Tumor suppressor p53 and its mutants in cancer metabolism. Cancer Lett 356(2 Pt A):197-203.

51. Ben Sahra, I., C. Regazzetti, G. Robert, K. Laurent, Y. Le Marchand-Brustel, P. Auberger, et al., (2011) Metformin, independent of AMPK, induces mTOR inhibition and cell-cycle arrest through REDD1. Cancer Res 71(13):4366-72.

52. Dallaglio, K., A. Bruno, A.R. Cantelmo, A.I. Esposito, L. Ruggiero, S. Orecchioni, et al., (2014) Paradoxic effects of metformin on endothelial cells and angiogenesis. Carcinogenesis 35(5):1055-66.

2.2 CHAPTER II: Additional experiments

2.2.1 Characterization of glioma stem-like cells

During this project, many of the questions were addressed on matched glioma differentiated (GDC) and glioma stem-like cells (GSC). For that purpose, we first characterized several GDC-GSC pairs originating from human GBM. In some cases, GSC were directly derived from the patients' tissue, but in other cases GSC were derived from GDC in culture.

In order to characterize the GSC population we performed a series of experiments to prove their stemness properties, that is, growth as neurospheres, differentiation and pluripotency capacities, expression of stemness markers, and clonogenicity. The following human cell lines were tested: Ge688, Ge738, Ge835, Ge869, Ge885, Ge898, Ge904, LN18, LN229, U251, and U87.

To make glioma cells grow as neurospheres we modified the composition of the media. Serum-containing media induces a differentiated phenotype supporting adherent form of growth, whereas a serum-free with additional growth factors can sustain a stem-like phenotype with growth as spheres (Fig 2.2.1.1A). Following retinoic acid and serum exposure, GSC can differentiate into GDC, changing their form of growth from neurospheres to adherent cells. Not all cell lines were able to satisfy these two criteria, and were either not able to directly grow as neurospheres or not able to differentiate into adherent cells.

We quantified the expression at the mRNA level of multiple known stemness and differentiation markers on matched GDC and GSC using Nanostring. We could again detect heterogeneity between cell lines, but overall, the GSC population expressed more

stemness markers (red), whereas the GDC population expressed more differentiation markers (blue) (Fig 2.2.1.1B).

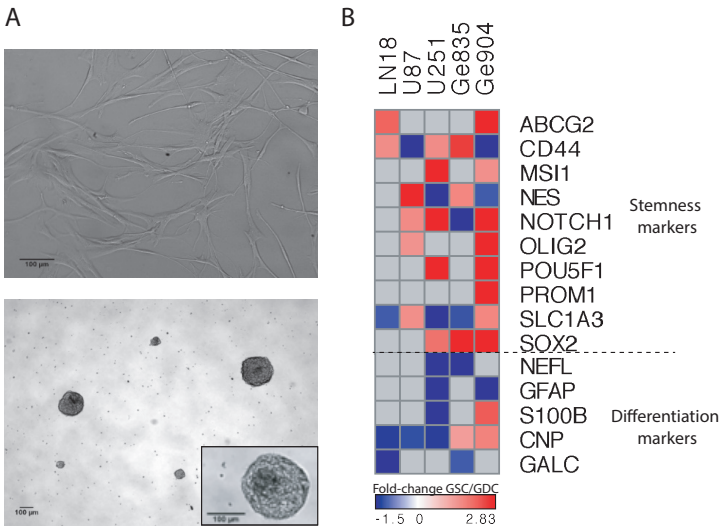

Figure 2.2.1.1. Glioma stem-like cells and glioma differentiated cells characterization. (A) Images of adherent Ge904 GDC (upper panel) and neurospheres Ge904 GSC (lower panel); scale bar set at 100 µm. (B) Heatmap of mRNA expression of stemness and differentiation markers quantified by Nanostring. Represented fold-change between the GSC over GDC of each cell line tested (calculated from the mean of 3 biological replicates).

From all the initial cell lines considered, only five fulfilled all the criteria. These five GDC-GSC pairs were HLA-typed and we confirmed same origin (data not shown). For the consequent hypoxia-related questions, we used these five matched human cell lines. All cell lines were tested for mycoplasma by PCR and were negative.

2.2.2 Analysis of differentially expressed genes under hypoxia

We performed whole transcriptomic analysis on 5 human cell lines by microarray and on 1 mouse glioma cell line by RNA-seq, and we selected genes that were modulated under hypoxia compared to physioxia that were either common or unique to specific cell lines. We did not consider those genes modulated under atmospheric conditions. We then chose those with higher modulation and/or those genes that could have a potential link to immunity, and we validated their differential expression in a more quantitative manner.

We quantified mRNA levels of 30 genes using Nanostring on the five matched GDC-GSC of 5 human cell lines: Ge835, Ge904, LN18, U251, and U87, which were exposed to hypoxia or physioxia for 48h (Fig 2.2.2.1).

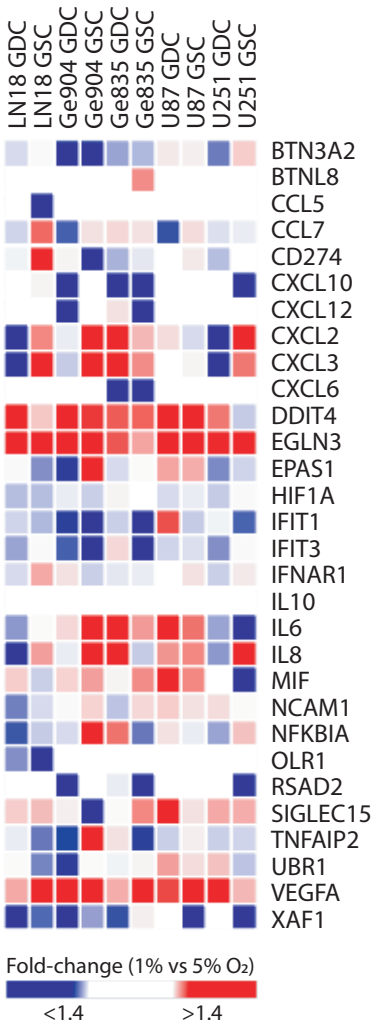

Figure 2.2.2.1. Heatmap from quantified mRNA levels of 5 human paired GDC-GSC cell lines using Nanostring. Each column represents the indicated cell line and each row is a different gene from the 30-gene selected list. Color code refers to the calculated fold-change between hypoxia (1% O_2) and physioxia (5% O_2), downregulation in blue and upregulation in red. (Fold-change calculated from the mean of 3 biological replicates).

We then sought to investigate multiple differentially expressed genes at the protein level of those genes that maintained a strong modulation under hypoxia at the mRNA level. We measured the protein levels of cytokines secreted by glioma cells that could impact immune cells: CXCL2, CXCL10, CXCL12, IL6, and IL8. For that, we used

Luminex, a multiplex assay, and we used VEGF as a positive control for hypoxia exposure. We did not detect major differences between hypoxia and physioxia (Fig 2.2.2.2).

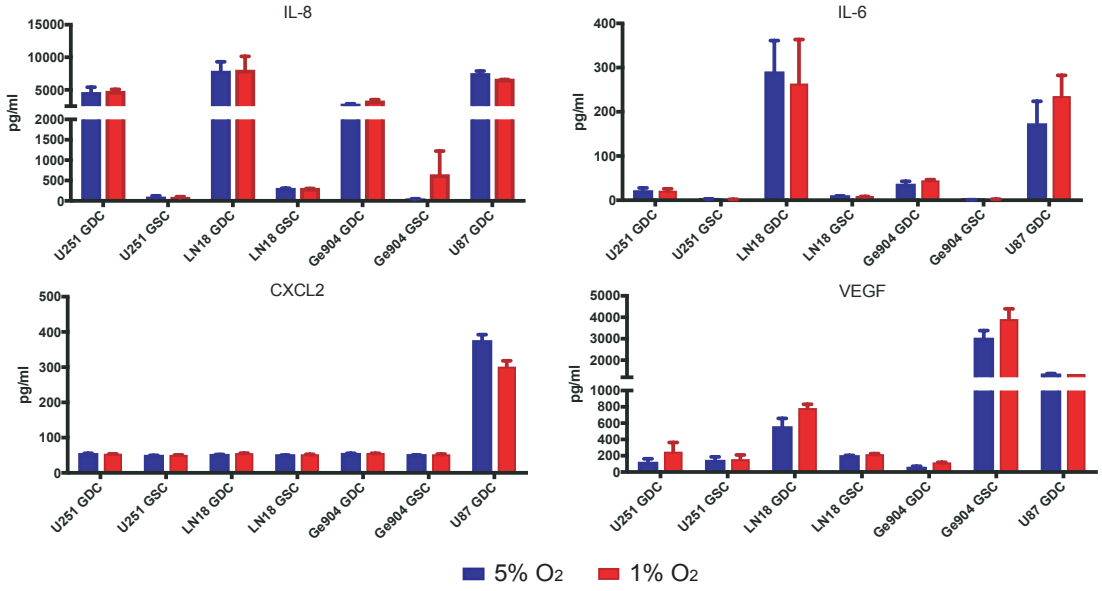

Figure 2.2.2.2. Protein expression quantification of IL-8, IL-6, CXCL2, and VEGF (CXCL10 and CXCL12 not shown) from supernatant of several glioma cell lines exposed to physioxia or hypoxia *in vitro* for 48h. (n=3; mean +/- SD).

We tested CD274 (PD-L1) by western blot and flow cytometry, even though its modulation under hypoxia at the mRNA level was only observed in one of the cell lines, LN18 GSC (Fig 2.2.2.1). As for the mRNA, we did not detect regulation of PD-L1 at the protein level in U87, U251, and LN18 glioma cell lines, together with reported B16 melanoma and MDA-MB-231 breast cancer cell lines (data not shown).

One gene that was consistently upregulated under hypoxia both at the mRNA and protein levels was REDD1. We further studied this protein in both human and mouse glioma cell lines. We first evaluated its expression when glioma cells were exposed to different oxygenation conditions, and we used metformin to modulate REDD1 expression (Fig 2.2.2.3). Again, we could segregate all cell lines into two groups depending on their response to metformin under hypoxia. However, this segregation did not overlap with the

p53 mutation-dependent classification associated with the effect of metformin on glioma cell viability. Here we observed one group of cell lines that invariably upregulated REDD1 levels upon exposure to metformin, such as LN18 GDC and Ge904 GDC. A second group showed a downregulation of REDD1 under hypoxia, such as U87 GDC, Ge835 GDC, and U251 GDC, although we observed heterogeneous responses under hyperoxia and physioxia. We observed the same results using the paired GSC version of all the tested cell lines (LN18, Ge904, U87, Ge835, U251, and GL261) (data not shown). We could not correlate such segregation of the cell lines with gene mutations, such as p53 or PTEN.

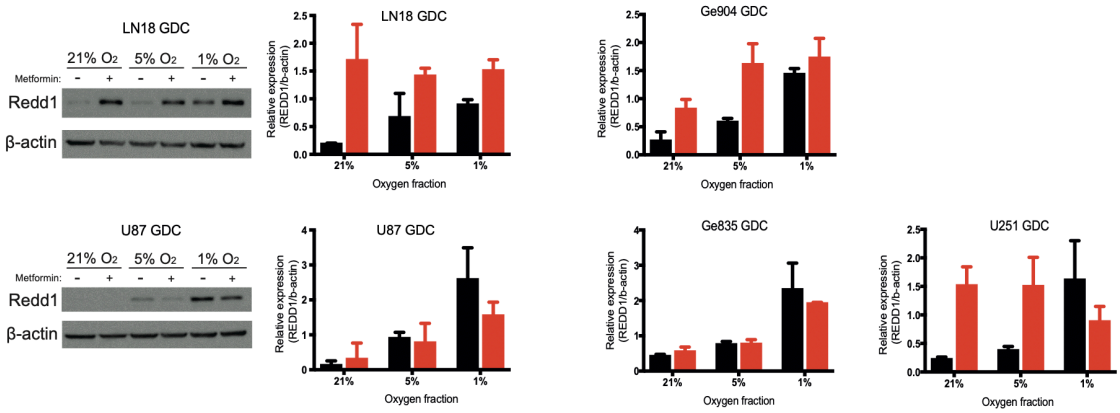

Figure 2.2.2.3 REDD1 protein expression of human glioma cell lines. Left panels: representative western blots of REDD1. Graphs represent the quantification of all western blots for each cell line (n=3; mean +/- SD).

We sought to investigate the involvement of REDD1 in the effects of metformin regarding the reduced viability of glioma cells, described in section 3.1. For that, we used the SB28 mouse glioma cell line and we successfully knocked-down *Redd1* by siRNA (Fig 2.2.2.4A). We observed an increase in cell viability after 48h culture under different oxygen conditions, especially under physiologic and hypoxic environments (Fig 2.2.2.4B). However, when we added metformin, *Redd1* levels were restored to basal levels (data not shown). This indicated that the methodology used to transiently knock-down the gene was not sufficient and permanent knock-down should be used instead.

We implemented a CRISPR/Cas9 approach on SB28 cells to reduce the levels of *Redd1*. We quantified the mRNA levels of SB28 transfected with non-targeting sequence or Redd1, and we did not significantly reduce Redd1 levels, but upon metformin treatment, Redd1 levels did not increase, as in our control (Fig 2.2.2.4C). We performed the same viability test, and we observed that under hyperoxia and physioxia, metformin was not able to reduce cell viability as much as in presence of *Redd1* (non-targeting CRISPR/Cas9 control), suggesting a partial role of Redd1 in the viability reduction induced by metformin (Fig 2.2.2.4D). However, under hypoxic conditions, absence or presence of *Redd1* did not modify the reduction in viability caused by metformin.

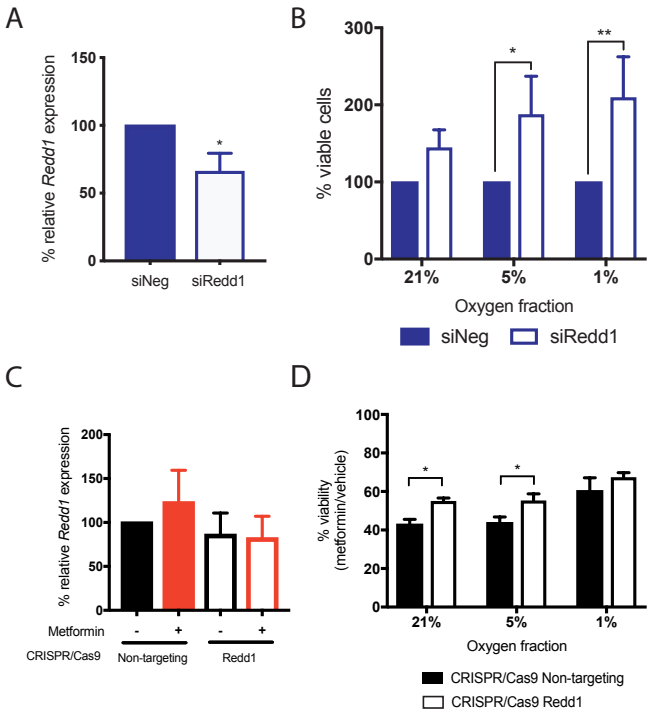

Figure 2.2.2.4 Modulation of Redd1 on SB28 glioma cell line. (A) Quantification of *Redd1* levels by qPCR on siNeg and siRedd1 cells (n=3; t-test. (B) Percentage of viable cells of siNeg and siRedd1 cells n=3; 2-way anova). (C) Quantification of *Redd1* levels by qPCR SB28 cells transfected with CRISPR/Cas9 with non-targeting sequence or against *Redd1* (n=3). (D) Percentage of viable cells treated with metformin normalized to vehicle-treated cells of CRISPR/Cas9 with non-targeting sequence or against *Redd1*. Represented mean +/- SD (2-way ANOVA; * $p<0.05$, ** $p<0.01$)

2.2.3 Metformin *in vitro*

We addressed whether metformin could modify immune-related molecules presented at the surface of glioma cells *in vitro*. For that, we used 2 glioma mouse models: SB28 and GL261-OVA. The latter consists in the carcinogen-induced glioma mouse model transfected with chicken ovalbumin (OVA) antigen. We used GL261-OVA GDC, and as well GL261-OVA GSC, which was derived in our laboratory. We calculated the protein levels by flow cytometry of Fas, CD80, CD86, MHC-I, MHC-II, PD-L1, CD40, ICAM-1, and CD44, following metformin treatment (Fig 2.2.3).

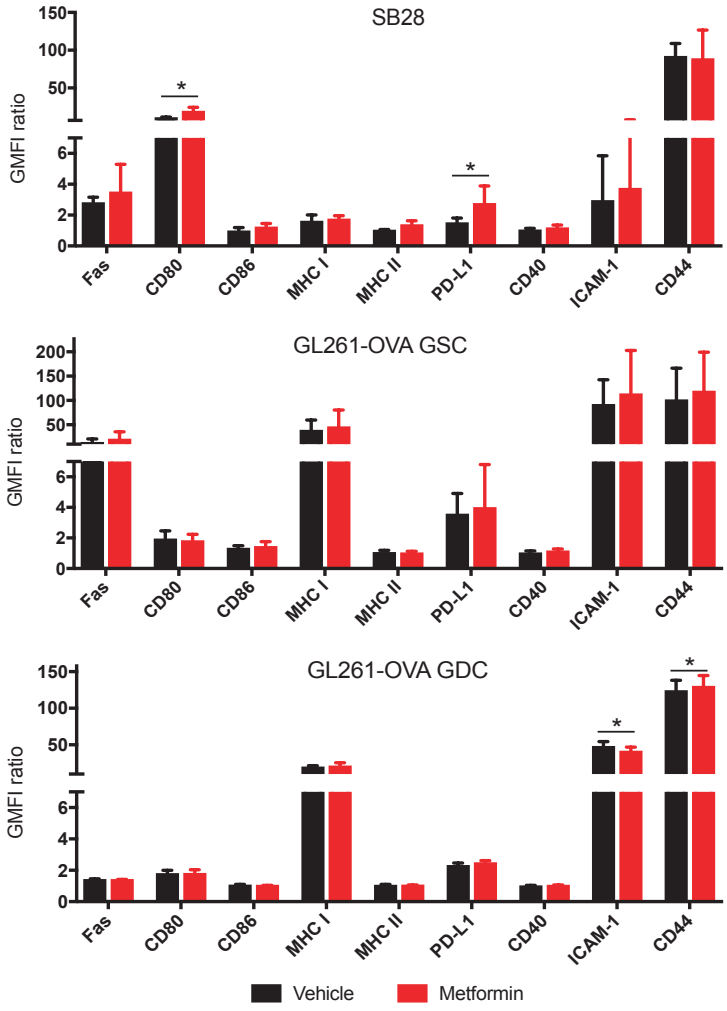

Figure 2.2.3. Expression of several surface molecules on 3 glioma mouse cell lines *in vitro*: SB28, GL261-OVA GSC, and GL261-OVA GDC following 48h exposure to vehicle or metformin (10 mM). One-way ANOVA test *p<0.05 (n=3; mean +/- SD)

SB28 cells constitutively express Fas, CD80, PD-L1, ICAM-1, and CD44, but only CD80 and PD-L1 expression was increased by metformin. GL261-OVA GDC had constitutive expression of CD80, MHC-I, and PD-L1, and this was unmodified by metformin. ICAM-1 and CD44, were both constitutively expressed and were modified by metformin, downregulated (FC=0.86, p=0.02) and upregulated (FC=1.05, p=0.04) respectively, although the fold-changes were small. GL261-OVA GSC showed expression of Fas, CD80, MHC-I, PD-L1, ICAM-1, and CD44, but these molecules were unmodified by metformin treatment.

2.2.4 Metformin *in vivo* in SB28 model

We continued to investigate the effect of metformin over SB28 regarding upregulation of CD80 and PD-L1 *in vivo*. We implanted 1'600 SB28 cells orthotopically in immunocompetent mice, and we treat them daily with oral metformin (6 mg/day-20g total weight) from day 5 until sacrifice at day 20 after tumor implantation. We isolated cancer cells using a brain dissociation kit and we evaluated the GFP^+ cells SB28 cells for expression of CD80, PD-L1, Fas, CD44, and MHC-I by flow cytometry. We did not observe statistically significant differences in the expression of any of the markers between metformin and control groups (Fig 2.2.4.1). The results were quite heterogeneous within each group. The only tendency we observed was a reduced percentage of positive PD-L1 GFP^+ cells on metformin-treated mice.

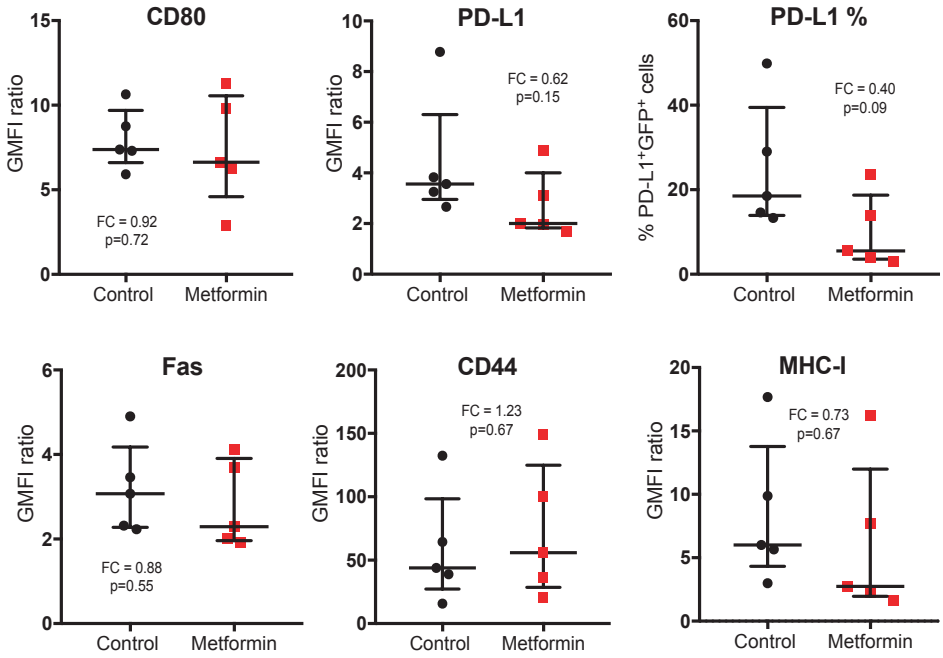

Figure 2.2.4.1. GMFI ratios of CD80, PD-L1, Fas, CD44, MHC-I, and percentage of PD-L1$^+$ cells on live GFP$^+$ ex vivo SB28 cells extracted from SB28-tumor bearing mice treated daily with vehicle (control) or metformin. Represented median with interquartile range with calculated fold-change (FC) (n=5; student's t-test).

We next evaluated tumor size using luciferase-based imaging at day 20 after tumor implantation. We did not detect a statistically significant difference between vehicle and metformin-treated mice, but we observed a tendency towards smaller tumor size in the metformin group (t-test, p=0.13) (Fig 2.2.4.2A). Probably statistical significance was not reached due to the small sample size used (n=6).

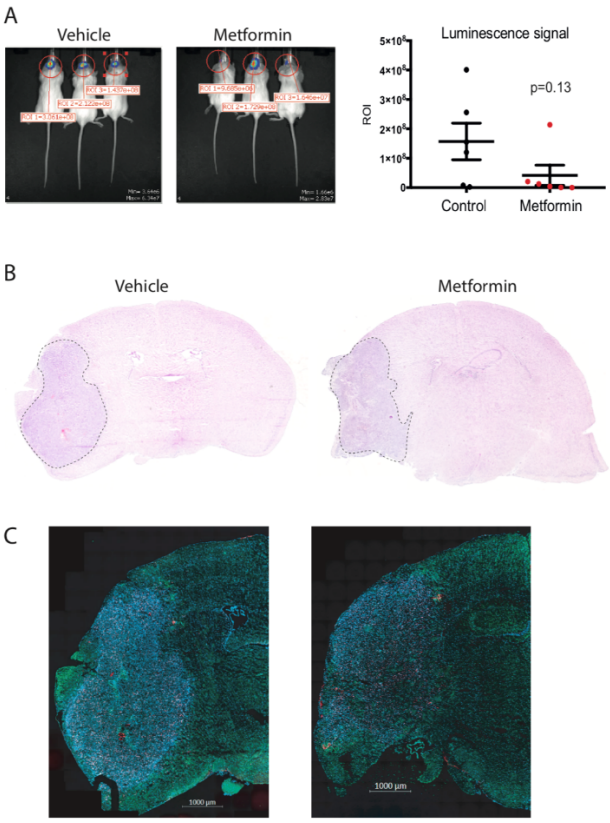

Figure 2.2.4.2. SB28 tumors growth *in vivo*. (A) Images of bioluminescence of vehicle or metformin-treated mice and quantification of bioluminescence (student's t-test). (B) H&E staining of SB28-bearing mouse brains; dashed black line delineating the tumor. (C) Immunofluorescence of hypoxia (Pimonidazole) in green, proliferation by ki67 in red, and cellular nuclei by DAPI in blue.

To study histological features of the brains, we used immunohistochemistry from frozen OCT-embedded sections. The size of the tumors was similar between the two treatment groups, as visualized with hematoxylin and eosin (H&E) staining (Fig 2.2.4.2B). We could detect presence of hypoxia using hypoxiprobe (pimonidazole: PIMO) immunofluorescence (IF) staining, which was comparable between the two groups (Fig 2.2.4.2C), validating this model at day 20 post-implantation as a good model to study hypoxia.

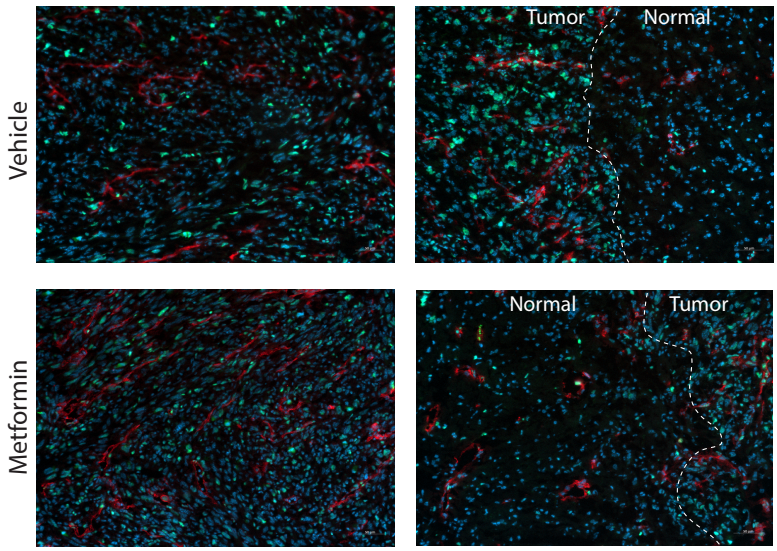

Figure 2.2.4.3. Immunofluorescence staining of the vasculature in SB28 tumors. Images on the left are in the core of the tumor; images on the right correspond to the edge of the tumor, delineated with the white discontinued line. Vessels CD31 in red, proliferating cells ki67 in green, DAPI in blue.

Moreover, we analyzed the tumor vasculature using CD31 staining, and we observed a tendency towards more vessels in the metformin group, although we could not quantify due to the small sample size of this pilot experiment.

We then repeated the experiment with a larger sample size (n=10). We implanted the SB28 glioma mouse model and followed the same treatment regimen. This time we performed a follow-up of tumor size by luminescence imaging at earlier time points to detect potential effects of metformin at earlier stages of tumor formation, but we did not observe any difference (Fig 2.2.4.4A). We followed mice until they showed symptoms or 15% weight loss, but we did not detect any difference in median survival either (Fig 2.2.4.4B).

To confirm that metformin was being injected we measured glucose levels in blood after fasting period. As metformin has anti-gluconeogenesis effect, we detected lower levels of glucose in blood following fasting in metformin-treated mice as compared to control mince (Fig 2.2.4.4C).

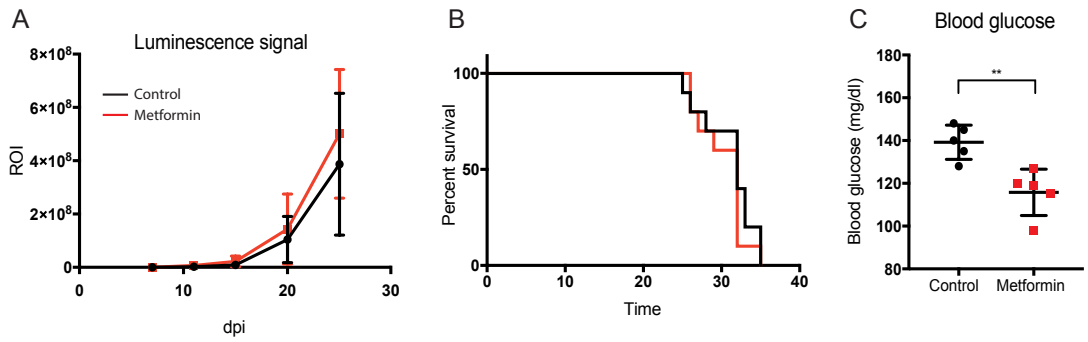

Figure 2.2.4.4. Follow-up of mice with intracranial implantation of SB28 cells treated with vehicle or metformin. (A) Bioluminescence signal quantified at days 7, 11, 15, 20, and 25 post-implantation. (B) Kaplan-Meier survival curve of control and metformin groups, both with median survival of 32 days (n=10). (C) Glucose levels in blood of vehicle or metformin treated mice 4 hours after treatment and fasting. Student's t-test **p<0.01 (n=5).

We evaluated tumor size using H&E staining, and we could quantify tumor area from several sections of each collected brain (Fig 2.2.4.5A). We quantified as well the size of hypoxic regions from several sections using PIMO IF staining (Fig 2.2.4.5B). The size of both tumors and hypoxic regions was heterogeneous between mice within the same treatment group.

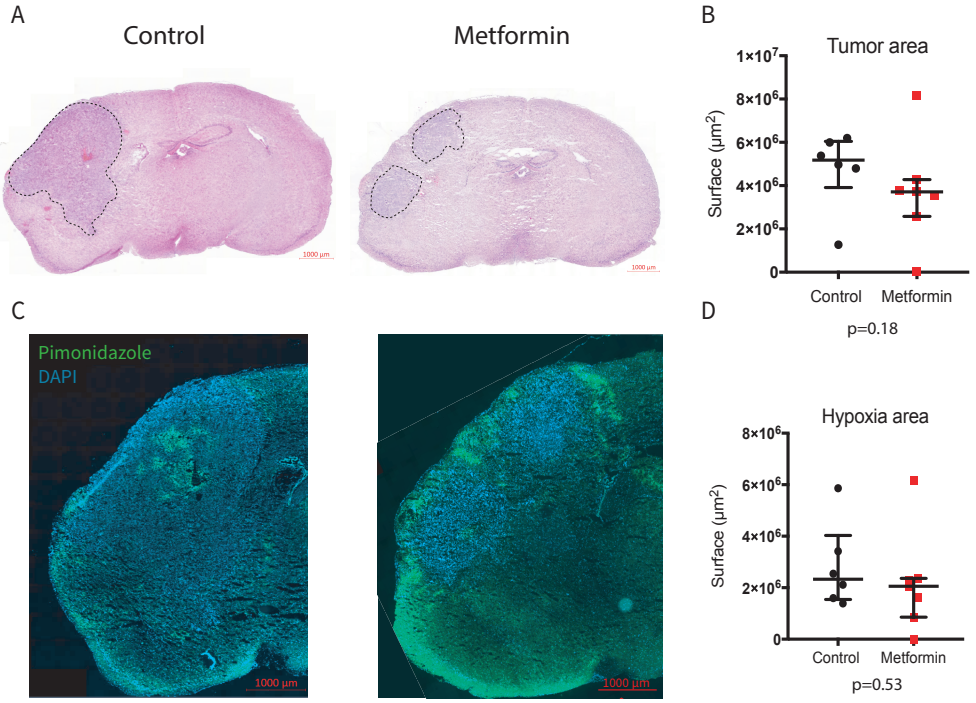

Figure 2.2.4.5. Histological staining of SB28 tumors ex vivo 20 days after implantation. (A) H&E staining and, (B) its quantification. (C) Hypoxia staining using pimonidazole and nuclei using DAPI and, (D) its quantification. Represented median with interquartile range. Mann-Whitney test (control: n=6; metformin n=7).

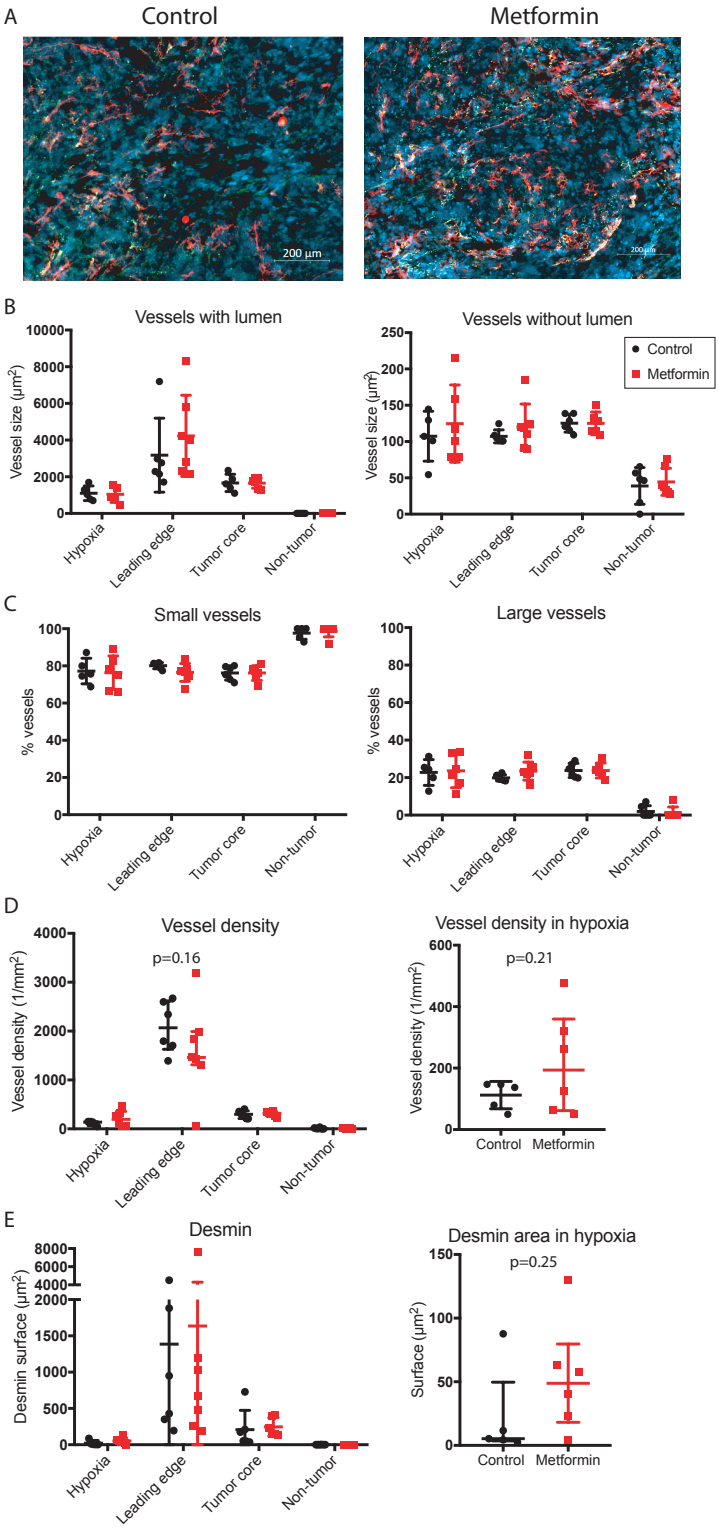

Figure 2.3.4.6. Vasculature *in vivo* of SB28 tumors. (A) Representative IF images of vehicle or metformin treated mice bearing intracranial SB28 tumors. CD31 in red, desmin in green, DAPI in blue. (B) Size of vessels with lumen and without lumen. (C) Percentage of small and large vessels. (D) Vessel density (left panel) and at larger scale for hypoxic regions (right panel). (E) Quantification of desmin surface (left panel) and at larger scale for hypoxic regions (right panel). (n=7; Two-way ANOVA).

We next evaluated the tumor vasculature using the marker CD31 for vessels, and desmin for pericytes, to assess vessel normalization (Fig 2.2.4.6A). We delineated several regions within each tumor according to their hypoxia staining, and localization in the tumor, that is: edge of the tumor, hypoxic region, tumor core (cellular tumor), and non-tumoral regions (normal brain tissue). From these 4 regions, we evaluated vessels and pericytes, calculating vessel size, percentage of vessels, and vessel density, differentiating between small (<50 μm) and large vessels (>50 μm), and vessels with and without lumen. All quantifications were performed using the automated software "definiens", except quantification of vessels with and without lumen, which was done manually (no differences observed, data not shown). We did not detect statistical differences between treatment regimens regarding all the above parameters (Fig 2.2.4.6B,C). However, we observed a tendency for vessel density to be slightly higher in hypoxic regions of tumors from mice treated with metformin (Fig 2.2.4.6D), which was accompanied by a higher desmin$^+$ surface area (Fig 2.2.4.6E).

In order to evaluate the immune infiltrate from those sections, we stained for the myeloid cell marker CD11b. We did not observe any difference between groups regarding the quantity of tumor infiltrating CD11b$^+$ cells. Although regardless of the treatment, we could observe different distributions of these cells around the tumor. In larger tumors, CD11b$^+$ cells were localized both at the edge and infiltrating the tumor (Fig 2.2.4.7A,B), and in smaller tumors or in the invasive front we could observe a higher accumulation of CD11b$^+$ cells at the tumor edges (Fig 2.2.4.7C).

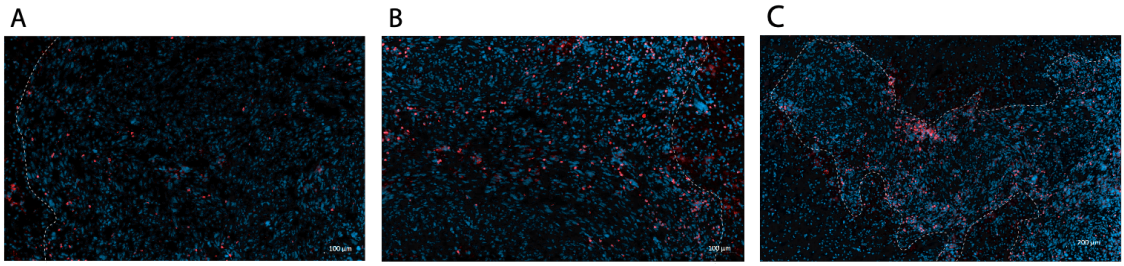

Figure 2.2.4.7. Infiltration of CD11b+ cells within SB28 tumors *in vivo* following daily vehicle or metformin treatment. CD11b in red, DAPI in blue.

We next continued metformin treatment until SB28 tumor-bearing mice were symptomatic and we then evaluated the immune infiltrate within the brain. We included a third group of mice with a combination treatment of oral daily metformin and intraperitoneal agonistic CD40 antibody administration (three times, on days 7, 12, and 16) to augment macrophage or dendritic cell activation with the aim to potentially help either innate or T cell-mediated anti-tumor immunity. Again, the median survival of both control and metformin groups was the same (Fig 2.2.4.8).

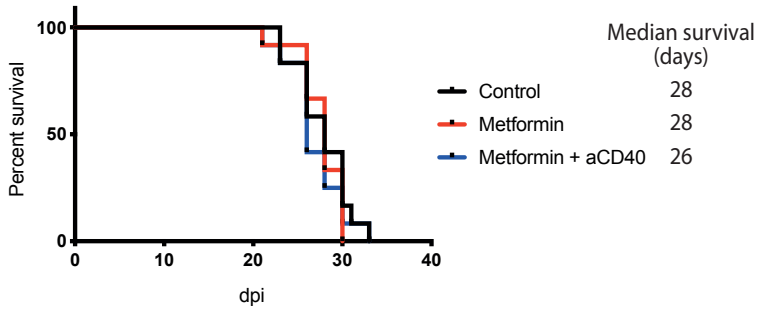

Figure 2.2.4.8. Kaplan-Meier survival curve of the three groups of mice: control, metformin, and metformin combined with agonistic anti-CD40 antibody (aCD40). Table with calculated median survival in days of each group (n=10).

In order to study the presence and status of the immune infiltrate, we digested the tumors after perfusion with Ringers solution to remove leukocytes trapped in vessels, then we isolated brain infiltrating leukocytes (BILs), and quantified them using flow cytometry. We evaluated CD8 and CD4 T cells, and the expression of PD-1, CD62L for $CD8^+$, and FoxP3 for $CD4^+$ cells. We also assessed myeloid cells: macrophages,

microglia, and granulocytes, and their expression of PD-L1 and MHC-II. We did not observe differences between treatment regimens in the percentage of cells and the expression of the listed molecules (data not shown).

2.2.5 Metformin *in vivo* in GL261 model

We investigated the impact of metformin in a second syngeneic mouse glioma model: GL261. To assess whether metformin could impact interactions between glioma and immune cells, we orthotopically implanted the OVA-transfected version: GL261-OVA GSC. The OVA expression of GL261 functions as a model tumor antigen, and we adoptively transferred OVA-specific OT-1 T cells through intra-venous (i.v.) injection. We performed adoptive cell transfer (ACT) of OT-1 T cells activated *in vitro* with OVA peptide at days 7 and 11 after tumor implantation, or with PBS, on both vehicle and metformin treated mice.

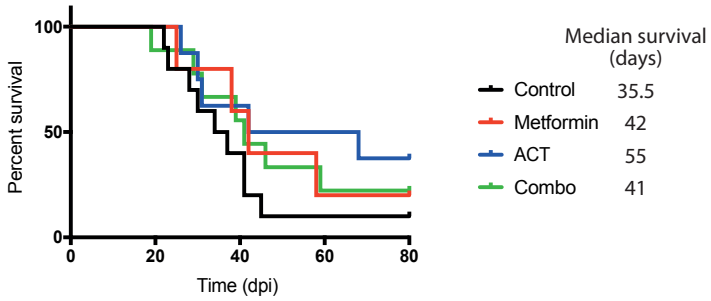

Figure 2.2.5. Kaplan-Meier survival curve of mice implanted intracranially with GL261-OVA GSC and treated with vehicle, metformin, ACT, or combination of metformin and ACT. ACT was performed on days 7 and 11 post-implantation; control and metformin groups received PBS i.v. The table shows the median survival of each group in days (n=10).

We followed the survival of mice from these 4 treatment groups. Metformin increased median survival (42 days) compared to the control group (35.5 days) (Fig 2.2.5). However, in this model, we did not observe 100% penetrance, and not all mice developed tumors, including one control mouse. ACT of OT-1 cells increased median

survival of GL261-OVA bearing mice (55 days), and addition of metformin eliminated the survival benefit provided by ACT and reduced survival (41 days) similar to the level of metformin as a monotherapy.

We evaluated the immune infiltration into the brain by flow cytometry after digestion of all brains, and we did not detect differences between any of the subsets of cells studied, similar to the results found with the SB28 model (data not shown).

In conclusion, metformin did not significantly modify tumor growth or immune infiltration in two syngeneic orthotopically implanted mouse glioma models, SB28 and GL261-OVA, neither as monotherapy, nor in the limited combinations tested. However, slight differences were observed at the level of the vasculature on the SB28 model, suggesting that optimized treatment protocols of metformin, or more potent combination therapies should be envisaged.

2.2.6 Identification of common glioma responses to hypoxia using standard culture conditions as a control

In this section, I provide data for the analysis performed when we compared hypoxic conditions (1% O_2) to standard culture conditions (21% O_2). We observed again the high degree of heterogeneity displayed by glioma cell lines, as demonstrated by the high number of individual differentially expressed genes of each cell line (Fig 2.2.6.1A). More importantly, our analysis identified two genes upregulated under hypoxia shared between all the cell lines tested: *ATF3* and *ZFP36* (Fig 2.2.6.1A). We validated their upregulation under hypoxia by qPCR (Fig 2.2.6.1B), consistent with data reporting ATF3 and ZFP36 involved in response to cellular stress, including hypoxia.

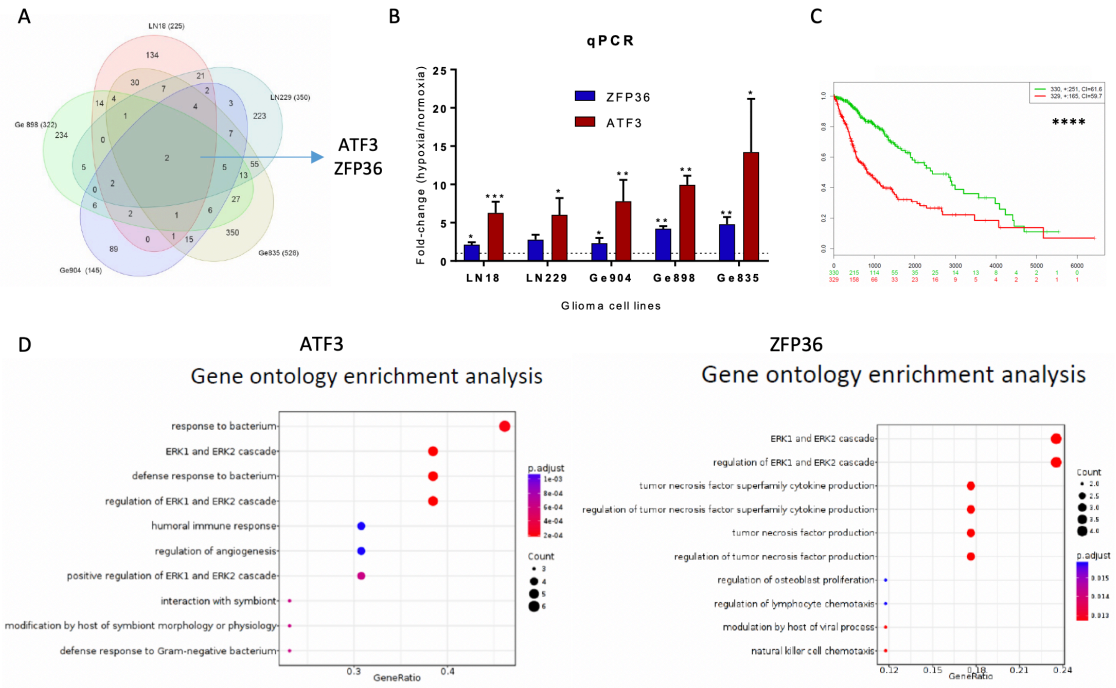

Figure 2.2.6.1. Identification of two common hypoxia-modulated genes. (A) Venn diagram of the differentially expressed genes individual to each cell line comparing glioma cells exposed to 1% O_2 with 21% O_2 (fold-change>1.5; p<0.05). The two common hypoxia-regulated genes identified in all 5 cell lines are indicated: ATF3 and ZFP36. (B) Gene expression of *ATF3* and *ZFP36* on the 5 human glioma cell lines assessed by qPCR (n=3; fold-changes represented, student's t-test). (C) Kaplan-Meier survival curve of high and low expression of *ATF3* and *ZFP36* on GBM patients from TCGA database. (D) Gene ontology enrichment analysis of *ATF3* (left panel) and *ZFP36* (right panel) using the TCGA database. (*p<0.05, **p<0.01, ***p<0.001, ****p<0.0001)

High expression of *ATF3* and *ZFP36* combined was associated with poor prognosis of GBM patients (Fig 2.2.6.1C). Gene ontology enrichment analysis of both genes revealed association with immune responses and extracellular matrix modification profile using data from TCGA (Fig 2.2.6.1D).

We further studied *in vitro* consequences following knock-down of *ATF3* and *ZFP36* individually and combined. We observed a decrease in cell viability and clonogenicity capacity when targeting *ZFP36* (Fig 2.2.6.2A,B). Interestingly, efficient knock-down of *ATF3* resulted in an increase in cell viability (Fig 2.2.6.2A). Two siRNA for each gene were tested, but only one of each showed successful downregulation of the gene.

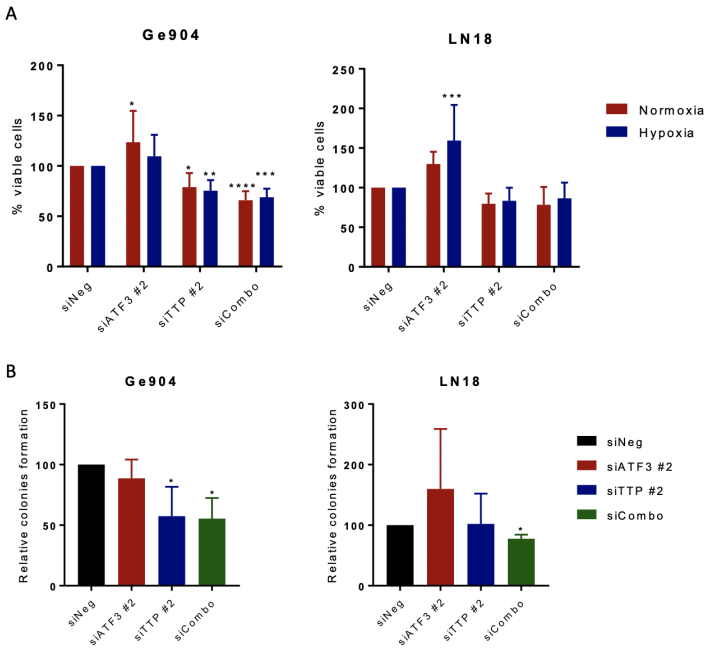

Figure 2.2.6.2. Effect of knock-down of *ATF3* and *ZFP36* on *in vitro* functional assays of two human glioma cell lines Ge904 and LN18. (A) Viability assay of Ge904 and LN18 (CellTiter Glo assay). (B) Clonogenicity capacity assay of Ge904 (n=3; normalized to siNeg control; represented mean +/- SEM; One-way ANOVA; *p<0.05,**p<0.01, ***p<0.001,****p<0.0001).

3 MATERIAL AND METHODS

This section contains detailed descriptions of the material methods used for both the manuscript in preparation (results chapter I) and all additional experiments (results chapter II).

3.1 Cell culture

Cell lines

Human established cell lines U251, U87, LN18 and LN229 were purchased from ATCC. Ge904, Ge835, Ge898 and Ge869 cell lines are primary cultures derived in-house from GBM patients from HUG (kindly provided by Valérie Dutoit, Translational Center of Research in Oncology and Hematology, UNIGE).

Murine carcinogenic-induced GL261 cell line was obtained from Serena Pellegatta (from Gaetano Finocchiaro group, Carlo Besta Institute, Department of Neuro-Oncology, Milan, Italy). OVA-transfected GL261 cell line was selected ex vivo from tumor-bearing mice and expanded *in vitro* by Dr. Cristina Riccadonna (from Paul Walker group). Engineered glioma mouse model SB28 was kindly provided by Dr. Hideo Okada (Department of Neurological Surgery, University of California, San Francisco, CA, USA).

All cell lines were tested for mycoplasma by PCR using antisense primer MGSO: TGCAC-CATCTGTCACTCTGTTAACCTC and sense primer GPO-3: GGGAGCAA-ACAGGATTAGA-TACCCT and resulted negative.

Media description

Adherent glioma differentiated cells grew in *GDC* media, composed of DMEM GlutaMAX (Life Technologies) containing high glucose (4.5 g/l) and 1 mM sodium pyruvate with additional 10% heat-inactivated fetal calf serum (FCS), 2.5% HEPES (Life Technologies), 1% non-essential amino acids (NEAA; Life Technologies) and 1% penicillin/streptomycin (P/S; Life Technologies). Induced differentiation was achieved in media based on DMEM/F-12 GlutaMAX (Life Technologies) containing high glucose and additional 10% FCS, 10 μM retinoic acid, 2.5% HEPES, 1% NEAA, 1% sodium pyruvate (Life Technologies) and 1% P/S.

Neurospheres in suspension formed by glioma stem-like cells were cultured in *GSC* media composed of DMEM/F-12 GlutaMAX (Life Technologies) containing high glucose media and additional B27 (Invitrogen), 2.5% HEPES, 1% NEAA, 1% sodium pyruvate, 1% P/S. Additional 20 ng/ml EGF and 20 ng/ml βFGF (Life Technologies) were freshly added at culture time at each passage. OVA-transfected GL261 cell line (both adherent and neurospheres) required selection with 200 μg/ml Geniticin (Life Technologies).

Cell lines were maintained in culture in humid regular incubators at 37°C and 5% CO_2. Splitting was performed every 2-3 days. Adherent cells were detached from the plastic and neurospheres dissociated using accutase (Life Technologies) by incubating cells for 5 min at 37°C.

Bone marrow-derived macrophages (BMDM) media composed of RPMI Glutamax media (Life Technologies) with additional 10% FCS, 2,5% HEPES, 1% NEAA, 1% P/S and 0.1% beta-mercaptoethanol (βME; Life Technologies). T

lymphocytes were cultured in DMEM media containing 4.5 g/l glucose, supplemented with 6% FCS, 2.5% HEPES, 1% NEAA, 1% P/S and 20 μM βME, at 37ºC and 8% CO_2.

Cell culture at different oxygen fractions

Cell culture under hypoxia (1% O_2) and normoxia (5% O_2) was performed in a hypoxic workstation Ruskinn 300 Invivo$_2$ (Baker), allowing both cell manipulation and incubation. Incubation was generally done in humidified hypoxic chambers (Billups-Rothenberg, Inc) flushed for 15 min at 20 l/min with the corresponding gas mix (1% O_2, 5% CO_2 and 94% N_2 or 5% O_2, 5% CO_2 and 90% N_2) and placed in conventional incubators to reach 37°C.

All solutions (GDC or GSC media, PBS and accutase) used at 1% or 5% O_2 were pre-equilibrated for at least 1 day at 4°C using the corresponding gas mix inside hypoxic chambers. Solutions were then aliquoted under the appropriate conditions inside the hypoxic workstation, sealed and stored at 4°C until usage for a maximum of 2 weeks.

Mouse-derived cells

T lymphocytes were isolated from OT-1 mouse spleen and inguinal lymph nodes, and dissociated through a 70-μm strainer. Red blood cells were lysed for 5 min at room temperature (RT) using ACK lysis buffer (Life Technologies) composed of 8.3 g/l NH_4Cl, 1 g/l $KHCO_3$, 37 mg/l EDTA. To achieve OVA-specific cytotoxic T lymphocyte activation *in vitro*, cells were resuspended at 1 million cells/ml in CTL media and pulsed with 10 nM OVA peptide (SIINFEKL, Proteintech). Every 2 days, T cells were diluted and 50 Units/ml (U/ml) of recombinant IL-2 was added. After 6 days, T cells were used for CTL *in vitro* killing assay or for adoptive cell transfer.

BMDM were extracted from *wild type* mice and dissociated through a 70-µm strainer. Cells were differentiated into *M0* phenotype by adding 10 ng/ml M-CSF; into *M1* with 5 ng/ml GM-CSF, and at day 5 with 20 ng/ml IFNγ for 1h and 100 ng/ml LPS for 48h; or into *M2* with 25 ng/ml M-CSF, 20 ng/ml IL-4 at day 5 and 20 ng/ml IL-13 at day 6.

3.2 Mice

In order to study gliomas *in vivo*, we implanted glioma cells in mice. Female C57BL/6J mice purchased from Charles River or bred at the animal facility from the Centre Médical Universitaire (CMU) of the University of Geneva. All procedures followed the Swiss federal law and were approved as the authorization GE/209/17.

Tumor implantation and follow-up

Mice aged between 5 and 6 weeks were anesthetized using 80 mg/kg Ketamine (Warner-Lambert, Baar, Switzerland) and 10 mg/kg Rompun (Bayer, Leverkusen, Germany) mix during intracranial implantations. Pre-surgery analgesic Temgesic was administered subcutaneously (15 µg/ml). Either 16'000 SB28 (in 2 µl) or 100'000 GL261 OVA GSC (in 4 µl; resuspension in methylcellulose to reduce leakage at implantation site) glioma mouse cells were implanted in the pallidum (2.6 mm lateral to bregma and 3.5 mm deep) using Hamilton syringes placed on a stereotactic apparatus (Stoelting, Indulab, Switzerland).

Tumor growth was monitored in some experimental setups using luminescence signal from SB28 glioma mouse model, following intraperitoneal injection of D-luciferin (15 mg/ml; GoldBio). Bioluminescence was detected on IVIS Spectrum System

(Xenogen, PerkinElmer) at the small animal Preclinical Imaging Platform (PIPPA; University of Geneva).

All mice were monitored daily by controlling their weight, and euthanized by CO_2 asphyxia when weight loss superior to 15% relative to their weight at implantation time was detected, or when symptomatic (hunched back, diminished activity, paralysis, convulsions).

Brain collection

Tumor bearing mice at mid-term tumor growth (day 20) or when symptomatic were sacrificed and organs were collected to study immune cells and tumor vasculature. Intraperitoneal pimonidazole (PIMO) injection (12 mg/ml, Hypoxiprobe) was performed 30 minutes prior to sacrifice of the mouse, followed by perfusion with Ringer's solution for 10 minutes.

Brains were either digested to purify brain infiltrating leukocytes (BILs) or frozen for histology. Digesting was performed with collagenase (Roche) and DNase D (Sigma) for 1 hour at 37°C, filtered and separated using 30% Percoll (Fluka) and ultracentrifuged at 30'000g for 1 hour. BILs were collected and stained for flow cytometry read-out. For histology purposes, brains were embedded in OCT (Tissue-Tek), rapidly frozen by close proximity to liquid nitrogen, and stored at -80ºC.

3.3 Nucleic acid analysis

RNA and DNA extractions

RNA extraction was performed using RNeasy Mini kit (Qiagen) following the manufacturer's instructions. RNA was quantified using the spectrophotometer

SpectraMax Gemini XPS (Molecular Devices) and tested for quality using 2100 Bioanalyzer (Agilent).

DNA extraction was performed using All Prep DNA/RNA Mini Kit (Qiagen) following the manufacturer's instructions. DNA quantity and quality were assessed using spectrophotometer and bioanalyzer, respectively. DNA samples were HLA-typed by Dr. Jean-Marie Tiercy (HUG, Geneva).

Whole transcriptome (microarray and RNA-seq)

Whole transcriptome of human samples was performed using Microarray PrimeView Human Gene Expression Array (Affymetrix, Applied Biosystems) at the Genomics platform from CMU. 500 ng of total RNA were reverse transcribed into cDNA, converted into biotin-labeled cRNA and was hybridized on the arrays and scanned in a *7G* scanner.

Mouse glioma cell line SB28 was sequenced using RNA-sequencing. mRNA fractions were purified by polyA capture and converted into cDNA. Libraries were sequenced on Illumina HiSeq 2500 at the Genomics platform.

qRT-PCR

250 to 500 ng of total RNA were converted into cDNA using PrimeScript RT Reagent Kit (Takara). mRNA levels of the following specificities were quantified using TB Green Premix Ex Taq II (Takara):

	Forward	**Reverse**
Mouse *Redd1*	CTTCGGGCCGGAGGAA	TCAAAGTCGGGAGGGAC
Human *ATF3*	TGCAGAGCTAAGCAGTCGTG	ATGGCTTCAGGGTTTTGGGT
Human *ZFP36*	GACTGAGCTATGTCGGACCTT	GAGTTCCGTCTTGTATTTGGGG

Table 3.3.1. Gene specificities quantified using qPCR

Nanostring

100 ng of total RNA was diluted in water and tested for the following specificities using nCounter from NanoString Technologies.

Gene ID	Ref Seq
ABCG2	NM_004827.2
BMI1	NM_005180.5
CD44	NM_001001392.1
DLX2	NM_004405.3
ERAS	NM_181532.2
FUT4	NM_002033.2
MET	NM_001127500.1
MSI1	NM_002442.3
NANOG	NM_024865.2
NES	NM_006617.1
NOTCH1	NM_017617.3
OLIG2	NM_005806.2
POU5F1	NM_002701.4
PROM1	NM_006017.1
SLC1A3	NM_004172.4
SOX2	NM_003106.2
VIM	NM_003380.2
NEFL	NM_006158.3
MAP2	NM_031845.2
GFAP	NM_002055.4
S100B	NM_006272.1
CNP	NM_033133.4
GALC	NM_000153.3
ACTB	*NM_001101.2*
TBP	*NM_001172085.1*
HPRT1	*NM_000194.1*

Gene ID	Ref Seq
BTN3A2	NM_007047.4
BTNL8	NM_024850.2
CCL5	NM_002985.2
CCL7	NM_006273.3
CD274	NM_014143.3
CXCL10	NM_001565.3
CXCL12	NM_199168.3
CXCL2	NM_002089.3
CXCL3	NM_002090.2
CXCL6	NM_002993.3
DDIT4	NM_019058.2
EGLN3	NM_022073.3
EPAS1	NM_001430.4
HIF1A	NM_001530.3
IFIT1	NM_001548.4
IFIT3	NM_001549.5
IFNAR1	NM_000629.2
IL10	NM_000572.2
IL6	NM_000600.4
IL8	NM_000584.3
MIF	NM_002415.1
NCAM1	NM_000615.6
NFKBIA	NM_020529.2
OLR1	NM_002543.3
RSAD2	NM_080657.4
SIGLEC15	NM_213602.2
TNFAIP2	NM_006291.2
UBR1	NM_174916.2
VEGFA	NM_001171623.1
XAF1	NM_017523.3

Table 3.3.2. Gene specificities quantified using Nanostring technologies. Left: gene list for stem cell characterization. Right: gene list used for glioma cell adaptations to hypoxia. Normalization genes (same for both tests) are shown in italics.

Knock-down

siRNA was employed to knock-down *Redd1* gene in SB28 cell line, and *ATF3* and *ZFP36* in several human glioma cell lines. Up to 5-30 nM siRNA on optiMEM (Life Technologies) mixed with lipofectamine 2000 (ThermoFisher) were added into adherent cell lines. 24h after transfection cells were used for *in vitro* assays.

Knock-out

CRISPR/Cas9 technology was used to knock-out *Redd1*on SB28 cells. Trueguide crRNA of nontarget or Redd1 (ThermoFisher), and TrueCut Cas9 protein (ThermoFisher) were transfected using Lipofectamine Crisprmax (ThermoFisher) following manufacturer's instructions. Clonal selection of successful knock-out was performed, and levels of *Redd1* were verified using qPCR.

3.4 Protein detection

Western Blot

Fresh or frozen dry samples were homogenized in lysis buffer containing 150 mM NaCl, 50 mM Tris, 1% NP-40 and Complete EDTA-free protease inhibitor (Roche) at pH 7.4 to obtain whole lysates. Separation of nuclear fractions were performed using NE-PER™ Nuclear and Cytoplasmic Extraction Reagents (ThermoFisher) for HIF-1α detection. BCA protein assay kit (Pierce; ThermoFisher) was used to assess protein concentration. Between 15 and 30 µg of protein from cell lysates were loaded onto 10 to 12.5% sodium dodecyl sulfate–polyacrylamide gel electrophoresis (SDS-PAGE) gels and transferred to nitrocellulose membranes (ThermoScientific). Blocking was performed using TBS 0.1% Tween containing 5% non-fat dry milk (AppliChem Panreac) or 5% bovine serum albumin (BSA; Sigma). Immune detection of rabbit anti-HIF-1α (1/1000,

Bethyl), mouse anti-TBP (1/1000, Novus Biologicals) or rabbit anti-REDD1 (1/1000, Proteintech) was performed at 4 °C overnight. Incubation of the horseradish peroxidase conjugated antibodies goat anti-rabbit IgG (1/2000, Abcam; 1/3000, Sigma), goat anti-mouse IgG (1/4000, Sigma) was performed at RT for at least 1h. Loading control anti-beta-actin HRP-conjugated (1/10'000, Sigma) was incubated at RT for 30 min. Enhanced chemiluminiscence (ECL) detection system (SuperSignal West Pico, ThermoFisher) was used to observe reactive bands. Quantification of bands was done using ImageJ.

Histology and immunofluorescence

OCT-embedded frozen mouse brains were cut into 5 μm sections using a cryostat. Hematoxylin and eosin (H&E) staining was performed for 5 min in each colorant. For immunostaining, sections were fixed in either 4% paraformaldehyde solution at RT, in 100% methanol, or 100% acetone at -20°C for 5 to 15 min. Blocking was performed in PBS containing 2.5% normal goat serum and 5% BSA for 1-2h. Primary antibodies rabbit anti-Ki67 (1/100, Abcam), rabbit anti-PD-L1 (1/100, Abcam), rat anti-CD31 GC-51[335] (1/100, kindly provided by Dr. Marijana Licina), mouse anti-PIMO-FITC (1/100, Hypoxiprobe), rat anti-CD11b (1/100, BD Biosciences) were incubated for 1h at RT. Mouse anti-desmin (1/100, Millipore) required prior mouse on mouse kit (Vector Labs) and incubation at 37ºC. Secondary antibodies goat anti-rat-AF568 (1/1000, ThermoFisher), donkey anti-mouse-AF488 (1/500, ThermoFisher), goat anti-rabbit-AF647 (1/500, ThermoFisher) were incubated for 1h at RT in the dark. Fluorescent images were obtained using Zeiss Axioscan.Z1 microscope, running Zen software, from the Bioimaging facility (CMU).

Flow cytometry

Murine cells were counted and incubated with Fc receptor block (2.4G2 hybridoma supernatant) for 10 min at 4°C. Both murine and human cells were stained for surface markers for 20 min at 4°C. Intracellular staining was performed following cell fixation and permeabilization (eBiosciences). Compensation was set performing single color staining. Gallios flow cytometer (Beckman Coulter) and Kaluza software were used to collect and analyze the data.

Target molecule	Fluorochrome	Clone	Company
Human CD80	AF700	L307.4	BD
Human PD-L1 (CD274)	PeCy7	MIH1	BD
Mouse CD80	APC	16-10A1	Biolegend
Mouse PD-L1 (CD274)	BV421	MIH5	BD
CD86	PeCy7	GL1	BD
CD40	APC	3/23	BD
Fas (CD95)	PE	Jo2	BD
ICAM-1 (CD54)	PE	3E2	BD
CD44	AF700	IM7	BD
MHC-I H-2Kd	Biotin	KH95	BD
MHC-II I-A/I-E	Biotin	2G9	BD
CD45	PE	30-F11	BD
CD11b	AF700	M1/70	BD
CD11b	PeCy7	M1/70	BD
CD8	APC	53-6.7	BD
CD62L	AF700	MEL-14	Biolegend
PD-1 (CD279)	PeCy7	29F.1A12	Biolegend
CD4	BV421	GK1.5	Biolegend
FoxP3	AF647	FJK-16s	eBioscience
Streptavidin	PeCy7		Biolegend
Streptavidin	APC-Cy7		BD

Table 3.3.1. Antibodies used to detect levels of surface or intracellular proteins by flow cytometry.

3.5 *In vitro* assays

Several *in vitro* assays were performed in order to assess the effect of hypoxia and/or metformin (1 to 10 mM, Sigma) on both mouse and human glioma cell lines.

Viability assay

Assessment of cell viability was done on cultured adherent cells or neurospheres in (flat-bottom or round-bottom, respectively) 96-well plates for 48h under the appropriate conditions and treatment. Viability read-out was performed using Cell Titer Glo (Promega) containing cell lysis buffer and luciferin to allow ATP quantification. Following incubation of 20 min at RT in the dark, lysates were transferred into flat-bottom white 96-well plates and luminescence signal was read within 10 min using a Cytation 3 plate reader.

Metabolic assay

Oxygen consumption rate (OCR) and extracellular acidification rate (ECAR) were measured using Seahorse XFe96 Analyzer (Agilent) at the READS unit (CMU). Cells were incubated in XF media (DMEM-based media) with additional 1 g/l glucose, 2 mM glutamine and 1 mM sodium pyruvate. Cell Mito Stress kit was used following manufacturer's instructions, treating cells with 2.25 µM Oligomycin, 2.25 µM FCCP and 1.13 µM Rotenone/Antimycin A. All wells were normalized to cell number.

Transmigration assay

24-well plate with 8-µm pore polycarbonate inserts (Corning, Vitaris) were used to assess attraction of BMDM by SB28 cells. The lower compartments were filled with either 50'000 SB28 cells, supernatant of SB28 cells or media containing 1% FCS at 21% O_2 or 1% O_2 for 48h. Differentiated BMDM on day 7 were seeded in the upper

compartment of the inserts for 24h. Cells on inserts were fixed in 4% PFA for 5 min, stained with 0.3% crystal violet for 30 min and counted. Supernatants in the lower compartments were collected and stained to detect transmigrating leukocytes by flow cytometry.

Scratch assay

Human glioma cells were seeded into 96-well plates and scratched using tips when confluence was reached. Images at scratch time, 12h and 24h later were taken using ImageXpress microscope and analyzed using MetaXpress software, at the Bioimaging facility.

3.6 Analysis

All experiments were analyzed using the indicated tests along the results section with R or GraphPad Prism 7 softwares to assess statistical significance (reached at p-values < 0.05).

The results from the Affymetrix microarray were analyzed after RMA normalization using Partek Genomics Suite software, version 6.6. ANOVA was performed to assess differential expression across all cell lines, and t-tests to compare each cell line individually. RNA-sequencing of SB28 was quality checked using FastQC v.0.11.2, mapped with TopHat v2.0.13 and analyzed with edgeR v.3.4.2.

4 DISCUSSION

4.1 Discussion and perspectives for additional experiments

The characterization of the GSC population is still controversial, with no standardized definition of markers expressed by these cells. In our study, we have used a panel with multiple markers that has allowed us to distinguish GSCs and GDCs. Using a panel of markers is useful, not only because of the high degree of heterogeneity of GBM, but also because each individual marker can be associated with other features of the tumor. For instance, the CD133 (Prom-1) marker has been used extensively in the field as the sole marker to identify GSC [169]; the expression of this marker has even been associated with worse clinical outcomes [336, 337]. However, CD133 has also been associated with hypoxia [108, 338], suggesting that the observed worse prognosis could refer to the presence of hypoxia and not the expression of that particular molecule. Moreover, CD133 is also expressed in differentiated cells [339]. We also investigated functional aspects of these cells to characterize them, although we did not assess tumorigenicity differences between GDC and GSC, which would ultimately support stemness properties.

Exploring data from a large transcriptome analysis can be challenging. We compared five human cell lines and obtained a restricted number of common genes. However, we observed many more individual differentially expressed genes between hypoxia and physioxia, indicating intertumoral heterogeneity. We sought to investigate those genes that have an impact on tumor immunology in more detail. One classic factor that is important in this field is PD-L1. It has been shown that hypoxia can upregulate PD-L1 in several cancer types [103, 104]. However, we observed no modulation of PD-

L1 at either the mRNA level or at the protein level in several glioma cell lines. In fact, we could not reproduce the published data in two of the cell lines reported, i.e. B16 and MDA-MB-231. While we used positive controls to ensure the validity of our read-out, this demonstrates the issue of reproducibility problems in research [340].

We analyzed other genes from this list of individual hypoxia-modulated genes but failed to find one that maintained such modulation at the protein level. The only gene that followed consistent upregulation, and which was common to all cell lines, was *REDD1*, which is involved in one of the downstream pathways affected by metformin. We then studied metformin as a means to modify glioma responses to hypoxia, both *in vitro* and *in vivo*. We evaluated the expression of REDD1 in glioma mouse and human cell lines, and its involvement in metformin-mediated effects. We also studied the potential modulation by metformin of several immune-related proteins on three mouse glioma cell lines.

Hypoxia strongly upregulated *REDD1* in both the common analysis (included in our hypoxia signature) and the individual analysis. REDD1 regulates the stress response of cells, for example, under hypoxic conditions (it contains the HRE sequence), it leads to the inhibition of mTOR to slow down protein translation and cellular proliferation [18, 325, 326, 341]. Our results are in accordance with these observations; when we knocked out *REDD1* from SB28 cells, we observed faster proliferation. REDD1 stability is regulated by ubiquitination to restore mTOR activity once hypoxia is resolved [342]; however, in our controlled conditions, we maintained a constant hypoxic environment. Moreover, REDD1 is reported to be upregulated following metformin treatment [343], as we observed mainly under hyperoxic and normoxic conditions. Under hypoxia, however, some cell lines showed metformin-induced upregulation of REDD1, while others maintained the same levels, or even decreased them. We could not relate this modulation

to the mutational status of several genes that we investigated (e.g. p53), though REDD1 expression has been linked to p53 [343]. Other regulators of REDD1 expression might be involved in these effects.

REDD1 will be upregulated under hypoxic conditions as a mechanism to promote cell survival; however, when metformin is added, this pathway is further potentiated, ending in sustained mTOR inhibition and stopping cell proliferation, even promoting cell death. We noted that cell viability of siREDD1 cells treated with metformin was higher than control cells, though we did not observe a restoration of viability, suggesting that REDD1 has only a partial role in this effect, and that other mechanisms are probably involved. We only investigated the expression and role of REDD1 in glioma cells, although it is also expressed in other cells and tissues (e.g. T cells [344]).

Regarding the expression of immune-related proteins, the expression of PD-L1 and CD80 was modulated following exposure to metformin *in vitro* in the SB28 model. However, when we administered the drug *in vivo*, the expression of these proteins was not modulated and, in fact, we observed a lower percentage of PD-L1$^+$ cells. One possible explanation for this could be that metformin did not reach the tumor at a sufficiently high concentration *in vivo*.

For our *in vivo* experiments, we sacrificed mice at day 20, because we wanted to study tumors large enough to create hypoxic regions, but before the mice were symptomatic. This timepoint was perhaps too late to visualize the differences between the treatment regimens since the sizes of all of the tumors were quite large. However, when we performed a follow-up on tumor growth at an earlier timepoint, we still did not detect any differences.

The lack of an effect from metformin treatment *in vivo* could be due to several factors, such as the doses used, the anatomical localization of the tumor, and the metformin route of administration. We tested the effect of metformin administration, but only peripherally, in the blood. We observed a decrease in blood glucose, due to the anti-gluconeogenesis effect of metformin [318, 345], proving that metformin was being administered and active. However, the BBB does not allow the transport of many compounds; although, in the case of GBM and glioma mouse models, the BBB can be disrupted, allowing more drugs through [203]. We did not assess the integrity of the BBB in our models, or whether metformin was found within the tumor or the brain; however, it could be possible to quantify levels of metformin in the CSF using methods such as high-performance liquid chromatography (HPLC) or mass spectrometry [346], which showed the presence of metformin in the CSF of rats with an intact BBB [347]. A study using a mouse orthotopic xenograft glioma model showed 10% of the administered metformin dose in the brain [315]. The dose we provided was in the range of biologically active concentrations of metformin (0.5–1.5g as used for humans, and adjusted for mouse administration [348, 349], 6mg/20g daily, comparable to other mouse studies using gavage administration [350]). The half-life of metformin in blood is calculated to be between 2–8h [349, 351]; therefore, at least one administration per day is recommended, but twice a day could have ensured a higher quantity within the brain.

However, since we did not measure the concentration of metformin in the brain, we need to consider the possibility that sufficient drug did not reach the brain in our models. An alternative could be to implant the tumor heterotopically, i.e. to implant the tumor elsewhere, not in the brain. Usually, tumors are implanted subcutaneously, which also offers the advantage of tumor growth follow-up because they are physically

measurable. For example, in a study using U87 xenografts implanted subcutaneously, daily administration of metformin reduced tumor growth [316].

The route of administration for metformin can also limit the quantity reaching the tumor. In our settings, we used gavage to provide the drug orally, comparable to oral administration using pills in diabetic human patients. Additionally, several preclinical models have shown an impact from metformin through oral administration either by gavage [350] or in drinking water [352, 353], though the latter does not allow proper monitoring of the administered dose. While we did not address different routes of administration for metformin in our model, an alternative could have been intraperitoneal (IP) administration, which could have delivered higher quantities of the drug to the tissues and has been shown to affect tumor growth in several mouse cancer models [323, 354], including gliomas [315, 316]. Another possibility would be to insert a pump that could deliver the drug directly into the brain, ensuring exposure of the tissue to the drug; the feasibility of this method has been validated in various brain pathologies, in rodents and humans [355-357].

Metformin as a monotherapy did not induce significant therapeutic effect in our models. It failed to extend overall survival; therefore, finding therapeutic combinations should be considered. The two combinations we tried failed: agonistic anti-CD40 in the SB28 model, and adoptive cell transfer of OT-1 T cells in the GL261-OVA model. This is in accordance with two studies showing a negative impact of metformin on the infiltrating immune cells, by increasing PD-1 or Tim-3; however, combining metformin with suitable immunotherapies resulted in a reduction in tumor growth [352, 354]. We sought to analyze the effects of metformin on the immune infiltrate, especially in a hypoxic context. To do this, we analyzed brain sections from our models, which allowed us to observe the distribution of some immune cells within the tumor. However, this

technique is not ideal for quantifying expression levels of particular markers on specific cell types. Instead, we used flow cytometry on isolated BILs after tumor digestion. In our setting, BILs analysis did not reveal an increase in PD-1 or Tim-3 expression on T cells, as previously reported. On the other hand, some studies have shown beneficial effects of metformin on the immune cells infiltrating the tumors, such as helping to skew TAMs from a protumoral phenotype towards antitumoral phenotype, and preventing lung metastasis [358]. Extensively studying the effect of metformin on the immune infiltrate could indicate which cell types are favorably modulated and which could be further stimulated by particular immunotherapies that could be combined with metformin.

Combining metformin with TMZ, an obvious combination for GBM, has already been tested, resulting in an enhanced effect of TMZ, especially in TMZ-resistant cell lines, both *in vitro* and *in vivo* [312, 359]. A preclinical model using U87 xenografts indicated that high doses of metformin combined with TMZ increased survival compared to monotherapy regimens [360]. *In vitro* data suggests that metformin and TMZ increase apoptosis in the GSC population [361]. Metformin combined with radiotherapy has also shown promising results in prostate cancer, increasing the radiotherapy response [332]; this therapy in GBM is under investigation in phase II trial, but no data is yet available (NCT02780024). Another combination proposed consists in administering metformin during hypoglycemic cycle in intermittent fasting, which lead to smaller tumors by activating Glycogen synthase kinase 3 beta (GSK3β) [362]. The possibilities for therapeutic combinations are vast. In order to choose proper therapeutic combinations, animal studies can provide information regarding overall survival and interactions with other cells within the tumor microenvironment. However, to test many drug combinations, prior *in vitro* screening may allow a reduction in the number of animals needed.

We observed some tendencies in our *in vivo* SB28 model regarding the tumor vasculature: more vessels in the hypoxic areas were accompanied by a higher expression of desmin. This suggested that hypoxic regions were becoming more vascularized and, importantly, more covered by pericytes, an indication of vasculature normalization. Normalized vasculature improves tumor perfusion and oxygenation [363]. This could help to overcome resistance to radiotherapy, since these vessels can bring back oxygen, one of the key molecules for radiosensitization. Normalizing vasculature could also potentially help to overcome chemotherapy resistance, not only by counterbalancing the effects of tumor hypoxia but also by providing the means for drugs to reach the tumor, and the hypoxic regions in particular. The need for pericytes around vessels is important for proper vessel function; however, too many pericytes could decrease vessel permeability and drug effusion, as demonstrated in a study targeting pericytes using ibrutinib [364].

We performed our *in vivo* experiments using two different mouse glioma models; however, both involved the injection of tumor cells orthotopically, which can disrupt the tissue during surgery, despite the fact that the volume injected, especially for the SB28 model, was small and glioma cells showed infiltration of the brain parenchyma. An alternative to such an intervention is to use spontaneously generated gliomas (e.g. [195, 365]). Although these models can help us to understand tumor formation, they still lack intratumoral heterogeneity, and homogeneity in relation to tumor initiation time [366].

In conclusion, metformin seems to modify tumor vasculature *in vivo*; however, we observed no changes regarding the immune infiltrate, despite changes we observed on SB28 cells *in vitro* which potentially could have been important for immune interactions *in vivo*. Optimizing the administration of metformin and investigating potential therapeutic combinations are justified.

Regarding the common adaptations of glioma cells to hypoxia using standard cultures conditions as a control, we showed an upregulation of *ATF3* and *ZFP36* in all glioma cell lines tested. The use of 21% O_2 as the control condition allowed us to detect a common response to hypoxia that was not observed at the 5% O_2. It is possible that the upregulation of *ATF3* and *ZFP36* took place in a physiologic range of oxygen (from 5% O_2 to around 9% O_2), but we did not address this point. For that, we could assess the expression of these factors at multiple oxygen conditions.

We demonstrated that the modulation of *ATF3* and *ZFP36* gene expression affected glioma cell viability and clonogenicity capacity. However, we did not detect differences between hypoxia and hyperoxia. These data suggest that these factors are expressed and necessary both at 1% O_2 and 21% O_2 conditions, and further downregulation will influence fundamental cell functioning, regardless of the oxygenation levels they are exposed to. Indeed, other regulators are reported to modulate ATF3 expression linked to the adaptation responses to cellular stress signals, not only involving hypoxia [28, 29].

ATF3 and ZFP36 seem to have independent roles in GBM biology even if they were both upregulated together under the same stress condition. We observed a negative impact of *ZFP36* knock-down in cell viability, but the contrary was observed for ATF3. Some studies associate *ATF3* expression with higher cancer cell proliferation, as demonstrated by knock-down of ATF on GBM cells growth *in vitro* and *in vivo,* resulting in reduced GBM cell growth [32]. However, another study using HepG2 cells showed a reduced cell proliferation upon overexpression of *ATF3* [33], which would be in accordance with our observation of increased cell viability after knock-down of *ATF3*. Further ectopic expression of this factor should be used to clarify these contradictions.

We observed a decreased viability and clonogenicity capacity following *ZFP36* knock-down, suggesting that ZFP36 participates in survival of hypoxic GBM cells. These observations are consistent with studies using the U87 GBM cell line where an increased *ZFP36* expression and activation were associated with increased GBM cell apoptosis and reduced cell growth *in vitro* [34, 35]. In contrast, another study using ln827 GBM cells showed opposite results, where ectopic expression of *ZFP36* decreased viability [36]. Detailed analysis of ZFP36 activation and consequent downstream cascades should be carried out to reveal the modulated pathways involved in these observations.

Our findings do not exclude that other mechanisms exist to compensate the induced gene expression loss of *ATF3* and/or *ZFP36*. In order to evaluate multiple consequences of *ATF3* and *ZFP36* loss, it would be necessary to investigate the transcriptional profiles of glioma cell lines with knock-down of *ATF3*, *ZFP36*, or both combined. Moreover, their reported roles in inflammation and extracellular matrix remodeling suggest important participation of ATF3 and ZFP36 in GBM biology and interaction with the microenvironment. This should be further addressed, for example, by testing chemotaxis of immune cells and migration capacity under 1% O_2 and 21% O_2.

4.2 General discussion

Interest in and understanding of hypoxia in a tumoral context have increased over the past decades, and continue to expand. Tumor hypoxia has a significant impact on clinical outcomes for GBM patients—it is associated with increasing malignancy grade in gliomas, and therefore with mortality [132]. Hypoxia and consequent HIF stabilization have been described in pseudopalisading areas around necrotic areas, both in mouse models and human GBM biopsies [213]. Unresolved hypoxia, as found in tumors, would normally induce cell death, but some tumors cells can survive such hostile microenvironments. Therefore, tumor hypoxia creates a selective pressure to already inherently adapted cells [367], or to those cells that can adapt [368], in any case promoting phenotypes of quiescence and/or migration.

Both *in vitro* and *in vivo* studies have supported the advances in the research on tumor hypoxia. We now have more tools and knowledge to work with in relation to hypoxia. However, the inaccurate use of physiological controls prevails [48]. As early as 1983, evidence of better translation to *in vivo* observations using 5% O_2 over 21% O_2 (atmospheric conditions) for cell culture were demonstrated [369]. In this project, we first set the various oxygen concentration exposures and timings. In a controlled setting, we cultured a monolayer of adherent cells exposed to 5% O_2 for physioxia, and 1% O_2 for hypoxia, which are *in vivo* relevant oxygen conditions [48]. We also included 21% O_2 as a control for atmospheric conditions, to compare our results with the data available in the literature.

Perhaps considering only one physiological control is too simplistic. The reality is that each tissue has an oxygen gradient, and our tested 5% O_2 cannot represent all physiological conditions. In fact, many changes could have occurred between our

observations at 21% O_2 and 5% O_2, as was likely in the results shown in 3.2. Moreover, the localization of the tumor within the brain can differ between patients, meaning that it is exposed to different oxygenation levels. In our glioma mouse models, we knew the exact location of the initial tumor formation since we always implanted stereotactically in the pallidum, a subcortical area, thus standardizing between our mouse subjects. It is worth noting that oxygen distribution *in vivo* changes spatially (differences in perfusion), but also temporally (metabolic changes). The technologies that provide this information have advanced, notably since the first electrodes that were capable of detecting partial pressures of oxygen were developed. In a clinical context, imaging techniques, principally based on PET and MRI, can detect changes in oxygenation, and could potentially be coupled with modern (fiber-optic based) sensors than can quantify pO_2. Visualization of the vasculature is possible *in vivo* in humans using vascular architecture mapping, based on MRI imaging, which, for example, allows the monitoring of changes in the vasculature of human GBM during bevacizumab therapy [370]. Some imaging tools have been developed for preclinical models for the study of hypoxia, such as quantifying the luciferase signal from luciferase with HRE reporter in GL261 glioma mouse cell lines [371]. We could not implement imaging techniques *in vivo* to quantify oxygenation levels, but we were able to evaluate hypoxia presence and vasculature *ex vivo* using a histologic approach.

As reviewed by Keeley and Mann, it is preferable to measure oxygenation using partial pressure units rather than percentages of oxygen [48]. The former is more accurate because partial pressures dictate the availability of oxygen in a given media, and will standardize working oxygen conditions across laboratories. In our study, however, we used percentages since our system did not measure partial pressures. In addition, we did not measure the exact partial pressures in our *in vitro* cultures. Many parameters in *in*

vitro cultures can impact the availability of oxygen for the cells; a way to normalize this is to use hypoxia stations, gas mixes, and pre-equilibrate the media and buffers to the desired oxygen condition to shorten the time needed for the cells to adapt to such an environment. Moreover, cell densities are a critical parameter to control. We implemented all of these actions in order to standardize the oxygen exposure in all of our cultures.

The timing of hypoxia exposure is important. The time frames of acute and chronic hypoxic exposure are still debated, and vary significantly between studies (reviewed in [70]). In this project, we used 48h because we sought to study consequences at the protein and functional levels, which would include HIF stabilization and subsequent signaling cascades involving further protein translation [62]. Indeed, we observed HIF-1α stabilization in those conditions, and also changes at the mRNA and protein levels.

Importantly, in our study, we modified the availability of oxygen in our cell cultures, thus allowing the cells to adapt to the hypoxic environment. We did not modify HIF stabilization or any signaling pathway, i.e. by using chemical hypoxia mimetics such as $CoCl_2$ [32]. Indeed, half of the genes in our described hypoxia signature have not been reported as having HRE in their sequences, suggesting the importance of directly modulating oxygen, and not just HIF. Moreover, despite the high heterogeneity of responses to hypoxia demonstrated from our data and some earlier studies [372], we obtained a hypoxia gene signature that was common to five glioma cell lines from our whole transcriptional analysis.

We are living in an era in which performing large-scale profiling analysis is common, and even expected, for example, using single-cell RNA sequencing [373]. The scientific community is thus generating enormous amounts of data that we are perhaps

not exploiting fully. Sharing data in publicly available databases is useful to expand research towards new horizons, enabling the scientific community to profit from multi-disciplinary points of view. However, the risk is that these databases contain data from a wide variety of fields under the same keywords—e.g. searching for hypoxia in such databases will provide data on hypoxia in a tumor context, probably including many studies using inadequate physiologic controls, but also in other biology fields such as ischemia and microbiology. This means that the gene sets taken into consideration are not ideal for comparison. We used gene set enrichment analysis (GSEA) in this type of approach; however, we also used databases that included only human GBM patient *ex vivo* data to validate our *in vitro* observations [163, 374].

Nowadays, plenty of information is available regarding the biology of GBM at multiple levels. However, the classification of GBM has evolved very little. Brain tumors have been categorized, since the first WHO classification in 1979, based on histological features, updated in 1993 [375]. Several subdivisions of GBM have been made since then, and are included in the latest WHO guidelines of 2016 [376], mainly through genetic and transcriptional profiles, which correlate better with survival than histological features [377]. Of note, different patterns of tumors are still considered as the same tumor type—GBM—because they share histological landscapes. Actually, given the high degree of heterogeneity, GBM is considered a family of tumor types. Our data provides more evidence of the intertumoral heterogeneity at the transcriptional level.

One example of GBM heterogeneity is the molecular subtyping based on the TCGA data [144, 147]. However, different subtypes have been observed within the same tumor, even though there might be a predominant subtype [162]. An important sub-classification of GBM is based on the methylation status of the MGMT promoter, which has been demonstrated to impact the response to TMZ [151]. Segregating GBM patients

according to their MGMT promoter methylation status could help to define differential treatments. However, many patients with unmethylated MGMT promoter continue to receive TMZ, even if they do not benefit from it, probably due to the lack of alternatives [378]. Molecular signatures are being studied as a means to subclassify patients according to common features, for differential treatments [379], for example, age-specific or self-renewal signatures of GBM patients [380, 381]. We have identified a common hypoxia gene signature that strongly correlates with poor survival, potentially helping to stratify patients that could benefit from hypoxia-targeting approaches.

Despite significant research effort in the scientific community to treat GBM, the prognosis for this disease is still very low. However, promising results have been achieved in recent clinical trials. The median survival of control groups (that is, the standard of care) is longer than that proposed by the landmark phase III trial for TMZ and radiotherapy in 2005. Although the treatment has remained the same, it has been demonstrated that improvement in diagnosis and surgical techniques has allowed an increase in the survival of GBM patients receiving the standard of care [382]. However, many phase I and II trials that show very promising positive results do not include a control-arm and instead continue to use such historical control, which could falsely lead to the assumption that the observed survival benefit originates from the investigated treatment.

New therapeutic approaches for GBM are needed; in this research project, we have studied the effects of metformin both *in vitro* and *in vivo*. Metformin is a repurposed drug originally used for type 2 diabetes mellitus, with observed effects on several tumor cell (including GBM) properties, such as viability, migration, and tumor growth [316, 383, 384]. We have validated *in vitro* that metformin reduces the viability of cancer cells, even under hypoxia, and reduces the oxygen consumption rate; we have confirmed these

observations at a physiological range of oxygen. The reduced oxygen consumption potentially results in higher tumor oxygenation, resolving hypoxia, and showing HIF inhibitory activity, as demonstrated in hepatocellular carcinoma [385]. In fact, many drugs available in the market for cancer treatment also show HIF inhibition, but are still fully unexploited for this purpose (summarized in [386]).

However, in our setting, we observed less impact from metformin under hypoxia regarding OCR. This is probably because, under hypoxia, there is already low oxygen consumption by the mitochondria. Supporting these observations, a study on pediatric sarcomas has indicated that hypoxia reduces the efficacy of metformin [387].

One of the most significant advantages of metformin is its low toxicity profile, in opposition to current second-line treatments for GBM targeting the tumor vasculature, bevacizumab (summarized in [388]). The aberrant angiogenic vasculature observed in GBM has been under the spotlight for many years, but bevacizumab treatment has several disadvantages, it is toxic, and in addition, some cells develop resistance and an invasive phenotype (reviewed in [389]). The approach of vascular normalization has gained attention, whereby the aim is to promote a proper structure and function of the tumor vasculature, which otherwise is aberrant, and limiting access to oxygen, nutrients, and eventually drugs [228]. A glioma mouse model showed tumor normalization following sunitinib treatment, which led to a better distribution of TMZ [390]. Nevertheless, tumor reoxygenation can also have negative consequences if not persistent and regulated. Cyclic and/or acute hypoxia following tumor reoxygenation can occur, and has been associated with increased production of ROS and DNA damage [391, 392], and a worse prognosis overall [70, 393].

Another important aspect of the tumor microenvironment is the immune infiltrate. It has been established that tumor hypoxia acts as a negative factor for the immune cells, both directly and indirectly, promoting an immunosuppressive microenvironment in many cancer types, including GBM [107]. Novel immunotherapy protocols have demonstrated outstanding results in GBM, encouraging further research.

Although different treatments have shown fairly positive results in preclinical GBM models, successful translation to humans is often problematic. An important limitation of animal models is that we cannot recapitulate the exact biology of human GBM, and equally important, there will never be enough animal models to incorporate the heterogeneity of human GBM. However, there are tools that can be used to generate meaningful information in a semi-controlled setting, such as CRISPR/Cas9 technologies [394], which allow screening of *in vivo* relevant genes. Graft implantation, such as those used in this study, may not reflect intertumoral heterogeneity of GBM; however, we have shown that this can be used to address hypoxia-related questions. However, without assessing any given therapeutic approaches in other models, this is unlikely to be directly translatable to clinics. We must be aware of the limitations of each technique and setting, and conclude accordingly.

In conclusion, our study has provided a common hypoxia gene signature using human GBM cell lines, despite the observed intertumoral heterogeneity. Additional use of metformin modified the hypoxia response, supporting further research on the use of metformin in the context of GBM. The use of appropriate preclinical models is key to optimizing drug combinations, for example, the use of metformin to normalize tumor vasculature and to enable oxygen and other drugs to reach the tumor. Therefore, in the context of the heterogeneity that characterizes GBM, finding common features such as the presence of hypoxia opens the possibility of finding new treatments (metformin or

other hypoxia modulators) from which many GBM patients can benefit. Such a common treatment can then be further optimized by considering GBM subclassifications to deliver a personalized therapy component to each patient.

5 CONCLUSIONS

This research shows that given the heterogeneity of GBM and its adaptations to hypoxia, we have identified common responses to low oxygenation. We have studied a compound that has potential to modify hypoxia, a common feature of the tumor microenvironment. Repurposing metformin to normalize the tumor vasculature can potentially reduce hypoxia in GBM. Our data suggest a justified continuation of the study of metformin to reverse hypoxia in the context of GBM.

6 REFERENCES

1. Semenza, G.L. and G.L. Wang, *A nuclear factor induced by hypoxia via de novo protein synthesis binds to the human erythropoietin gene enhancer at a site required for transcriptional activation*. Mol Cell Biol, 1992. **12**(12): p. 5447-54.
2. Iyer, N.V., et al., *Cellular and developmental control of O2 homeostasis by hypoxia-inducible factor 1 alpha*. Genes Dev, 1998. **12**(2): p. 149-62.
3. Bruick, R.K. and S.L. McKnight, *A conserved family of prolyl-4-hydroxylases that modify HIF*. Science, 2001. **294**(5545): p. 1337-40.
4. Ivan, M., et al., *Biochemical purification and pharmacological inhibition of a mammalian prolyl hydroxylase acting on hypoxia-inducible factor*. Proc Natl Acad Sci U S A, 2002. **99**(21): p. 13459-64.
5. Epstein, A.C., et al., *C. elegans EGL-9 and mammalian homologs define a family of dioxygenases that regulate HIF by prolyl hydroxylation*. Cell, 2001. **107**(1): p. 43-54.
6. Jaakkola, P., et al., *Targeting of HIF-alpha to the von Hippel-Lindau ubiquitylation complex by O2-regulated prolyl hydroxylation*. Science, 2001. **292**(5516): p. 468-72.
7. Ivan, M., et al., *HIFalpha targeted for VHL-mediated destruction by proline hydroxylation: implications for O2 sensing*. Science, 2001. **292**(5516): p. 464-8.
8. Hewitson, K.S., et al., *Hypoxia-inducible factor (HIF) asparagine hydroxylase is identical to factor inhibiting HIF (FIH) and is related to the cupin structural family*. J Biol Chem, 2002. **277**(29): p. 26351-5.
9. Lando, D., et al., *FIH-1 is an asparaginyl hydroxylase enzyme that regulates the transcriptional activity of hypoxia-inducible factor*. Genes Dev, 2002. **16**(12): p. 1466-71.
10. Lando, D., et al., *Asparagine hydroxylation of the HIF transactivation domain a hypoxic switch*. Science, 2002. **295**(5556): p. 858-61.
11. Peng, J., et al., *The transcription factor EPAS-1/hypoxia-inducible factor 2alpha plays an important role in vascular remodeling*. Proc Natl Acad Sci U S A, 2000. **97**(15): p. 8386-91.
12. Compernolle, V., et al., *Loss of HIF-2alpha and inhibition of VEGF impair fetal lung maturation, whereas treatment with VEGF prevents fatal respiratory distress in premature mice*. Nat Med, 2002. **8**(7): p. 702-10.
13. Wenger, R.H., D.P. Stiehl, and G. Camenisch, *Integration of oxygen signaling at the consensus HRE*. Sci STKE, 2005. **2005**(306): p. re12.
14. Uchida, T., et al., *Prolonged hypoxia differentially regulates hypoxia-inducible factor (HIF)-1alpha and HIF-2alpha expression in lung epithelial cells: implication of natural antisense HIF-1alpha*. J Biol Chem, 2004. **279**(15): p. 14871-8.
15. Hara, S., et al., *Expression and characterization of hypoxia-inducible factor (HIF)-3alpha in human kidney: suppression of HIF-mediated gene expression by HIF-3alpha*. Biochem Biophys Res Commun, 2001. **287**(4): p. 808-13.
16. Makino, Y., et al., *Inhibitory PAS domain protein is a negative regulator of hypoxia-inducible gene expression*. Nature, 2001. **414**(6863): p. 550-4.
17. Schofield, C.J. and P.J. Ratcliffe, *Oxygen sensing by HIF hydroxylases*. Nat Rev Mol Cell Biol, 2004. **5**(5): p. 343-54.

18. Schodel, J., et al., *High-resolution genome-wide mapping of HIF-binding sites by ChIP-seq*. Blood, 2011. **117**(23): p. e207-17.
19. Pugh, C.W. and P.J. Ratcliffe, *Regulation of angiogenesis by hypoxia: role of the HIF system*. Nat Med, 2003. **9**(6): p. 677-84.
20. Semenza, G.L., *HIF-1: upstream and downstream of cancer metabolism*. Curr Opin Genet Dev, 2010. **20**(1): p. 51-6.
21. Wang, H., et al., *Negative regulation of Hif1a expression and TH17 differentiation by the hypoxia-regulated microRNA miR-210*. Nat Immunol, 2014. **15**(4): p. 393-401.
22. Ginouves, A., et al., *PHDs overactivation during chronic hypoxia "desensitizes" HIFalpha and protects cells from necrosis*. Proc Natl Acad Sci U S A, 2008. **105**(12): p. 4745-50.
23. Jewell, U.R., et al., *Induction of HIF-1alpha in response to hypoxia is instantaneous*. FASEB J, 2001. **15**(7): p. 1312-4.
24. Cramer, T., et al., *HIF-1alpha is essential for myeloid cell-mediated inflammation*. Cell, 2003. **112**(5): p. 645-57.
25. Finlay, D.K., et al., *PDK1 regulation of mTOR and hypoxia-inducible factor 1 integrate metabolism and migration of CD8+ T cells*. J Exp Med, 2012. **209**(13): p. 2441-53.
26. Palazon, A., et al., *An HIF-1alpha/VEGF-A Axis in Cytotoxic T Cells Regulates Tumor Progression*. Cancer Cell, 2017. **32**(5): p. 669-683 e5.
27. Knowles, H.J., et al., *Normoxic stabilization of hypoxia-inducible factor-1alpha by modulation of the labile iron pool in differentiating U937 macrophages: effect of natural resistance-associated macrophage protein 1*. Cancer Res, 2006. **66**(5): p. 2600-7.
28. Arsham, A.M., J.J. Howell, and M.C. Simon, *A novel hypoxia-inducible factor-independent hypoxic response regulating mammalian target of rapamycin and its targets*. J Biol Chem, 2003. **278**(32): p. 29655-60.
29. Park, E.C., et al., *Hypoxia regulates glutamate receptor trafficking through an HIF-independent mechanism*. EMBO J, 2012. **31**(6): p. 1379-93.
30. Lluis, J.M., et al., *Dual role of mitochondrial reactive oxygen species in hypoxia signaling: activation of nuclear factor-{kappa}B via c-SRC and oxidant-dependent cell death*. Cancer Res, 2007. **67**(15): p. 7368-77.
31. Tafani, M., et al., *The Interplay of Reactive Oxygen Species, Hypoxia, Inflammation, and Sirtuins in Cancer Initiation and Progression*. Oxid Med Cell Longev, 2016. **2016**: p. 3907147.
32. Yuan, Y., et al., *Cobalt inhibits the interaction between hypoxia-inducible factor-alpha and von Hippel-Lindau protein by direct binding to hypoxia-inducible factor-alpha*. J Biol Chem, 2003. **278**(18): p. 15911-6.
33. Wang, G.L. and G.L. Semenza, *Desferrioxamine induces erythropoietin gene expression and hypoxia-inducible factor 1 DNA-binding activity: implications for models of hypoxia signal transduction*. Blood, 1993. **82**(12): p. 3610-5.
34. O'Connor, J.P.B., S.P. Robinson, and J.C. Waterton, *Imaging tumour hypoxia with oxygen-enhanced MRI and BOLD MRI*. Br J Radiol, 2019. **92**(1095): p. 20180642.
35. Clark, L.C., Jr., et al., *Monitor and control of blood oxygen tension and pH during total body perfusion*. J Thorac Surg, 1958. **36**(4): p. 488-96.
36. Vanderkooi, J.M., et al., *An optical method for measurement of dioxygen concentration based upon quenching of phosphorescence*. J Biol Chem, 1987. **262**(12): p. 5476-82.

37. Lecoq, J., et al., *Simultaneous two-photon imaging of oxygen and blood flow in deep cerebral vessels*. Nat Med, 2011. **17**(7): p. 893-8.
38. Lord, E.M., L. Harwell, and C.J. Koch, *Detection of hypoxic cells by monoclonal antibody recognizing 2-nitroimidazole adducts*. Cancer Res, 1993. **53**(23): p. 5721-6.
39. Raleigh, J.A., et al., *Comparisons among pimonidazole binding, oxygen electrode measurements, and radiation response in C3H mouse tumors*. Radiat Res, 1999. **151**(5): p. 580-9.
40. van Brussel, A.S., et al., *Molecular imaging with a fluorescent antibody targeting carbonic anhydrase IX can successfully detect hypoxic ductal carcinoma in situ of the breast*. Breast Cancer Res Treat, 2013. **140**(2): p. 263-72.
41. Hoogsteen, I.J., et al., *Hypoxia in larynx carcinomas assessed by pimonidazole binding and the value of CA-IX and vascularity as surrogate markers of hypoxia*. Eur J Cancer, 2009. **45**(16): p. 2906-14.
42. Sobhanifar, S., et al., *Reduced expression of hypoxia-inducible factor-1alpha in perinecrotic regions of solid tumors*. Cancer Res, 2005. **65**(16): p. 7259-66.
43. Bruehlmeier, M., et al., *Assessment of hypoxia and perfusion in human brain tumors using PET with 18F-fluoromisonidazole and 15O-H2O*. J Nucl Med, 2004. **45**(11): p. 1851-9.
44. Stadlbauer, A., et al., *Development of a Non-invasive Assessment of Hypoxia and Neovascularization with Magnetic Resonance Imaging in Benign and Malignant Breast Tumors: Initial Results*. Mol Imaging Biol, 2018.
45. Christen, T., et al., *Measuring brain oxygenation in humans using a multiparametric quantitative blood oxygenation level dependent MRI approach*. Magn Reson Med, 2012. **68**(3): p. 905-11.
46. la Cour, A., G. Greisen, and S. Hyttel-Sorensen, *In vivo validation of cerebral near-infrared spectroscopy: a review*. Neurophotonics, 2018. **5**(4): p. 040901.
47. Swartz, H.M., et al., *Advances in probes and methods for clinical EPR oximetry*. Adv Exp Med Biol, 2014. **812**: p. 73-79.
48. Keeley, T.P. and G.E. Mann, *Defining Physiological Normoxia for Improved Translation of Cell Physiology to Animal Models and Humans*. Physiol Rev, 2019. **99**(1): p. 161-234.
49. Cater, D.B., et al., *Changes of oxygen tension in brain and somatic tissues induced by vasodilator and vasoconstrictor drugs*. Royal Society, 1961. **155**(958): p. 136-157.
50. Sakadzic, S., et al., *Two-photon high-resolution measurement of partial pressure of oxygen in cerebral vasculature and tissue*. Nat Methods, 2010. **7**(9): p. 755-9.
51. Metzger, H. and S. Heuber, *Local oxygen tension and spike activity of the cerebral grey matter of the rat and its response to short intervals of O2 deficiency or CO2 excess*. Pflugers Arch, 1977. **370**(2): p. 201-9.
52. Nair, P., W.J. Whalen, and D. Buerk, *PO2 of cat cerebral cortex: response to breathing N2 and 100 per cent O21*. Microvasc Res, 1975. **9**(2): p. 158-65.
53. Hoffman, W.E., F.T. Charbel, and G. Edelman, *Brain tissue oxygen, carbon dioxide, and pH in neurosurgical patients at risk for ischemia*. Anesth Analg, 1996. **82**(3): p. 582-6.
54. Liu, K.J., et al., *Assessment of cerebral pO2 by EPR oximetry in rodents: effects of anesthesia, ischemia, and breathing gas*. Brain Res, 1995. **685**(1-2): p. 91-8.
55. Dings, J., et al., *Clinical experience with 118 brain tissue oxygen partial pressure catheter probes*. Neurosurgery, 1998. **43**(5): p. 1082-95.

56. Smith, R.H., E.J. Guilbeau, and D.D. Reneau, *The oxygen tension field within a discrete volume of cerebral cortex*. Microvasc Res, 1977. **13**(2): p. 233-40.
57. Rosenthal, G., et al., *Brain tissue oxygen tension is more indicative of oxygen diffusion than oxygen delivery and metabolism in patients with traumatic brain injury*. Crit Care Med, 2008. **36**(6): p. 1917-24.
58. Parpaleix, A., Y. Goulam Houssen, and S. Charpak, *Imaging local neuronal activity by monitoring PO(2) transients in capillaries*. Nat Med, 2013. **19**(2): p. 241-6.
59. Lyons, D.G., et al., *Mapping oxygen concentration in the awake mouse brain*. Elife, 2016. **5**.
60. Seylaz, J. and E. Pinard, *Continuous measurement of gas partial pressures in intracerebral tissue*. J Appl Physiol Respir Environ Exerc Physiol, 1978. **44**(4): p. 528-33.
61. Zauner, A., et al., *Brain oxygen, CO2, pH, and temperature monitoring: evaluation in the feline brain*. Neurosurgery, 1995. **37**(6): p. 1168-76; discussion 1176-7.
62. Carreau, A., et al., *Why is the partial oxygen pressure of human tissues a crucial parameter? Small molecules and hypoxia*. J Cell Mol Med, 2011. **15**(6): p. 1239-53.
63. Timpano, S., et al., *Physioxic human cell culture improves viability, metabolism, and mitochondrial morphology while reducing DNA damage*. FASEB J, 2019: p. fj201802279R.
64. Ferguson, D.C.J., et al., *Altered cellular redox homeostasis and redox responses under standard oxygen cell culture conditions versus physioxia*. Free Radic Biol Med, 2018. **126**: p. 322-333.
65. Atkuri, K.R., L.A. Herzenberg, and L.A. Herzenberg, *Culturing at atmospheric oxygen levels impacts lymphocyte function*. Proc Natl Acad Sci U S A, 2005. **102**(10): p. 3756-9.
66. Bhandari, V., et al., *Molecular landmarks of tumor hypoxia across cancer types*. Nat Genet, 2019. **51**(2): p. 308-318.
67. Hanahan, D. and R.A. Weinberg, *Hallmarks of cancer: the next generation*. Cell, 2011. **144**(5): p. 646-74.
68. Vaupel, P., M. Hockel, and A. Mayer, *Detection and characterization of tumor hypoxia using pO2 histography*. Antioxid Redox Signal, 2007. **9**(8): p. 1221-35.
69. Vaupel, P. and A. Mayer, *Hypoxia in cancer: significance and impact on clinical outcome*. Cancer Metastasis Rev, 2007. **26**(2): p. 225-39.
70. Bayer, C. and P. Vaupel, *Acute versus chronic hypoxia in tumors: Controversial data concerning time frames and biological consequences*. Strahlenther Onkol, 2012. **188**(7): p. 616-27.
71. Algire, G.H. and H.W. Chalkley, *Vascular reactions of normal and malignant tissues in vivo. I. Vascular reactions of mice to wounds and to normal and neoplastic transplants*. J Natl Cancer Inst, 1945. **6**(1): p. 73-85.
72. Nagy, J.A., et al., *Why are tumour blood vessels abnormal and why is it important to know?* Br J Cancer, 2009. **100**(6): p. 865-9.
73. Dvorak, H.F., *How tumors make bad blood vessels and stroma*. Am J Pathol, 2003. **162**(6): p. 1747-57.
74. Krock, B.L., N. Skuli, and M.C. Simon, *Hypoxia-induced angiogenesis: good and evil*. Genes Cancer, 2011. **2**(12): p. 1117-33.
75. Hockel, M., et al., *Association between tumor hypoxia and malignant progression in advanced cancer of the uterine cervix*. Cancer Res, 1996. **56**(19): p. 4509-15.

76. Young, S.D., R.S. Marshall, and R.P. Hill, *Hypoxia induces DNA overreplication and enhances metastatic potential of murine tumor cells*. Proc Natl Acad Sci U S A, 1988. **85**(24): p. 9533-7.
77. Miyazaki, Y., et al., *The effect of hypoxic microenvironment on matrix metalloproteinase expression in xenografts of human oral squamous cell carcinoma*. Int J Oncol, 2008. **32**(1): p. 145-51.
78. Du, R., et al., *HIF1alpha induces the recruitment of bone marrow-derived vascular modulatory cells to regulate tumor angiogenesis and invasion*. Cancer Cell, 2008. **13**(3): p. 206-20.
79. Coquelle, A., et al., *A new role for hypoxia in tumor progression: induction of fragile site triggering genomic rearrangements and formation of complex DMs and HSRs*. Mol Cell, 1998. **2**(2): p. 259-65.
80. Reynolds, T.Y., S. Rockwell, and P.M. Glazer, *Genetic instability induced by the tumor microenvironment*. Cancer Res, 1996. **56**(24): p. 5754-7.
81. Koshiji, M., et al., *HIF-1alpha induces genetic instability by transcriptionally downregulating MutSalpha expression*. Mol Cell, 2005. **17**(6): p. 793-803.
82. Mihaylova, V.T., et al., *Decreased expression of the DNA mismatch repair gene Mlh1 under hypoxic stress in mammalian cells*. Mol Cell Biol, 2003. **23**(9): p. 3265-73.
83. Graeber, T.G., et al., *Hypoxia-mediated selection of cells with diminished apoptotic potential in solid tumours*. Nature, 1996. **379**(6560): p. 88-91.
84. Soengas, M.S., et al., *Apaf-1 and caspase-9 in p53-dependent apoptosis and tumor inhibition*. Science, 1999. **284**(5411): p. 156-9.
85. Greijer, A.E. and E. van der Wall, *The role of hypoxia inducible factor 1 (HIF-1) in hypoxia induced apoptosis*. J Clin Pathol, 2004. **57**(10): p. 1009-14.
86. Zhang, L. and R.P. Hill, *Hypoxia enhances metastatic efficiency by up-regulating Mdm2 in KHT cells and increasing resistance to apoptosis*. Cancer Res, 2004. **64**(12): p. 4180-9.
87. Schwartz, G., *Ueber Desensibilisierung gegen röntgen- und radiumstrahlen*. Munchener Medizinische Wochenschrift, 1909. **24**: p. 1-2.
88. Gray, L.H., et al., *The concentration of oxygen dissolved in tissues at the time of irradiation as a factor in radiotherapy*. Br J Radiol, 1953. **26**(312): p. 638-48.
89. Quintiliani, M., *The oxygen effect in radiation inactivation of DNA and enzymes*. Int J Radiat Biol Relat Stud Phys Chem Med, 1986. **50**(4): p. 573-94.
90. Tredan, O., et al., *Drug resistance and the solid tumor microenvironment*. J Natl Cancer Inst, 2007. **99**(19): p. 1441-54.
91. Minchinton, A.I. and I.F. Tannock, *Drug penetration in solid tumours*. Nat Rev Cancer, 2006. **6**(8): p. 583-92.
92. Comerford, K.M., et al., *Hypoxia-inducible factor-1-dependent regulation of the multidrug resistance (MDR1) gene*. Cancer Res, 2002. **62**(12): p. 3387-94.
93. Warburg, O., *On the origin of cancer cells*. Science, 1956. **123**(3191): p. 309-14.
94. Vander Heiden, M.G., L.C. Cantley, and C.B. Thompson, *Understanding the Warburg effect: the metabolic requirements of cell proliferation*. Science, 2009. **324**(5930): p. 1029-33.
95. Chen, C., et al., *Regulation of glut1 mRNA by hypoxia-inducible factor-1. Interaction between H-ras and hypoxia*. J Biol Chem, 2001. **276**(12): p. 9519-25.
96. Semenza, G.L., et al., *Hypoxia response elements in the aldolase A, enolase 1, and lactate dehydrogenase A gene promoters contain essential binding sites for hypoxia-inducible factor 1*. J Biol Chem, 1996. **271**(51): p. 32529-37.

97. Yamagata, M., et al., *The contribution of lactic acid to acidification of tumours: studies of variant cells lacking lactate dehydrogenase*. Br J Cancer, 1998. **77**(11): p. 1726-31.
98. Wykoff, C.C., et al., *Hypoxia-inducible expression of tumor-associated carbonic anhydrases*. Cancer Res, 2000. **60**(24): p. 7075-83.
99. Chiche, J., et al., *Hypoxia-inducible carbonic anhydrase IX and XII promote tumor cell growth by counteracting acidosis through the regulation of the intracellular pH*. Cancer Res, 2009. **69**(1): p. 358-68.
100. Sitkovsky, M.V., et al., *Hostile, hypoxia-A2-adenosinergic tumor biology as the next barrier to overcome for tumor immunologists*. Cancer Immunol Res, 2014. **2**(7): p. 598-605.
101. Vuillefroy de Silly, R., et al., *Phenotypic switch of CD8(+) T cells reactivated under hypoxia toward IL-10 secreting, poorly proliferative effector cells*. Eur J Immunol, 2015. **45**(8): p. 2263-75.
102. Noman, M.Z., et al., *Blocking hypoxia-induced autophagy in tumors restores cytotoxic T-cell activity and promotes regression*. Cancer Res, 2011. **71**(18): p. 5976-86.
103. Barsoum, I.B., et al., *A mechanism of hypoxia-mediated escape from adaptive immunity in cancer cells*. Cancer Res, 2014. **74**(3): p. 665-74.
104. Noman, M.Z., et al., *PD-L1 is a novel direct target of HIF-1alpha, and its blockade under hypoxia enhanced MDSC-mediated T cell activation*. J Exp Med, 2014. **211**(5): p. 781-90.
105. Murdoch, C., A. Giannoudis, and C.E. Lewis, *Mechanisms regulating the recruitment of macrophages into hypoxic areas of tumors and other ischemic tissues*. Blood, 2004. **104**(8): p. 2224-34.
106. Facciabene, A., et al., *Tumour hypoxia promotes tolerance and angiogenesis via CCL28 and T(reg) cells*. Nature, 2011. **475**(7355): p. 226-30.
107. Wei, J., et al., *Hypoxia potentiates glioma-mediated immunosuppression*. PLoS One, 2011. **6**(1): p. e16195.
108. Bar, E.E., et al., *Hypoxia increases the expression of stem-cell markers and promotes clonogenicity in glioblastoma neurospheres*. Am J Pathol, 2010. **177**(3): p. 1491-502.
109. Das, B., et al., *Hypoxia enhances tumor stemness by increasing the invasive and tumorigenic side population fraction*. Stem Cells, 2008. **26**(7): p. 1818-30.
110. Toustrup, K., et al., *Validation of a 15-gene hypoxia classifier in head and neck cancer for prospective use in clinical trials*. Acta Oncol, 2016. **55**(9-10): p. 1091-1098.
111. Toustrup, K., et al., *Development of a hypoxia gene expression classifier with predictive impact for hypoxic modification of radiotherapy in head and neck cancer*. Cancer Res, 2011. **71**(17): p. 5923-31.
112. Ge, L., et al., *Differential glioma-associated tumor antigen expression profiles of human glioma cells grown in hypoxia*. PLoS One, 2012. **7**(9): p. e42661.
113. Ostrom, Q.T., et al., *CBTRUS Statistical Report: Primary Brain and Other Central Nervous System Tumors Diagnosed in the United States in 2011-2015*. Neuro Oncol, 2018. **20**(suppl_4): p. iv1-iv86.
114. Tykocki, T. and M. Eltayeb, *Ten-year survival in glioblastoma. A systematic review*. J Clin Neurosci, 2018. **54**: p. 7-13.
115. Crocetti, E., et al., *Epidemiology of glial and non-glial brain tumours in Europe*. Eur J Cancer, 2012. **48**(10): p. 1532-42.

116. Louis, D.N., et al., *The 2007 WHO classification of tumours of the central nervous system*. Acta Neuropathol, 2007. **114**(2): p. 97-109.
117. Diamandis, P. and K. Aldape, *World Health Organization 2016 Classification of Central Nervous System Tumors*. Neurol Clin, 2018. **36**(3): p. 439-447.
118. Venneti, S. and J.T. Huse, *The evolving molecular genetics of low-grade glioma*. Adv Anat Pathol, 2015. **22**(2): p. 94-101.
119. Ohgaki, H. and P. Kleihues, *Epidemiology and etiology of gliomas*. Acta Neuropathol, 2005. **109**(1): p. 93-108.
120. Grimm, S.A. and M.C. Chamberlain, *Anaplastic astrocytoma*. CNS Oncol, 2016. **5**(3): p. 145-57.
121. Yan, H., et al., *IDH1 and IDH2 mutations in gliomas*. N Engl J Med, 2009. **360**(8): p. 765-73.
122. Batash, R., et al., *Glioblastoma Multiforme, Diagnosis and Treatment; Recent Literature Review*. Curr Med Chem, 2017. **24**(27): p. 3002-3009.
123. Ichimura, K., et al., *Molecular pathogenesis of astrocytic tumours*. J Neurooncol, 2004. **70**(2): p. 137-60.
124. Alcantara Llaguno, S., et al., *Malignant astrocytomas originate from neural stem/progenitor cells in a somatic tumor suppressor mouse model*. Cancer Cell, 2009. **15**(1): p. 45-56.
125. Nguyen, L.V., et al., *Cancer stem cells: an evolving concept*. Nat Rev Cancer, 2012. **12**(2): p. 133-43.
126. Lee, J.H., et al., *Human glioblastoma arises from subventricular zone cells with low-level driver mutations*. Nature, 2018. **560**(7717): p. 243-247.
127. Ratai, E.M., et al., *ACRIN 6684: Multicenter, phase II assessment of tumor hypoxia in newly diagnosed glioblastoma using magnetic resonance spectroscopy*. PLoS One, 2018. **13**(6): p. e0198548.
128. Quartuccio, N. and M.C. Asselin, *The Validation Path of Hypoxia PET Imaging: Focus on Brain Tumours*. Curr Med Chem, 2018. **25**(26): p. 3074-3095.
129. Fleming, I.N., et al., *Imaging tumour hypoxia with positron emission tomography*. Br J Cancer, 2015. **112**(2): p. 238-50.
130. Brat, D.J., et al., *Pseudopalisades in glioblastoma are hypoxic, express extracellular matrix proteases, and are formed by an actively migrating cell population*. Cancer Res, 2004. **64**(3): p. 920-7.
131. Rong, Y., et al., *'Pseudopalisading' necrosis in glioblastoma: a familiar morphologic feature that links vascular pathology, hypoxia, and angiogenesis*. J Neuropathol Exp Neurol, 2006. **65**(6): p. 529-39.
132. Evans, S.M., et al., *Hypoxia is important in the biology and aggression of human glial brain tumors*. Clin Cancer Res, 2004. **10**(24): p. 8177-84.
133. Scherer, H.J., *The forms of growth in gliomas and their practical significance*. Brain, 1940. **40**: p. 631-635.
134. Batzdorf, U. and N. Malamud, *The Problem of Multicentric Gliomas*. J Neurosurg, 1963. **20**: p. 122-36.
135. Muller, C., et al., *Hematogenous dissemination of glioblastoma multiforme*. Sci Transl Med, 2014. **6**(247): p. 247ra101.
136. Sullivan, J.P., et al., *Brain tumor cells in circulation are enriched for mesenchymal gene expression*. Cancer Discov, 2014. **4**(11): p. 1299-309.
137. Beauchesne, P., *Extra-neural metastases of malignant gliomas: myth or reality?* Cancers (Basel), 2011. **3**(1): p. 461-77.

138. Hamilton, J.D., et al., *Glioblastoma multiforme metastasis outside the CNS: three case reports and possible mechanisms of escape*. J Clin Oncol, 2014. **32**(22): p. e80-4.
139. Parsons, D.W., et al., *An integrated genomic analysis of human glioblastoma multiforme*. Science, 2008. **321**(5897): p. 1807-12.
140. Ohgaki, H. and P. Kleihues, *The definition of primary and secondary glioblastoma*. Clin Cancer Res, 2013. **19**(4): p. 764-72.
141. Godard, S., et al., *Classification of human astrocytic gliomas on the basis of gene expression: a correlated group of genes with angiogenic activity emerges as a strong predictor of subtypes*. Cancer Res, 2003. **63**(20): p. 6613-25.
142. Lawrence, M.S., et al., *Mutational heterogeneity in cancer and the search for new cancer-associated genes*. Nature, 2013. **499**(7457): p. 214-218.
143. Vogelstein, B., et al., *Cancer genome landscapes*. Science, 2013. **339**(6127): p. 1546-58.
144. Cancer Genome Atlas Research, N., *Comprehensive genomic characterization defines human glioblastoma genes and core pathways*. Nature, 2008. **455**(7216): p. 1061-8.
145. Furnari, F.B., et al., *Malignant astrocytic glioma: genetics, biology, and paths to treatment*. Genes Dev, 2007. **21**(21): p. 2683-710.
146. Freije, W.A., et al., *Gene expression profiling of gliomas strongly predicts survival*. Cancer Res, 2004. **64**(18): p. 6503-10.
147. Verhaak, R.G., et al., *Integrated genomic analysis identifies clinically relevant subtypes of glioblastoma characterized by abnormalities in PDGFRA, IDH1, EGFR, and NF1*. Cancer Cell, 2010. **17**(1): p. 98-110.
148. Van Meir, E.G., et al., *Exciting new advances in neuro-oncology: the avenue to a cure for malignant glioma*. CA Cancer J Clin, 2010. **60**(3): p. 166-93.
149. Phillips, H.S., et al., *Molecular subclasses of high-grade glioma predict prognosis, delineate a pattern of disease progression, and resemble stages in neurogenesis*. Cancer Cell, 2006. **9**(3): p. 157-73.
150. Wang, Q., et al., *Tumor Evolution of Glioma-Intrinsic Gene Expression Subtypes Associates with Immunological Changes in the Microenvironment*. Cancer Cell, 2017. **32**(1): p. 42-56 e6.
151. Hegi, M.E., et al., *MGMT gene silencing and benefit from temozolomide in glioblastoma*. N Engl J Med, 2005. **352**(10): p. 997-1003.
152. Esteller, M., et al., *Inactivation of the DNA repair gene O6-methylguanine-DNA methyltransferase by promoter hypermethylation is a common event in primary human neoplasia*. Cancer Res, 1999. **59**(4): p. 793-7.
153. Noushmehr, H., et al., *Identification of a CpG island methylator phenotype that defines a distinct subgroup of glioma*. Cancer Cell, 2010. **17**(5): p. 510-22.
154. de Souza, C.F., et al., *A Distinct DNA Methylation Shift in a Subset of Glioma CpG Island Methylator Phenotypes during Tumor Recurrence*. Cell Rep, 2018. **23**(2): p. 637-651.
155. consortium, B., *Quantitative comparison of DNA methylation assays for biomarker development and clinical applications*. Nat Biotechnol, 2016. **34**(7): p. 726-37.
156. Klughammer, J., et al., *The DNA methylation landscape of glioblastoma disease progression shows extensive heterogeneity in time and space*. Nat Med, 2018. **24**(10): p. 1611-1624.

157. Itakura, H., et al., *Magnetic resonance image features identify glioblastoma phenotypic subtypes with distinct molecular pathway activities*. Sci Transl Med, 2015. **7**(303): p. 303ra138.
158. Rayfield, C.A., et al., *Distinct Phenotypic Clusters of Glioblastoma Growth and Response Kinetics Predict Survival*. JCO Clin Cancer Inform, 2018. **2**: p. 1-14.
159. Li, R., et al., *Identification of intrinsic subtype-specific prognostic microRNAs in primary glioblastoma*. J Exp Clin Cancer Res, 2014. **33**: p. 9.
160. Chen, X., et al., *Characterization of microRNAs in serum: a novel class of biomarkers for diagnosis of cancer and other diseases*. Cell Res, 2008. **18**(10): p. 997-1006.
161. Santangelo, A., et al., *Circulating microRNAs as emerging non-invasive biomarkers for gliomas*. Ann Transl Med, 2017. **5**(13): p. 277.
162. Sottoriva, A., et al., *Intratumor heterogeneity in human glioblastoma reflects cancer evolutionary dynamics*. Proc Natl Acad Sci U S A, 2013. **110**(10): p. 4009-14.
163. Puchalski, R.B., et al., *An anatomic transcriptional atlas of human glioblastoma*. Science, 2018. **360**(6389): p. 660-663.
164. Kumar, A., et al., *Deep sequencing of multiple regions of glial tumors reveals spatial heterogeneity for mutations in clinically relevant genes*. Genome Biol, 2014. **15**(12): p. 530.
165. Consortium, G., *Glioma through the looking GLASS: molecular evolution of diffuse gliomas and the Glioma Longitudinal Analysis Consortium*. Neuro Oncol, 2018. **20**(7): p. 873-884.
166. Spiteri, I., et al., *Evolutionary dynamics of residual disease in human glioblastoma*. Ann Oncol, 2018.
167. Kim, J., et al., *Spatiotemporal Evolution of the Primary Glioblastoma Genome*. Cancer Cell, 2015. **28**(3): p. 318-28.
168. Mazor, T., et al., *DNA Methylation and Somatic Mutations Converge on the Cell Cycle and Define Similar Evolutionary Histories in Brain Tumors*. Cancer Cell, 2015. **28**(3): p. 307-317.
169. Singh, S.K., et al., *Identification of human brain tumour initiating cells*. Nature, 2004. **432**(7015): p. 396-401.
170. Galli, R., et al., *Isolation and characterization of tumorigenic, stem-like neural precursors from human glioblastoma*. Cancer Res, 2004. **64**(19): p. 7011-21.
171. Glumac, P.M. and A.M. LeBeau, *The role of CD133 in cancer: a concise review*. Clin Transl Med, 2018. **7**(1): p. 18.
172. De Bacco, F., et al., *The MET oncogene is a functional marker of a glioblastoma stem cell subtype*. Cancer Res, 2012. **72**(17): p. 4537-50.
173. Kelly, P.N., et al., *Tumor growth need not be driven by rare cancer stem cells*. Science, 2007. **317**(5836): p. 337.
174. Patel, A.P., et al., *Single-cell RNA-seq highlights intratumoral heterogeneity in primary glioblastoma*. Science, 2014. **344**(6190): p. 1396-401.
175. Meyer, M., et al., *Single cell-derived clonal analysis of human glioblastoma links functional and genomic heterogeneity*. Proc Natl Acad Sci U S A, 2015. **112**(3): p. 851-6.
176. Lee, J., et al., *Tumor stem cells derived from glioblastomas cultured in bFGF and EGF more closely mirror the phenotype and genotype of primary tumors than do serum-cultured cell lines*. Cancer Cell, 2006. **9**(5): p. 391-403.
177. Hubert, C.G., et al., *A Three-Dimensional Organoid Culture System Derived from Human Glioblastomas Recapitulates the Hypoxic Gradients and Cancer Stem*

Cell Heterogeneity of Tumors Found In Vivo. Cancer Res, 2016. **76**(8): p. 2465-77.
178. Vlachogiannis, G., et al., *Patient-derived organoids model treatment response of metastatic gastrointestinal cancers*. Science, 2018. **359**(6378): p. 920-926.
179. Calabrese, C., et al., *A perivascular niche for brain tumor stem cells*. Cancer Cell, 2007. **11**(1): p. 69-82.
180. Shiraki, Y., et al., *Significance of perivascular tumour cells defined by CD109 expression in progression of glioma*. J Pathol, 2017. **243**(4): p. 468-480.
181. Seidel, S., et al., *A hypoxic niche regulates glioblastoma stem cells through hypoxia inducible factor 2 alpha*. Brain, 2010. **133**(Pt 4): p. 983-95.
182. Inukai, M., et al., *Hypoxia-mediated cancer stem cells in pseudopalisades with activation of hypoxia-inducible factor-1alpha/Akt axis in glioblastoma*. Hum Pathol, 2015. **46**(10): p. 1496-505.
183. Man, J., et al., *Hypoxic Induction of Vasorin Regulates Notch1 Turnover to Maintain Glioma Stem-like Cells*. Cell Stem Cell, 2018. **22**(1): p. 104-118 e6.
184. Li, Z., et al., *Hypoxia-inducible factors regulate tumorigenic capacity of glioma stem cells*. Cancer Cell, 2009. **15**(6): p. 501-13.
185. Calinescu, A.A., et al., *Survival and Proliferation of Neural Progenitor-Derived Glioblastomas Under Hypoxic Stress is Controlled by a CXCL12/CXCR4 Autocrine-Positive Feedback Mechanism*. Clin Cancer Res, 2017. **23**(5): p. 1250-1262.
186. Suva, M.L., et al., *Reconstructing and reprogramming the tumor-propagating potential of glioblastoma stem-like cells*. Cell, 2014. **157**(3): p. 580-94.
187. Liau, B.B., et al., *Adaptive Chromatin Remodeling Drives Glioblastoma Stem Cell Plasticity and Drug Tolerance*. Cell Stem Cell, 2017. **20**(2): p. 233-246 e7.
188. Bao, S., et al., *Glioma stem cells promote radioresistance by preferential activation of the DNA damage response*. Nature, 2006. **444**(7120): p. 756-60.
189. Chen, J., et al., *A restricted cell population propagates glioblastoma growth after chemotherapy*. Nature, 2012. **488**(7412): p. 522-6.
190. Louveau, A., T.H. Harris, and J. Kipnis, *Revisiting the Mechanisms of CNS Immune Privilege*. Trends Immunol, 2015. **36**(10): p. 569-577.
191. Louveau, A., et al., *Structural and functional features of central nervous system lymphatic vessels*. Nature, 2015. **523**(7560): p. 337-41.
192. Dunn, G.P., et al., *Cancer immunoediting: from immunosurveillance to tumor escape*. Nat Immunol, 2002. **3**(11): p. 991-8.
193. Quail, D.F. and J.A. Joyce, *The Microenvironmental Landscape of Brain Tumors*. Cancer Cell, 2017. **31**(3): p. 326-341.
194. Sorensen, M.D., et al., *Tumour-associated microglia/macrophages predict poor prognosis in high-grade gliomas and correlate with an aggressive tumour subtype*. Neuropathol Appl Neurobiol, 2018. **44**(2): p. 185-206.
195. Pyonteck, S.M., et al., *CSF-1R inhibition alters macrophage polarization and blocks glioma progression*. Nat Med, 2013. **19**(10): p. 1264-72.
196. Saha, D., R.L. Martuza, and S.D. Rabkin, *Macrophage Polarization Contributes to Glioblastoma Eradication by Combination Immunovirotherapy and Immune Checkpoint Blockade*. Cancer Cell, 2017. **32**(2): p. 253-267 e5.
197. Wallmann, T., et al., *Microglia Induce PDGFRB Expression in Glioma Cells to Enhance Their Migratory Capacity*. iScience, 2018. **9**: p. 71-83.
198. Markovic, D.S., et al., *Microglia stimulate the invasiveness of glioma cells by increasing the activity of metalloprotease-2*. J Neuropathol Exp Neurol, 2005. **64**(9): p. 754-62.

199. Woroniecka, K.I., et al., *T-cell Dysfunction in Glioblastoma: Applying a New Framework*. Clin Cancer Res, 2018. **24**(16): p. 3792-3802.
200. Quezada, C., et al., *Role of extracellular vesicles in glioma progression*. Mol Aspects Med, 2018. **60**: p. 38-51.
201. Pavlyukov, M.S., et al., *Apoptotic Cell-Derived Extracellular Vesicles Promote Malignancy of Glioblastoma Via Intercellular Transfer of Splicing Factors*. Cancer Cell, 2018. **34**(1): p. 119-135 e10.
202. Abbott, N.J., *Blood-brain barrier structure and function and the challenges for CNS drug delivery*. J Inherit Metab Dis, 2013. **36**(3): p. 437-49.
203. Wolburg, H., et al., *The disturbed blood-brain barrier in human glioblastoma*. Mol Aspects Med, 2012. **33**(5-6): p. 579-89.
204. Obermeier, B., R. Daneman, and R.M. Ransohoff, *Development, maintenance and disruption of the blood-brain barrier*. Nat Med, 2013. **19**(12): p. 1584-96.
205. Agarwal, S., et al., *Function of the blood-brain barrier and restriction of drug delivery to invasive glioma cells: findings in an orthotopic rat xenograft model of glioma*. Drug Metab Dispos, 2013. **41**(1): p. 33-9.
206. Sarkaria, J.N., et al., *Is the blood-brain barrier really disrupted in all glioblastomas? A critical assessment of existing clinical data*. Neuro Oncol, 2018. **20**(2): p. 184-191.
207. Harder, B.G., et al., *Developments in Blood-Brain Barrier Penetrance and Drug Repurposing for Improved Treatment of Glioblastoma*. Front Oncol, 2018. **8**: p. 462.
208. Vittori, M., H. Motaln, and T.L. Turnsek, *The study of glioma by xenotransplantation in zebrafish early life stages*. J Histochem Cytochem, 2015. **63**(10): p. 749-61.
209. Yang, X.J., et al., *A novel zebrafish xenotransplantation model for study of glioma stem cell invasion*. PLoS One, 2013. **8**(4): p. e61801.
210. Inda, M.M., et al., *Tumor heterogeneity is an active process maintained by a mutant EGFR-induced cytokine circuit in glioblastoma*. Genes Dev, 2010. **24**(16): p. 1731-45.
211. Miller, T.E., et al., *Transcription elongation factors represent in vivo cancer dependencies in glioblastoma*. Nature, 2017. **547**(7663): p. 355-359.
212. Jacobs, V.L., et al., *Current review of in vivo GBM rodent models: emphasis on the CNS-1 tumour model*. ASN Neuro, 2011. **3**(3): p. e00063.
213. Zagzag, D., et al., *Expression of hypoxia-inducible factor 1alpha in brain tumors: association with angiogenesis, invasion, and progression*. Cancer, 2000. **88**(11): p. 2606-18.
214. Grobben, B., P.P. De Deyn, and H. Slegers, *Rat C6 glioma as experimental model system for the study of glioblastoma growth and invasion*. Cell Tissue Res, 2002. **310**(3): p. 257-70.
215. Genoud, V., et al., *Responsiveness to anti-PD-1 and anti-CTLA-4 immune checkpoint blockade in SB28 and GL261 mouse glioma models*. Oncoimmunology, 2018. **7**(12): p. e1501137.
216. Nowak-Sliwinska, P., et al., *Consensus guidelines for the use and interpretation of angiogenesis assays*. Angiogenesis, 2018. **21**(3): p. 425-532.
217. Hagedorn, M., et al., *Accessing key steps of human tumor progression in vivo by using an avian embryo model*. Proc Natl Acad Sci U S A, 2005. **102**(5): p. 1643-8.

218. Hatfield, S.M., et al., *Systemic oxygenation weakens the hypoxia and hypoxia inducible factor 1alpha-dependent and extracellular adenosine-mediated tumor protection*. J Mol Med (Berl), 2014. **92**(12): p. 1283-92.
219. Jayaprakash, P., et al., *Targeted hypoxia reduction restores T cell infiltration and sensitizes prostate cancer to immunotherapy*. J Clin Invest, 2018. **128**(11): p. 5137-5149.
220. Ryan, H.E., J. Lo, and R.S. Johnson, *HIF-1 alpha is required for solid tumor formation and embryonic vascularization*. EMBO J, 1998. **17**(11): p. 3005-15.
221. Maxwell, P.H., et al., *Hypoxia-inducible factor-1 modulates gene expression in solid tumors and influences both angiogenesis and tumor growth*. Proc Natl Acad Sci U S A, 1997. **94**(15): p. 8104-9.
222. Semenza, G.L., *Hypoxia-inducible factors: mediators of cancer progression and targets for cancer therapy*. Trends Pharmacol Sci, 2012. **33**(4): p. 207-14.
223. Fallah, J. and B.I. Rini, *HIF Inhibitors: Status of Current Clinical Development*. Curr Oncol Rep, 2019. **21**(1): p. 6.
224. Galanis, E., et al., *Phase II trial of vorinostat in recurrent glioblastoma multiforme: a north central cancer treatment group study*. J Clin Oncol, 2009. **27**(12): p. 2052-8.
225. Friday, B.B., et al., *Phase II trial of vorinostat in combination with bortezomib in recurrent glioblastoma: a north central cancer treatment group study*. Neuro Oncol, 2012. **14**(2): p. 215-21.
226. Ramjiawan, R.R., A.W. Griffioen, and D.G. Duda, *Anti-angiogenesis for cancer revisited: Is there a role for combinations with immunotherapy?* Angiogenesis, 2017. **20**(2): p. 185-204.
227. Fenton, B.M., S.F. Paoni, and I. Ding, *Effect of VEGF receptor-2 antibody on vascular function and oxygenation in spontaneous and transplanted tumors*. Radiother Oncol, 2004. **72**(2): p. 221-30.
228. Jain, R.K., *Normalization of tumor vasculature: an emerging concept in antiangiogenic therapy*. Science, 2005. **307**(5706): p. 58-62.
229. Batchelor, T.T., et al., *Improved tumor oxygenation and survival in glioblastoma patients who show increased blood perfusion after cediranib and chemoradiation*. Proc Natl Acad Sci U S A, 2013. **110**(47): p. 19059-64.
230. Zhou, Q., P. Guo, and J.M. Gallo, *Impact of angiogenesis inhibition by sunitinib on tumor distribution of temozolomide*. Clin Cancer Res, 2008. **14**(5): p. 1540-9.
231. Stylianopoulos, T. and R.K. Jain, *Combining two strategies to improve perfusion and drug delivery in solid tumors*. Proc Natl Acad Sci U S A, 2013. **110**(46): p. 18632-7.
232. Brown, J.M., *SR 4233 (tirapazamine): a new anticancer drug exploiting hypoxia in solid tumours*. Br J Cancer, 1993. **67**(6): p. 1163-70.
233. Borad, M.J., et al., *Randomized Phase II Trial of Gemcitabine Plus TH-302 Versus Gemcitabine in Patients With Advanced Pancreatic Cancer*. J Clin Oncol, 2015. **33**(13): p. 1475-81.
234. Tap, W.D., et al., *Doxorubicin plus evofosfamide versus doxorubicin alone in locally advanced, unresectable or metastatic soft-tissue sarcoma (TH CR-406/SARC021): an international, multicentre, open-label, randomised phase 3 trial*. Lancet Oncol, 2017. **18**(8): p. 1089-1103.
235. Rischin, D., et al., *Tirapazamine, cisplatin, and radiation versus cisplatin and radiation for advanced squamous cell carcinoma of the head and neck (TROG 02.02, HeadSTART): a phase III trial of the Trans-Tasman Radiation Oncology Group*. J Clin Oncol, 2010. **28**(18): p. 2989-95.

236. Laurence, V.M., et al., *Carbogen breathing with nicotinamide improves the oxygen status of tumours in patients*. Br J Cancer, 1995. **72**(1): p. 198-205.
237. Janssens, G.O., et al., *Accelerated radiotherapy with carbogen and nicotinamide for laryngeal cancer: results of a phase III randomized trial*. J Clin Oncol, 2012. **30**(15): p. 1777-83.
238. Brizel, D.M., et al., *The mechanisms by which hyperbaric oxygen and carbogen improve tumour oxygenation*. Br J Cancer, 1995. **72**(5): p. 1120-4.
239. Beppu, T., et al., *Change of oxygen pressure in glioblastoma tissue under various conditions*. J Neurooncol, 2002. **58**(1): p. 47-52.
240. Graham, K. and E. Unger, *Overcoming tumor hypoxia as a barrier to radiotherapy, chemotherapy and immunotherapy in cancer treatment*. Int J Nanomedicine, 2018. **13**: p. 6049-6058.
241. Gaspar, L.E., et al., *Supratentorial malignant glioma: patterns of recurrence and implications for external beam local treatment*. Int J Radiat Oncol Biol Phys, 1992. **24**(1): p. 55-7.
242. Berens, M.E. and A. Giese, "*...those left behind.*" *Biology and oncology of invasive glioma cells*. Neoplasia, 1999. **1**(3): p. 208-19.
243. Orzan, F., et al., *Genetic Evolution of Glioblastoma Stem-Like Cells From Primary to Recurrent Tumor*. Stem Cells, 2017. **35**(11): p. 2218-2228.
244. Friedman, H.S., T. Kerby, and H. Calvert, *Temozolomide and treatment of malignant glioma*. Clin Cancer Res, 2000. **6**(7): p. 2585-97.
245. Stupp, R., et al., *Radiotherapy plus concomitant and adjuvant temozolomide for glioblastoma*. N Engl J Med, 2005. **352**(10): p. 987-96.
246. Esteller, M., et al., *Inactivation of the DNA-repair gene MGMT and the clinical response of gliomas to alkylating agents*. N Engl J Med, 2000. **343**(19): p. 1350-4.
247. Wick, W., et al., *MGMT testing--the challenges for biomarker-based glioma treatment*. Nat Rev Neurol, 2014. **10**(7): p. 372-85.
248. Hegi, M.E., et al., *MGMT Promoter Methylation Cutoff with Safety Margin for Selecting Glioblastoma Patients into Trials Omitting Temozolomide: A Pooled Analysis of Four Clinical Trials*. Clin Cancer Res, 2019. **25**(6): p. 1809-1816.
249. Johnson, B.E., et al., *Mutational analysis reveals the origin and therapy-driven evolution of recurrent glioma*. Science, 2014. **343**(6167): p. 189-193.
250. Wang, J., et al., *Clonal evolution of glioblastoma under therapy*. Nat Genet, 2016. **48**(7): p. 768-76.
251. Young, B., et al., *Reoperation for glioblastoma*. J Neurosurg, 1981. **55**(6): p. 917-21.
252. Robin, A.M., I. Lee, and S.N. Kalkanis, *Reoperation for Recurrent Glioblastoma Multiforme*. Neurosurg Clin N Am, 2017. **28**(3): p. 407-428.
253. Perry, J., et al., *Gliadel wafers in the treatment of malignant glioma: a systematic review*. Curr Oncol, 2007. **14**(5): p. 189-94.
254. Ashby, L.S., K.A. Smith, and B. Stea, *Gliadel wafer implantation combined with standard radiotherapy and concurrent followed by adjuvant temozolomide for treatment of newly diagnosed high-grade glioma: a systematic literature review*. World J Surg Oncol, 2016. **14**(1): p. 225.
255. Herrlinger, U., et al., *Lomustine-temozolomide combination therapy versus standard temozolomide therapy in patients with newly diagnosed glioblastoma with methylated MGMT promoter (CeTeG/NOA-09): a randomised, open-label, phase 3 trial*. Lancet, 2019. **393**(10172): p. 678-688.

256. Cohen, M.H., et al., *FDA drug approval summary: bevacizumab (Avastin) as treatment of recurrent glioblastoma multiforme*. Oncologist, 2009. **14**(11): p. 1131-8.
257. Chinot, O.L., et al., *Bevacizumab plus radiotherapy-temozolomide for newly diagnosed glioblastoma*. N Engl J Med, 2014. **370**(8): p. 709-22.
258. Bottsford-Miller, J.N., R.L. Coleman, and A.K. Sood, *Resistance and escape from antiangiogenesis therapy: clinical implications and future strategies*. J Clin Oncol, 2012. **30**(32): p. 4026-34.
259. Keunen, O., et al., *Anti-VEGF treatment reduces blood supply and increases tumor cell invasion in glioblastoma*. Proc Natl Acad Sci U S A, 2011. **108**(9): p. 3749-54.
260. Wick, W., et al., *Lomustine and Bevacizumab in Progressive Glioblastoma*. N Engl J Med, 2017. **377**(20): p. 1954-1963.
261. Stupp, R., et al., *Effect of Tumor-Treating Fields Plus Maintenance Temozolomide vs Maintenance Temozolomide Alone on Survival in Patients With Glioblastoma: A Randomized Clinical Trial*. JAMA, 2017. **318**(23): p. 2306-2316.
262. Brennan, C.W., et al., *The somatic genomic landscape of glioblastoma*. Cell, 2013. **155**(2): p. 462-77.
263. Wong, A.J., et al., *Increased expression of the epidermal growth factor receptor gene in malignant gliomas is invariably associated with gene amplification*. Proc Natl Acad Sci U S A, 1987. **84**(19): p. 6899-903.
264. Rich, J.N., et al., *Phase II trial of gefitinib in recurrent glioblastoma*. J Clin Oncol, 2004. **22**(1): p. 133-42.
265. van den Bent, M.J., et al., *Randomized phase II trial of erlotinib versus temozolomide or carmustine in recurrent glioblastoma: EORTC brain tumor group study 26034*. J Clin Oncol, 2009. **27**(8): p. 1268-74.
266. Neyns, B., et al., *Stratified phase II trial of cetuximab in patients with recurrent high-grade glioma*. Ann Oncol, 2009. **20**(9): p. 1596-603.
267. Westphal, M., et al., *A randomised, open label phase III trial with nimotuzumab, an anti-epidermal growth factor receptor monoclonal antibody in the treatment of newly diagnosed adult glioblastoma*. Eur J Cancer, 2015. **51**(4): p. 522-32.
268. Stupp, R., et al., *Cilengitide combined with standard treatment for patients with newly diagnosed glioblastoma with methylated MGMT promoter (CENTRIC EORTC 26071-22072 study): a multicentre, randomised, open-label, phase 3 trial*. Lancet Oncol, 2014. **15**(10): p. 1100-8.
269. Nabors, L.B., et al., *Two cilengitide regimens in combination with standard treatment for patients with newly diagnosed glioblastoma and unmethylated MGMT gene promoter: results of the open-label, controlled, randomized phase II CORE study*. Neuro Oncol, 2015. **17**(5): p. 708-17.
270. Fridman, W.H., et al., *The immune contexture in cancer prognosis and treatment*. Nat Rev Clin Oncol, 2017. **14**(12): p. 717-734.
271. Chen, D.S. and I. Mellman, *Oncology meets immunology: the cancer-immunity cycle*. Immunity, 2013. **39**(1): p. 1-10.
272. Everson, R.G., et al., *Efficacy of systemic adoptive transfer immunotherapy targeting NY-ESO-1 for glioblastoma*. Neuro Oncol, 2016. **18**(3): p. 368-78.
273. Riccadonna, C., et al., *Decitabine Treatment of Glioma-Initiating Cells Enhances Immune Recognition and Killing*. PLoS One, 2016. **11**(8): p. e0162105.
274. Hodi, F.S., et al., *Improved survival with ipilimumab in patients with metastatic melanoma*. N Engl J Med, 2010. **363**(8): p. 711-23.

275. Schalper, K.A., et al., *Neoadjuvant nivolumab modifies the tumor immune microenvironment in resectable glioblastoma*. Nat Med, 2019. **25**(3): p. 470-476.
276. Cloughesy, T.F., et al., *Neoadjuvant anti-PD-1 immunotherapy promotes a survival benefit with intratumoral and systemic immune responses in recurrent glioblastoma*. Nat Med, 2019. **25**(3): p. 477-486.
277. Zhao, J., et al., *Immune and genomic correlates of response to anti-PD-1 immunotherapy in glioblastoma*. Nat Med, 2019. **25**(3): p. 462-469.
278. Quezada, S.A., et al., *CD40/CD154 interactions at the interface of tolerance and immunity*. Annu Rev Immunol, 2004. **22**: p. 307-28.
279. Chonan, M., et al., *CD40/CD40L expression correlates with the survival of patients with glioblastomas and an augmentation in CD40 signaling enhances the efficacy of vaccinations against glioma models*. Neuro Oncol, 2015. **17**(11): p. 1453-62.
280. Alexandroff, A.B., et al., *Role for CD40-CD40 ligand interactions in the immune response to solid tumours*. Mol Immunol, 2000. **37**(9): p. 515-26.
281. Calvo Tardon, M., et al., *Peptides as cancer vaccines*. Curr Opin Pharmacol, 2019. **47**: p. 20-26.
282. van Willigen, W.W., et al., *Dendritic Cell Cancer Therapy: Vaccinating the Right Patient at the Right Time*. Front Immunol, 2018. **9**: p. 2265.
283. Brown, C.E., et al., *Bioactivity and Safety of IL13Ralpha2-Redirected Chimeric Antigen Receptor CD8+ T Cells in Patients with Recurrent Glioblastoma*. Clin Cancer Res, 2015. **21**(18): p. 4062-72.
284. Brown, C.E., et al., *Regression of Glioblastoma after Chimeric Antigen Receptor T-Cell Therapy*. N Engl J Med, 2016. **375**(26): p. 2561-9.
285. O'Rourke, D.M., et al., *A single dose of peripherally infused EGFRvIII-directed CAR T cells mediates antigen loss and induces adaptive resistance in patients with recurrent glioblastoma*. Sci Transl Med, 2017. **9**(399).
286. Bielamowicz, K., et al., *Trivalent CAR T cells overcome interpatient antigenic variability in glioblastoma*. Neuro Oncol, 2018. **20**(4): p. 506-518.
287. Cobbs, C.S., et al., *Human cytomegalovirus infection and expression in human malignant glioma*. Cancer Res, 2002. **62**(12): p. 3347-50.
288. Stragliotto, G., et al., *Effects of valganciclovir as an add-on therapy in patients with cytomegalovirus-positive glioblastoma: a randomized, double-blind, hypothesis-generating study*. Int J Cancer, 2013. **133**(5): p. 1204-13.
289. Soderberg-Naucler, C., A. Rahbar, and G. Stragliotto, *Survival in patients with glioblastoma receiving valganciclovir*. N Engl J Med, 2013. **369**(10): p. 985-6.
290. Batich, K.A., et al., *Long-term Survival in Glioblastoma with Cytomegalovirus pp65-Targeted Vaccination*. Clin Cancer Res, 2017. **23**(8): p. 1898-1909.
291. Reap, E.A., et al., *Dendritic Cells Enhance Polyfunctionality of Adoptively Transferred T Cells That Target Cytomegalovirus in Glioblastoma*. Cancer Res, 2018. **78**(1): p. 256-264.
292. Park, N.I., et al., *ASCL1 Reorganizes Chromatin to Direct Neuronal Fate and Suppress Tumorigenicity of Glioblastoma Stem Cells*. Cell Stem Cell, 2017. **21**(3): p. 411.
293. Caren, H., et al., *Glioblastoma Stem Cells Respond to Differentiation Cues but Fail to Undergo Commitment and Terminal Cell-Cycle Arrest*. Stem Cell Reports, 2015. **5**(5): p. 829-842.
294. Jin, X., et al., *Targeting glioma stem cells through combined BMI1 and EZH2 inhibition*. Nat Med, 2017. **23**(11): p. 1352-1361.

295. Yu, D., et al., *Multiplexed RNAi therapy against brain tumor-initiating cells via lipopolymeric nanoparticle infusion delays glioblastoma progression*. Proc Natl Acad Sci U S A, 2017. **114**(30): p. E6147-E6156.
296. Vengoji, R., et al., *Natural products: a hope for glioblastoma patients*. Oncotarget, 2018. **9**(31): p. 22194-22219.
297. Trogrlic, I., et al., *Treatment of glioblastoma with herbal medicines*. World J Surg Oncol, 2018. **16**(1): p. 28.
298. Elsakka, A.M.A., et al., *Management of Glioblastoma Multiforme in a Patient Treated With Ketogenic Metabolic Therapy and Modified Standard of Care: A 24-Month Follow-Up*. Front Nutr, 2018. **5**: p. 20.
299. Safdie, F., et al., *Fasting enhances the response of glioma to chemo- and radiotherapy*. PLoS One, 2012. **7**(9): p. e44603.
300. Vanderbeek, A.M., et al., *The clinical trials landscape for glioblastoma: is it adequate to develop new treatments?* Neuro Oncol, 2018. **20**(8): p. 1034-1043.
301. Shchors, K., A. Massaras, and D. Hanahan, *Dual Targeting of the Autophagic Regulatory Circuitry in Gliomas with Repurposed Drugs Elicits Cell-Lethal Autophagy and Therapeutic Benefit*. Cancer Cell, 2015. **28**(4): p. 456-471.
302. Rao Kondapally Seshasai, S., et al., *Diabetes mellitus, fasting glucose, and risk of cause-specific death*. N Engl J Med, 2011. **364**(9): p. 829-841.
303. Evans, J.M., et al., *Metformin and reduced risk of cancer in diabetic patients*. BMJ, 2005. **330**(7503): p. 1304-5.
304. Bowker, S.L., et al., *Increased cancer-related mortality for patients with type 2 diabetes who use sulfonylureas or insulin*. Diabetes Care, 2006. **29**(2): p. 254-8.
305. Scarpello, J.H. and H.C. Howlett, *Metformin therapy and clinical uses*. Diab Vasc Dis Res, 2008. **5**(3): p. 157-67.
306. Kasznicki, J., A. Sliwinska, and J. Drzewoski, *Metformin in cancer prevention and therapy*. Ann Transl Med, 2014. **2**(6): p. 57.
307. Higurashi, T., et al., *Metformin for chemoprevention of metachronous colorectal adenoma or polyps in post-polypectomy patients without diabetes: a multicentre double-blind, placebo-controlled, randomised phase 3 trial*. Lancet Oncol, 2016. **17**(4): p. 475-483.
308. Mantovani, A. and G. Targher, *Type 2 diabetes mellitus and risk of hepatocellular carcinoma: spotlight on nonalcoholic fatty liver disease*. Ann Transl Med, 2017. **5**(13): p. 270.
309. De Souza, A., et al., *Diabetes Type 2 and Pancreatic Cancer: A History Unfolding*. JOP, 2016. **17**(2): p. 144-148.
310. Coyle, C., et al., *Metformin as an adjuvant treatment for cancer: a systematic review and meta-analysis*. Ann Oncol, 2016. **27**(12): p. 2184-2195.
311. Kordes, S., et al., *Metformin in patients with advanced pancreatic cancer: a double-blind, randomised, placebo-controlled phase 2 trial*. Lancet Oncol, 2015. **16**(7): p. 839-47.
312. Valtorta, S., et al., *Metformin and temozolomide, a synergic option to overcome resistance in glioblastoma multiforme models*. Oncotarget, 2017. **8**(68): p. 113090-113104.
313. Maraka, S., et al., *Phase 1 lead-in to a phase 2 factorial study of temozolomide plus memantine, mefloquine, and metformin as postradiation adjuvant therapy for newly diagnosed glioblastoma*. Cancer, 2019. **125**(3): p. 424-433.
314. Al Hassan, M., et al., *Metformin Treatment Inhibits Motility and Invasion of Glioblastoma Cancer Cells*. Anal Cell Pathol (Amst), 2018. **2018**: p. 5917470.

315. Kim, E.H., et al., *Inhibition of glioblastoma tumorspheres by combined treatment with 2-deoxyglucose and metformin*. Neuro Oncol, 2017. **19**(2): p. 197-207.
316. Sesen, J., et al., *Metformin inhibits growth of human glioblastoma cells and enhances therapeutic response*. PLoS One, 2015. **10**(4): p. e0123721.
317. Wang, G.S. and C. Hoyte, *Review of Biguanide (Metformin) Toxicity*. J Intensive Care Med, 2018: p. 885066618793385.
318. Rena, G., D.G. Hardie, and E.R. Pearson, *The mechanisms of action of metformin*. Diabetologia, 2017. **60**(9): p. 1577-1585.
319. Goodwin, P.J., et al., *Insulin-lowering effects of metformin in women with early breast cancer*. Clin Breast Cancer, 2008. **8**(6): p. 501-5.
320. Pollak, M., *The insulin and insulin-like growth factor receptor family in neoplasia: an update*. Nat Rev Cancer, 2012. **12**(3): p. 159-69.
321. Pollak, M., *Potential applications for biguanides in oncology*. J Clin Invest, 2013. **123**(9): p. 3693-700.
322. Dowling, R.J., et al., *Metformin inhibits mammalian target of rapamycin-dependent translation initiation in breast cancer cells*. Cancer Res, 2007. **67**(22): p. 10804-12.
323. Memmott, R.M., et al., *Metformin prevents tobacco carcinogen--induced lung tumorigenesis*. Cancer Prev Res (Phila), 2010. **3**(9): p. 1066-76.
324. Wilson, W.R. and M.P. Hay, *Targeting hypoxia in cancer therapy*. Nat Rev Cancer, 2011. **11**(6): p. 393-410.
325. Brugarolas, J., et al., *Regulation of mTOR function in response to hypoxia by REDD1 and the TSC1/TSC2 tumor suppressor complex*. Genes Dev, 2004. **18**(23): p. 2893-904.
326. Shoshani, T., et al., *Identification of a novel hypoxia-inducible factor 1-responsive gene, RTP801, involved in apoptosis*. Mol Cell Biol, 2002. **22**(7): p. 2283-93.
327. Pencreach, E., et al., *Marked activity of irinotecan and rapamycin combination toward colon cancer cells in vivo and in vitro is mediated through cooperative modulation of the mammalian target of rapamycin/hypoxia-inducible factor-1alpha axis*. Clin Cancer Res, 2009. **15**(4): p. 1297-307.
328. Ma, D.J., et al., *A phase II trial of everolimus, temozolomide, and radiotherapy in patients with newly diagnosed glioblastoma: NCCTG N057K*. Neuro Oncol, 2015. **17**(9): p. 1261-9.
329. Wick, W., et al., *Phase II Study of Radiotherapy and Temsirolimus versus Radiochemotherapy with Temozolomide in Patients with Newly Diagnosed Glioblastoma without MGMT Promoter Hypermethylation (EORTC 26082)*. Clin Cancer Res, 2016. **22**(19): p. 4797-4806.
330. Andrzejewski, S., et al., *Metformin directly acts on mitochondria to alter cellular bioenergetics*. Cancer Metab, 2014. **2**: p. 12.
331. Wheaton, W.W., et al., *Metformin inhibits mitochondrial complex I of cancer cells to reduce tumorigenesis*. Elife, 2014. **3**: p. e02242.
332. Zannella, V.E., et al., *Reprogramming metabolism with metformin improves tumor oxygenation and radiotherapy response*. Clin Cancer Res, 2013. **19**(24): p. 6741-50.
333. Wang, J., et al., *Suppression of tumor angiogenesis by metformin treatment via a mechanism linked to targeting of HER2/HIF-1alpha/VEGF secretion axis*. Oncotarget, 2015. **6**(42): p. 44579-92.
334. Weiss, A., et al., *Rapid optimization of drug combinations for the optimal angiostatic treatment of cancer*. Angiogenesis, 2015. **18**(3): p. 233-44.

335. Piali, L., et al., *Murine platelet endothelial cell adhesion molecule (PECAM-1)/CD31 modulates beta 2 integrins on lymphokine-activated killer cells*. Eur J Immunol, 1993. **23**(10): p. 2464-71.
336. Zeppernick, F., et al., *Stem cell marker CD133 affects clinical outcome in glioma patients*. Clin Cancer Res, 2008. **14**(1): p. 123-9.
337. Shibahara, I., et al., *The expression status of CD133 is associated with the pattern and timing of primary glioblastoma recurrence*. Neuro Oncol, 2013. **15**(9): p. 1151-9.
338. Soeda, A., et al., *Hypoxia promotes expansion of the CD133-positive glioma stem cells through activation of HIF-1alpha*. Oncogene, 2009. **28**(45): p. 3949-59.
339. Holmberg Olausson, K., et al., *Prominin-1 (CD133) defines both stem and non-stem cell populations in CNS development and gliomas*. PLoS One, 2014. **9**(9): p. e106694.
340. Baker, M., *1,500 scientists lift the lid on reproducibility*. Nature, 2016. **533**(7604): p. 452-4.
341. Dennis, M.D., et al., *REDD1 enhances protein phosphatase 2A-mediated dephosphorylation of Akt to repress mTORC1 signaling*. Sci Signal, 2014. **7**(335): p. ra68.
342. Katiyar, S., et al., *REDD1, an inhibitor of mTOR signalling, is regulated by the CUL4A-DDB1 ubiquitin ligase*. EMBO Rep, 2009. **10**(8): p. 866-72.
343. Ben Sahra, I., et al., *Metformin, independent of AMPK, induces mTOR inhibition and cell-cycle arrest through REDD1*. Cancer Res, 2011. **71**(13): p. 4366-72.
344. Reuschel, E.L., et al., *REDD1 Is Essential for Optimal T Cell Proliferation and Survival*. PLoS One, 2015. **10**(8): p. e0136323.
345. Yu, B., S. Pugazhenthi, and R.L. Khandelwal, *Effects of metformin on glucose and glucagon regulated gluconeogenesis in cultured normal and diabetic hepatocytes*. Biochem Pharmacol, 1994. **48**(5): p. 949-54.
346. Mandal, R., et al., *Multi-platform characterization of the human cerebrospinal fluid metabolome: a comprehensive and quantitative update*. Genome Med, 2012. **4**(4): p. 38.
347. Labuzek, K., et al., *Quantification of metformin by the HPLC method in brain regions, cerebrospinal fluid and plasma of rats treated with lipopolysaccharide*. Pharmacol Rep, 2010. **62**(5): p. 956-65.
348. Reagan-Shaw, S., M. Nihal, and N. Ahmad, *Dose translation from animal to human studies revisited*. FASEB J, 2008. **22**(3): p. 659-61.
349. Tucker, G.T., et al., *Metformin kinetics in healthy subjects and in patients with diabetes mellitus*. Br J Clin Pharmacol, 1981. **12**(2): p. 235-46.
350. Nath, N., et al., *Metformin attenuated the autoimmune disease of the central nervous system in animal models of multiple sclerosis*. J Immunol, 2009. **182**(12): p. 8005-14.
351. Graham, G.G., et al., *Clinical pharmacokinetics of metformin*. Clin Pharmacokinet, 2011. **50**(2): p. 81-98.
352. Eikawa, S., et al., *Immune-mediated antitumor effect by type 2 diabetes drug, metformin*. Proc Natl Acad Sci U S A, 2015. **112**(6): p. 1809-14.
353. Incio, J., et al., *Metformin Reduces Desmoplasia in Pancreatic Cancer by Reprogramming Stellate Cells and Tumor-Associated Macrophages*. PLoS One, 2015. **10**(12): p. e0141392.
354. Scharping, N.E., et al., *Efficacy of PD-1 Blockade Is Potentiated by Metformin-Induced Reduction of Tumor Hypoxia*. Cancer Immunol Res, 2017. **5**(1): p. 9-16.

355. Proctor, C.M., et al., *Electrophoretic drug delivery for seizure control*. Sci Adv, 2018. **4**(8): p. eaau1291.
356. Dagdeviren, C., et al., *Miniaturized neural system for chronic, local intracerebral drug delivery*. Sci Transl Med, 2018. **10**(425).
357. Vogelbaum, M.A. and M.K. Aghi, *Convection-enhanced delivery for the treatment of glioblastoma*. Neuro Oncol, 2015. **17 Suppl 2**: p. ii3-ii8.
358. Ding, L., et al., *Metformin prevents cancer metastasis by inhibiting M2-like polarization of tumor associated macrophages*. Oncotarget, 2015. **6**(34): p. 36441-55.
359. Yang, S.H., et al., *Metformin treatment reduces temozolomide resistance of glioblastoma cells*. Oncotarget, 2016. **7**(48): p. 78787-78803.
360. Lee, J.E., et al., *High-Dose Metformin Plus Temozolomide Shows Increased Anti-tumor Effects in Glioblastoma In Vitro and In Vivo Compared with Monotherapy*. Cancer Res Treat, 2018. **50**(4): p. 1331-1342.
361. Yu, Z., et al., *Temozolomide in combination with metformin act synergistically to inhibit proliferation and expansion of glioma stem-like cells*. Oncol Lett, 2016. **11**(4): p. 2792-2800.
362. Elgendy, M., et al., *Combination of Hypoglycemia and Metformin Impairs Tumor Metabolic Plasticity and Growth by Modulating the PP2A-GSK3beta-MCL-1 Axis*. Cancer Cell, 2019.
363. Goel, S., A.H. Wong, and R.K. Jain, *Vascular normalization as a therapeutic strategy for malignant and nonmalignant disease*. Cold Spring Harb Perspect Med, 2012. **2**(3): p. a006486.
364. Zhou, W., et al., *Targeting Glioma Stem Cell-Derived Pericytes Disrupts the Blood-Tumor Barrier and Improves Chemotherapeutic Efficacy*. Cell Stem Cell, 2017. **21**(5): p. 591-603 e4.
365. Tran Thang, N.N., et al., *Immune infiltration of spontaneous mouse astrocytomas is dominated by immunosuppressive cells from early stages of tumor development*. Cancer Res, 2010. **70**(12): p. 4829-39.
366. Lenting, K., et al., *Glioma: experimental models and reality*. Acta Neuropathol, 2017. **133**(2): p. 263-282.
367. Kim, H., et al., *The hypoxic tumor microenvironment in vivo selects the cancer stem cell fate of breast cancer cells*. Breast Cancer Res, 2018. **20**(1): p. 16.
368. Taddei, M.L., et al., *Microenvironment and tumor cell plasticity: an easy way out*. Cancer Lett, 2013. **341**(1): p. 80-96.
369. Sridhar, K.S., et al., *Effects of physiological oxygen concentration on human tumor colony growth in soft agar*. Cancer Res, 1983. **43**(10): p. 4629-31.
370. Stadlbauer, A., et al., *Vascular Hysteresis Loops and Vascular Architecture Mapping in Patients with Glioblastoma treated with Antiangiogenic Therapy*. Sci Rep, 2017. **7**(1): p. 8508.
371. Burgi, S., et al., *In vivo imaging of hypoxia-inducible factor regulation in a subcutaneous and orthotopic GL261 glioma tumor model using a reporter gene assay*. Mol Imaging, 2014. **13**.
372. Denko, N.C., et al., *Investigating hypoxic tumor physiology through gene expression patterns*. Oncogene, 2003. **22**(37): p. 5907-14.
373. Darmanis, S., et al., *Single-Cell RNA-Seq Analysis of Infiltrating Neoplastic Cells at the Migrating Front of Human Glioblastoma*. Cell Rep, 2017. **21**(5): p. 1399-1410.
374. Bowman, R.L., et al., *GlioVis data portal for visualization and analysis of brain tumor expression datasets*. Neuro Oncol, 2017. **19**(1): p. 139-141.

375. Kleihues, P., P.C. Burger, and B.W. Scheithauer, *The new WHO classification of brain tumours*. Brain Pathol, 1993. **3**(3): p. 255-68.
376. Louis, D.N., et al., *The 2016 World Health Organization Classification of Tumors of the Central Nervous System: a summary*. Acta Neuropathol, 2016. **131**(6): p. 803-20.
377. Nutt, C.L., et al., *Gene expression-based classification of malignant gliomas correlates better with survival than histological classification*. Cancer Res, 2003. **63**(7): p. 1602-7.
378. Hegi, M.E. and R. Stupp, *Withholding temozolomide in glioblastoma patients with unmethylated MGMT promoter--still a dilemma?* Neuro Oncol, 2015. **17**(11): p. 1425-7.
379. Mamatjan, Y., et al., *Molecular Signatures for Tumor Classification: An Analysis of The Cancer Genome Atlas Data*. J Mol Diagn, 2017. **19**(6): p. 881-891.
380. Bozdag, S., et al., *Age-specific signatures of glioblastoma at the genomic, genetic, and epigenetic levels*. PLoS One, 2013. **8**(4): p. e62982.
381. Murat, A., et al., *Stem cell-related "self-renewal" signature and high epidermal growth factor receptor expression associated with resistance to concomitant chemoradiotherapy in glioblastoma*. J Clin Oncol, 2008. **26**(18): p. 3015-24.
382. deSouza, R.M., et al., *Has the survival of patients with glioblastoma changed over the years?* Br J Cancer, 2016. **114**(12): p. e20.
383. Ferla, R., E. Haspinger, and E. Surmacz, *Metformin inhibits leptin-induced growth and migration of glioblastoma cells*. Oncol Lett, 2012. **4**(5): p. 1077-1081.
384. Ucbek, A., et al., *Effect of metformin on the human T98G glioblastoma multiforme cell line*. Exp Ther Med, 2014. **7**(5): p. 1285-1290.
385. Zhou, X., et al., *Metformin suppresses hypoxia-induced stabilization of HIF-1alpha through reprogramming of oxygen metabolism in hepatocellular carcinoma*. Oncotarget, 2016. **7**(1): p. 873-84.
386. Burroughs, S.K., et al., *Hypoxia inducible factor pathway inhibitors as anticancer therapeutics*. Future Med Chem, 2013. **5**(5): p. 553-72.
387. Garofalo, C., et al., *Metformin as an adjuvant drug against pediatric sarcomas: hypoxia limits therapeutic effects of the drug*. PLoS One, 2013. **8**(12): p. e83832.
388. Brandes, A.A., et al., *Practical management of bevacizumab-related toxicities in glioblastoma*. Oncologist, 2015. **20**(2): p. 166-75.
389. Hardee, M.E. and D. Zagzag, *Mechanisms of glioma-associated neovascularization*. Am J Pathol, 2012. **181**(4): p. 1126-41.
390. Zhou, Q. and J.M. Gallo, *Differential effect of sunitinib on the distribution of temozolomide in an orthotopic glioma model*. Neuro Oncol, 2009. **11**(3): p. 301-10.
391. Dewhirst, M.W., Y. Cao, and B. Moeller, *Cycling hypoxia and free radicals regulate angiogenesis and radiotherapy response*. Nat Rev Cancer, 2008. **8**(6): p. 425-37.
392. Hammond, E.M., M.J. Dorie, and A.J. Giaccia, *ATR/ATM targets are phosphorylated by ATR in response to hypoxia and ATM in response to reoxygenation*. J Biol Chem, 2003. **278**(14): p. 12207-13.
393. Rofstad, E.K., et al., *Tumors exposed to acute cyclic hypoxic stress show enhanced angiogenesis, perfusion and metastatic dissemination*. Int J Cancer, 2010. **127**(7): p. 1535-46.
394. Chen, S., et al., *Genome-wide CRISPR screen in a mouse model of tumor growth and metastasis*. Cell, 2015. **160**(6): p. 1246-60.

Available online at www.sciencedirect.com

ScienceDirect

Current Opinion in Pharmacology

Peptides as cancer vaccines

Marta Calvo Tardón[1], Mathilde Allard[1], Valérie Dutoit[2], Pierre-Yves Dietrich[2] and Paul R Walker[1]

Cancer vaccines based on synthetic peptides are a safe, well-tolerated immunotherapy able to specifically stimulate tumor-reactive T cells. However, their clinical efficacy does not approach that achieved with other immunotherapies such as immune checkpoint blockade. Nevertheless, major advances have been made in selecting tumor antigens to target, identifying epitopes binding to classical and non-classical HLA molecules, and incorporating these into optimal sized peptides for formulation into a vaccine. Limited potency of currently used adjuvants and the immunosuppressive tumor microenvironment are now understood to be major impediments to vaccine efficacy that need to be overcome. Rationally designed combination therapies are now being tested and should ultimately enable peptide vaccination to be added to immuno-oncology treatment options.

Addresses
[1] Center for Translational Research in Onco-Hematology, Division of Oncology, Geneva University Hospitals and University of Geneva, Geneva, Switzerland
[2] Center for Translational Research in Onco-Hematology, Department of Oncology, Geneva University Hospitals and University of Geneva, Geneva, Switzerland

Corresponding author: Walker, Paul R (Paul.Walker@unige.ch)

Current Opinion in Pharmacology 2019, **47**:20–26

This review comes from a themed issue on **Cancer**

Edited by **Laura Soucek** and **Jonathan Whitfield**

https://doi.org/10.1016/j.coph.2019.01.007

Introduction

Therapeutic cancer vaccines based on peptides have been envisaged and developed for almost 40 years and yet the approach remains in a status of 'potential' interest for cancer therapy rather than one with unequivocal clinical benefit. Notwithstanding this stark appraisal of the current situation and the absence of FDA-approval for peptide cancer vaccines, there have been major advances in the field. Peptide vaccines are able to elicit an immune response against a tumor [1,2], and hundreds of clinical trials [3•] are providing a wealth of information that is driving the field forward. A realistic roadmap for clinical development will take into account the lessons learned from suboptimal vaccination protocols, the resistance of tumor cells and the hostility of the tumor microenvironment, and the opportunities of combinations with other forms of immunotherapy such as immune checkpoint blockade (ICB).

Cancer vaccines targeting defined antigens aim to induce or expand cancer-specific T cells and rely on DNA, RNA, proteins or peptides. The latter offer the most direct way of targeting a specific epitope, the portion of the antigen that is recognized by the T-cell receptor in association with human leukocyte antigen (HLA) molecules, thus stimulating T cells with defined tumor specificity. This precision targeting contrasts with the broad immunity (including autoimmune responses) induced by immune checkpoint blocking antibodies and contributes to the excellent safety and tolerability profile of peptide vaccines. Moreover, synthesis of clinical grade peptides of virtually any specificity is achieved more rapidly and cost-effectively than a human or humanized therapeutic antibody. Nevertheless, these advantages are offset by the fact that a given peptide epitope will efficiently bind to only one or a few HLA alleles, thus limiting a particular peptide vaccine formulation to a subset of cancer patients. In many clinical trials using peptide vaccines in Europe and the USA, HLA-A2 binding peptides are used and inclusion criteria require expression of this allele, a condition satisfied by around one third of patients. Choice of the peptide sequence is the first essential requirement of a peptide vaccine, but this is not sufficient to elicit an effective immune response. Peptide length or other modifications, administration regimen, adjuvants and combinations with other therapies are all key in determining final clinical efficacy of therapeutic peptide vaccines.

Antigens to target

Many therapeutic vaccines have targeted non-mutated tumor-associated antigens (TAA), which are shared between healthy and tumor cells, but are overexpressed by cancer cells. The advantage of targeting TAA is their expression by cancers from many individuals. However, since these TAA are self-proteins, the repertoire of high avidity T cells with corresponding specificity can be restricted due to immunological tolerance. Whether this significantly impacts clinical vaccination has been difficult to directly assess, because immunomonitoring is often relatively insensitive and never exhaustive. More recent advances may address this issue more adequately, although with the limitations of clinical sampling in the

peripheral blood rather than at the tumor site [4,5]. Results of phase III trials of such TAA vaccines have been disappointing in the case of pancreatic cancer, non-small-cell lung cancer and renal cell carcinoma [6–8]. Nevertheless, the approach continues in other indications, including bladder cancer, prostate cancer, and glioma [9–11]. Although data are only reported for pilot studies and phase I/II trials to date, the results are promising as they show peptide-specific CD8 T cell-responses in several patients, which was correlated with longer survival.

Targeting epitopes expressed only in cancer cells and absent in healthy tissue, the so-called tumor-specific antigens (TSA), can obviate the limitations of a partially tolerant T-cell repertoire. These antigens can originate from viruses associated with certain cancers (e.g. HPV and HBV) or from mutated proteins, termed neoantigens. In the former category, several phase I and II clinical trials targeting HPV are underway or have been completed (as recently reviewed [12]). Although peptide vaccination alone may be insufficient for tumor regression, encouraging results from a phase II trial in patients with incurable HPV-16 related malignances point to the interest of long-peptide vaccination combined with ICB [13]. However, human cancers with a known viral etiology are the exception, and most TSA derive from mutated epitopes. These neoantigens can arise from point mutations, but other genetic rearrangements such as insertions and deletions can also be the underlying cause [14]. Some of these may be common to multiple tumors, such as the neoepitope expressed by many glioblastomas, EGFRvIII, as a result of a truncation in the wild-type EGFR. However, a phase III clinical trial targeting this epitope with rindopepimut vaccine in addition to chemotherapy did not improve survival over chemotherapy alone [15]. This study assessed humoral responses but did not address the role of vaccine-induced T cells. Since the best described mechanism of action of peptide vaccines for cancer is induction of tumor-specific T cells, it is difficult to judge whether failure of this trial was a result of an absence of such a cellular response.

An additional problem of targeting only one epitope, as performed in the previous study, is the heterogeneous antigen expression and the outgrowth of antigen-negative tumor cells. Multi-peptide vaccines are one solution to this, as long as sufficient tumor antigens are identified. For TAAs, this was achieved by peptide elution from tumor cells for the IMA901 vaccine for renal cell carcinoma [8] and the IMA950 vaccine for glioblastoma using as adjuvants GM-CSF [16] or poly-ICLC [17], and from *in vitro* predictions for other multi-peptide vaccines for pediatric glioma and multiple myeloma [11,18]. These studies showed immune responses against multiple peptides in several patients, encouraging further development of multiple TAA peptide vaccines. However, the magnitude and/or therapeutic efficacy of these responses still need to be improved, as shown by the IMA901 phase III clinical trial that showed no improvement in overall survival [8]. For TSA, there have been major advances in genome mapping technologies to identify neoepitopes even in cancers from individual patients [19,20••,21], thus opening the way to personalized peptide vaccines [22•], which has yielded particularly encouraging results in a phase I trial for melanoma, in which up to 20 personalized long peptides were administered to patients [20••]. Other studies in glioblastoma are following the same approach, such as the phase I GAPVAC trial and the phase I/Ib trial of a personalized neoantigen vaccine; both showing sustained CD8 and CD4 T cell responses [23•,24•]. Although multi-peptide vaccines are the most direct way to broaden anti-tumor immunity and avoid immune escape, significant tumor cell killing can liberate additional tumor antigens, promote epitope spreading, and expand T cells of different specificities to that induced by the vaccine or other immunotherapy [25,26].

HLA binding and peptide length

Minimal peptide epitopes of 8–11 amino acids with appropriate binding motifs can associate with certain HLA class I (HLA-I) alleles without further processing, thereby forming ligands for CD8 T cells. Similarly, longer peptides of 13–18 amino acids can directly bind to HLA class II (HLA-II) alleles and stimulate CD4 T cells. However, the simplicity of administering peptide vaccines based on minimal peptide epitopes must be balanced with the risk that most injected peptides will exogenously bind to HLA expressing cells that do not express costimulatory molecules and do not, therefore, efficiently stimulate T cells [27,28]. This is principally a problem for HLA-I, which is expressed by most nucleated cells of the body. The implications of this may even lead to tolerance induction rather than activation [29]. Synthetic long peptides are now routinely employed in many clinical trials; they are generally more than 20 amino acids long, require processing and so favor presentation by professional antigen presenting cells such as dendritic cells, ideally suited for T-cell priming. Judicious choice of long peptide sequences can select regions encompassing both HLA-I and HLA-II binding epitopes; moreover, binding motifs for multiple HLA alleles may be present, which can be further increased by using multiple long peptides in individual patients, as recently described in the previously mentioned phase I trial for melanoma [20••]. Nevertheless, generation of HLA-I binding peptides requires processing of peptides that enter the cytosol, which may not occur efficiently for all peptides. Future trials may employ long peptides modified by the addition of a cell penetrating peptide sequence, shown to induce superior CD8 T-cell responses to long peptides alone in animal models [30,31]. Interestingly, although this approach promoted CD8 T-cell induction, this was not at the expense of CD4 T-cell immune responses, which are increasingly recognized as being an essential component of

anti-cancer immunity [32•,33]. Indeed, CD4 T cells, particularly Th1 cells, are not only important for efficient CD8 T-cell priming, recruitment at the tumor site and establishing memory, but they may also exert CD8-independent anti-tumor effect functions, justifying CD4-inducing approaches in peptide vaccination [22•,34,35].

Epitope prediction

Approaches to select peptide vaccine epitopes differ according to whether the epitope is a TSA derived from a mutated gene, or a non-mutated TAA. For the latter, it is essential to determine preferential expression of the protein by the tumor, and ideally (as for TSA) presentation of the peptide on tumor cell HLA molecules. This is most directly determined by elution of peptide bound to HLA from tumor cells, with subsequent detection and characterization by mass spectrometry [36–38]. For mutated epitopes, the development of faster and cheaper deep-sequencing techniques has revolutionized identification of putative neoepitopes [39], even at the single-cell level [40]. This can be followed by bioinformatics algorithms to predict peptide–HLA binding [41], which can be combined with peptide characterization [37,38,42]. Regardless of the sophistication of epitope prediction from TAA or TSA, it is also essential to prove T-cell recognition. Here, the original techniques of reverse immunology that opened the era of tumor immunotherapy have been brought up to date with 21st century technology. Culture of fastidious T-cell clones from cancer patients is no longer a bottleneck, with TCR transduction, or healthy donor T cells being used to validate epitope recognition [43,44]. Furthermore, the relationship between TCR sequences and epitope specificity is becoming progressively unraveled [45], opening future possibilities for combining *in silico* approaches with cellular immunology to determine whether predicted epitopes should be targeted by vaccines [21].

HLA-E-binding peptides as potential universal tumor epitopes

To date therapeutic cancer vaccines have mostly focused on antigenic peptides presented by classical HLA-I molecules. However, the existence of unconventional CD8 T-cell responses restricted by the non-classical HLA-I molecule HLA-E has recently emerged, offering the opportunity to identify alternative peptide targets in cancer patients [46•]. As for classical HLA-I, HLA-E is broadly expressed and assembles with β2-microglobulin to present intracellular-derived peptides at the cell surface [47]. However, whereas classical HLA-I has thousands of allotypes, HLA-E shows little polymorphism, with only two alleles that differ outside the peptide-binding groove [48]. Thus, while the highly polymorphic classical HLA-I molecules imposes diverse peptide repertoires among patents, HLA-E–peptide complexes could provide universal antigenic targets. Furthermore, while classical HLA-I alleles are frequently down modulated in cancer cells, promoting immune escape from CD8 T cells [49•], HLA-E expression is retained in numerous hematopoietic and solid malignancies, and for certain of these, levels are correlated with prognosis and/or immune infiltration [50]. Hence, HLA-E binding peptides may represent attractive therapeutic targets, especially when classical HLA-I expression is lost. However, an HLA-E-restricted anti-tumor T-cell response remains unexplored.

The role of HLA-E is best characterized as an NK receptor ligand; a restricted peptide-set derived from the signal sequences of others HLA-I molecules is presented and protects healthy cells from NK cytotoxicity through interaction with the inhibitory CD94/NKG2A receptor. Nonetheless, during cellular stress, infection or malignant transformation, HLA-E can present a more diverse repertoire of peptides recognized by CD8 T cells and can contribute to immunity in various infections (reviewed in Ref. [51]). Indeed, HLA-E-restricted pathogen-specific CD8 T cells can display polyclonality, polyfunctionality, and long-term persistence, that is, features that would be appropriate for anti-tumor immunity. In mice, *in vivo* studies convincingly demonstrated immune surveillance of tumors with TAP [52,53•] or ERAPP [54] deficiencies by T cells restricted by the functional homolog of HLA-E, Qa-1 [49•]. Moreover, Qa-1 restricted CD8 T cells could be induced by peptide vaccination [52,53•]. In human *in vitro* studies using classical HLA-I negative cells, HLA-E was shown to bind a set of self-derived peptides related to heat shock responses [55,56] and defective antigen-processing [57]. Collectively, these data encourage future efforts to identify and address immunogenicity of the HLA-E–peptidome naturally presented in human tumors, and to test the feasibility of therapeutic vaccination. Finally, while HLA-E binding-peptide may represent potent therapeutic targets when expressed at the surface of malignant cells, their self-origin mandates vigilance; any on-target autoimmune side effects must be assessed.

Adjuvants and vaccine formulation

The formulation of a peptide vaccine and the choice of adjuvant are critical for vaccine efficacy, with no consensus concerning what is optimal for therapeutic vaccination in cancer. The primary role of the adjuvant in any vaccine is to ensure sufficient costimulation by the antigen presenting cells that prime T cells. There are additional requirements for a therapeutic peptide vaccine: facilitating cross-presentation of the vaccine peptides to stimulate CD8 T cells, protecting the peptides from too rapid degradation, and promoting effector T-cell homing to the tumor site. Current vaccines have mostly employed a restricted range of adjuvants, including Montanide ISA-51 (IFA), TLR agonists, and GM-CSF. Caution in clinical trials has generally resulted in the use of single

Figure 1

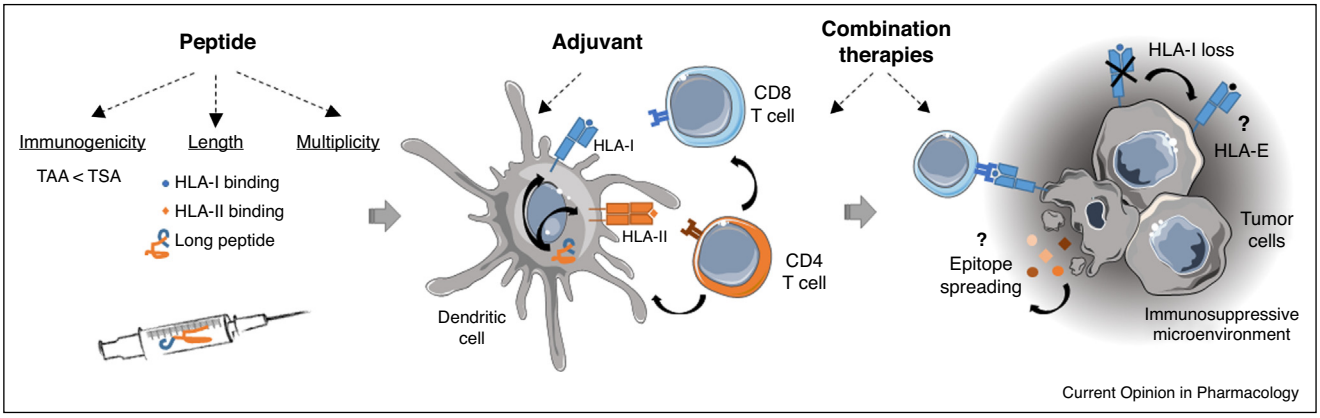

The figure is an original scheme using modified images from smart Servier Medical Art (using license Creative Commons Attribution 3.0 France https://creativecommons.org/licenses/by/3.0/).

adjuvants, but multiple adjuvants may ultimately be necessary, as recently discussed [58,59]. Future developments will also need to consider modulating the duration of antigen presentation [60], and minimizing the retention and inactivation of activated T cells in water-in-oil depots (Montanide, IFA) at the injection site [61,62•].

Synergistic combination therapies

High magnitude, highly functional, tumor-specific T cells induced by the most optimal peptide vaccine that can be envisaged still face a final formidable hurdle: the tumor microenvironment. Tumor cells, myeloid cells, regulatory T cells, an aberrant vasculature and physicochemical features of the tumor microenvironment such as hypoxia and lactate accumulation, all contribute to inhibit T-cell infiltration or function. Fortunately, the revolution in clinical cancer immunotherapy offers a multitude of opportunities for rational combinations with peptide vaccination, many of which are already under clinical trial [3•]. These can use peptide vaccination to sensitize to the immunomodulator (e.g. ICB), or use ICB antibodies to maintain the functionality of vaccine-induced T cells. Although the end result, clinical efficacy, might be the same, the underlying mechanism will influence the choice and sequence of administering the different therapies. Combinations are not only restricted to immunotherapy, but can include radiotherapy, targeted therapy, anti-angiogenic therapy and chemotherapy. Certain chemotherapeutic agents, when used in the right sequence, can promote anti-tumor immunity by eliciting immunogenic tumor cell death [63], and anti-angiogenic strategies can enhance T-cell infiltration [64].

Perspectives

The future for therapeutic peptide vaccines is encouraging, because we have tools to identify target antigens, adjuvants to potentially combine for enhanced immunogenicity and a multitude of clinically relevant immunomodulators (Figure 1). A major challenge of this cornucopia of opportunities is how to rationally combine and test a multimodal cancer therapy in a clinical context. Tumor immunity requires investigation *in vivo*, which obligates uses of immunocompetent animals in preclinical testing, and yet the targeted antigens will be of human origin in the clinical vaccine. Despite advances in using humanized animals and more sophisticated *in vitro* cultures, these must be used in addition to biological and clinical information, with improved immunomonitoring from clinical trials. We should be inspired by the cancer immunotherapy revolution of ICB that was built on deciphering conserved immune mechanisms between mice and humans, to develop a next generation of potent peptide vaccines to incorporate into new multimodality treatments for cancer patients.

Funding

This work was supported by the Association Frédéric Fellay and Fond'action contre le cancer.

Conflict of interest statement

P.R.W. and P.-Y.D. have ownership interest in patents related to cell penetrating peptides and are consultant/advisory board members for Amal Therapeutics.

References and recommended reading

Papers of particular interest, published within the period of review, have been highlighted as:

- • of special interest
- •• of outstanding interest

1. Kumai T, Fan A, Harabuchi Y, Celis E: **Cancer immunotherapy: moving forward with peptide T cell vaccines**. *Curr Opin Immunol* 2017, **47**:57-63.

2. Van der Burg SH: **Correlates of immune and clinical activity of novel cancer vaccines**. *Semin Immunol* 2018, **39**:119-136.

3. • Bezu L, Kepp O, Cerrato G, Pol J, Fucikova J, Spisek R, Zitvogel L, Kroemer G, Galluzzi L: **Trial watch: peptide-based vaccines in anticancer therapy**. *Oncoimmunology* 2018, **7**:e1511506.
Useful and comprehensive review of clinical trials (and some preclinical studies) using peptide vaccines from 2015 until mid 2018.

4. Muller S, Agnihotri S, Shoger KE, Myers MI, Smith N, Chaparala S, Villanueva CR, Chattopadhyay A, Lee AV, Butterfield LH *et al.*: **Peptide vaccine immunotherapy biomarkers and response patterns in pediatric gliomas**. *JCI Insight* 2018, **3**.

5. Dimitrov S, Gouttefangeas C, Besedovsky L, Jensen ATR, Chandran PA, Rusch E, Businger R, Schindler M, Lange T, Born J *et al.*: **Activated integrins identify functional antigen-specific CD8(+) T cells within minutes after antigen stimulation**. *Proc Natl Acad Sci U S A* 2018, **115**:E5536-E5545.

6. Middleton G, Silcocks P, Cox T, Valle J, Wadsley J, Propper D, Coxon F, Ross P, Madhusudan S, Roques T *et al.*: **Gemcitabine and capecitabine with or without telomerase peptide vaccine GV1001 in patients with locally advanced or metastatic pancreatic cancer (TeloVac): an open-label, randomised, phase 3 trial**. *Lancet Oncol* 2014, **15**:829-840.

7. Mitchell P, Thatcher N, Socinski MA, Wasilewska-Tesluk E, Horwood K, Szczesna A, Martin C, Ragulin Y, Zukin M, Helwig C *et al.*: **Tecemotide in unresectable stage III non-small-cell lung cancer in the phase III START study: updated overall survival and biomarker analyses**. *Ann Oncol* 2015, **26**:1134-1142.

8. Rini BI, Stenzl A, Zdrojowy R, Kogan M, Shkolnik M, Oudard S, Weikert S, Bracarda S, Crabb SJ, Bedke J *et al.*: **IMA901, a multipeptide cancer vaccine, plus sunitinib versus sunitinib alone, as first-line therapy for advanced or metastatic renal cell carcinoma (IMPRINT): a multicentre, open-label, randomised, controlled, phase 3 trial**. *Lancet Oncol* 2016, **17**:1599-1611.

9. Obara W, Eto M, Mimata H, Kohri K, Mitsuhata N, Miura I, Shuin T, Miki T, Koie T, Fujimoto H *et al.*: **A phase I/II study of cancer peptide vaccine S-288310 in patients with advanced urothelial carcinoma of the bladder**. *Ann Oncol* 2017, **28**:798-803.

10. Obara W, Sato F, Takeda K, Kato R, Kato Y, Kanehira M, Takata R, Mimata H, Sugai T, Nakamura Y *et al.*: **Phase I clinical trial of cell division associated 1 (CDCA1) peptide vaccination for castration resistant prostate cancer**. *Cancer Sci* 2017, **108**:1452-1457.

11. Pollack IF, Jakacki RI, Butterfield LH, Hamilton RL, Panigrahy A, Normolle DP, Connelly AK, Dibridge S, Mason G, Whiteside TL *et al.*: **Antigen-specific immunoreactivity and clinical outcome following vaccination with glioma-associated antigen peptides in children with recurrent high-grade gliomas: results of a pilot study**. *J Neurooncol* 2016, **130**:517-527.

12. Chabeda A, Yanez RJR, Lamprecht R, Meyers AE, Rybicki EP, Hitzeroth II: **Therapeutic vaccines for high-risk HPV-associated diseases**. *Papillomavirus Res* 2018, **5**:46-58.

13. Massarelli E, William W, Johnson F, Kies M, Ferrarotto R, Guo M, Feng L, Lee JJ, Tran H, Kim YU *et al.*: **Combining immune checkpoint blockade and tumor-specific vaccine for patients with incurable human papillomavirus 16-related cancer: a phase 2 clinical trial**. *JAMA Oncol* 2018, **5**:67-73.

14. Turajlic S, Litchfield K, Xu H, Rosenthal R, McGranahan N, Reading JL, Wong YNS, Rowan A, Kanu N, Al Bakir M *et al.*: **Insertion-and-deletion-derived tumour-specific neoantigens and the immunogenic phenotype: a pan-cancer analysis**. *Lancet Oncol* 2017, **18**:1009-1021.

15. Weller M, Butowski N, Tran DD, Recht LD, Lim M, Hirte H, Ashby L, Mechtler L, Goldlust SA, Iwamoto F *et al.*: **Rindopepimut with temozolomide for patients with newly diagnosed, EGFRvIII-expressing glioblastoma (ACT IV): a randomised, double-blind, international phase 3 trial**. *Lancet Oncol* 2017, **18**:1373-1385.

16. Rampling R, Peoples S, Mulholland PJ, James A, Al-Salihi O, Twelves CJ, McBain C, Jefferies S, Jackson A, Stewart W *et al.*: **A cancer research UK first time in human phase I trial of IMA950 (novel multipeptide therapeutic vaccine) in patients with newly diagnosed glioblastoma**. *Clin Cancer Res* 2016, **22**:4776-4785.

17. Migliorini D, Dutoit V, Allard M, Grandjean Hallez N, Marinari E, Widmer V, Philippin G, Corlazzoli F, Gustave R, Kreutzfeldt M *et al.*: **Phase I/II trial testing safety and immunogenicity of the multipeptide IMA950/poly-ICLC vaccine in newly diagnosed adult malignant astrocytoma patients**. *Neuro-Oncology* 2019: noz040 http://dx.doi.org/10.1093/neuonc/noz040.

18. Nooka AK, Wang ML, Yee AJ, Kaufman JL, Bae J, Peterkin D, Richardson PG, Raje NS: **Assessment of safety and immunogenicity of PVX-410 vaccine with or without lenalidomide in patients with smoldering multiple myeloma: a nonrandomized clinical trial**. *JAMA Oncol* 2018:e183267.

19. Gubin MM, Artyomov MN, Mardis ER, Schreiber RD: **Tumor neoantigens: building a framework for personalized cancer immunotherapy**. *J Clin Invest* 2015, **125**:3413-3421.

20. •• Ott PA, Hu Z, Keskin DB, Shukla SA, Sun J, Bozym DJ, Zhang W, Luoma A, Giobbie-Hurder A, Peter L *et al.*: **An immunogenic personal neoantigen vaccine for patients with melanoma**. *Nature* 2017, **547**:217-221.
A landmark study in personalized peptide vaccination, showing the feasibility of targeting multiple neoantigens from melanoma patients with a multiple long peptide vaccine. The vaccine was safe and immunogenic, with induction of both CD4 and CD8 T cells, and showed clinical efficacy in some patients. Moreover, subsequent anti-PD1 treatment in 2 patients with tumor recurrence resulted in broadening of the anti-tumor response and tumor regression.

21. Schumacher TN, Schreiber RD: **Neoantigens in cancer immunotherapy**. *Science* 2015, **348**:69-74.

22. • Sahin U, Tureci O: **Personalized vaccines for cancer immunotherapy**. *Science* 2018, **359**:1355-1360.
An up to date review of the cutting edge technological advances for personalized vaccines (including peptide vaccines) targeting tumor mutations from individual patients.

23. • Hilf N, Kuttruff-Coqui S, Frenzel K, Bukur V, Stevanovic S, Gouttefangeas C, Platten M, Tabatabai G, Dutoit V, van der Burg SH *et al.*: **Actively personalized vaccination trial for newly diagnosed glioblastoma**. *Nature* 2019, **565**:240-245.
A technologically sophisticated personalized peptide vaccine trial for glioblastoma targeting sequentially non-mutated antigens from a 'warehouse' of previously defined antigens, and then mutated neoantigens for each patient. The former antigens induced CD8 T cell responses, the latter category induced CD4 T cell responses. In view of the limited number of mutations and neoantigens in glioblastoma and the apparent CD4 T cell bias of the vaccine induced responses, this study revives the interest and necessity of targeting both non-mutated antigens (TAA) and mutated neoantigens (TSA).

24. • Keskin DB, Anandappa AJ, Sun J, Tirosh I, Mathewson ND, Li S, Oliveira G, Giobbie-Hurder A, Felt K, Gjini E *et al.*: **Neoantigen vaccine generates intratumoral T cell responses in phase Ib glioblastoma trial**. *Nature* 2019, **565**:234-239.
A personalized peptide vaccine phase I/Ib trial for glioblastoma targeting only neoantigens. Immunogenicity of the vaccine was validated, but principally in patients that did not require dexamethasone (which was required to limit brain edema) during priming. In these patients there was a CD4 T cell dominance of the induced response, despite epitope identification based on HLA class I binding algorithms. Importantly, there was evidence for vaccine-induced T-cell infiltration of the tumor site, but also signs of an exhaustion phenotype.

25. Gulley JL, Madan RA, Pachynski R, Mulders P, Sheikh NA, Trager J, Drake CG: **Role of antigen spread and distinctive characteristics of immunotherapy in cancer treatment**. *J Natl Cancer Inst* 2017, **109**.

26. Verdegaal EM, de Miranda NF, Visser M, Harryvan T, van Buuren MM, Andersen RS, Hadrup SR, van der Minne CE, Schotte R, Spits H *et al.*: **Neoantigen landscape dynamics during human melanoma-T cell interactions**. *Nature* 2016, **536**:91-95.

27. Eisen HN, Hou XH, Shen C, Wang K, Tanguturi VK, Smith C, Kozyrytska K, Nambiar L, McKinley CA, Chen J *et al.*: **Promiscuous binding of extracellular peptides to cell surface class I MHC protein**. *Proc Natl Acad Sci U S A* 2012, **109**:4580-4585.

28. Santambrogio L, Sato AK, Fischer FR, Dorf ME, Stern LJ: **Abundant empty class II MHC molecules on the surface of**

immature dendritic cells. *Proc Natl Acad Sci U S A* 1999, **96**:15050-15055.

29. Melief CJ, van Hall T, Arens R, Ossendorp F, van der Burg SH: **Therapeutic cancer vaccines**. *J Clin Invest* 2015, **125**:3401-3412.

30. Derouazi M, Di Berardino-Besson W, Belnoue E, Hoepner S, Walther R, Benkhoucha M, Teta P, Dufour Y, Yacoub Maroun C, Salazar AM *et al.*: **Novel cell-penetrating peptide-based vaccine induces robust CD4+ and CD8+ T cell-mediated antitumor immunity**. *Cancer Res* 2015, **75**:3020-3031.

31. Belnoue E, Di Berardino-Besson W, Gaertner H, Carboni S, Dunand-Sauthier I, Cerini F, Suso-Inderberg EM, Walchli S, Konig S, Salazar AM *et al.*: **Enhancing antitumor immune responses by optimized combinations of cell-penetrating peptide-based vaccines and adjuvants**. *Mol Ther* 2016, **24**:1675-1685.

32. • Marty R, Thompson WK, Salem RM, Zanetti M, Carter H: **Evolutionary pressure against MHC class II binding cancer mutations**. *Cell* 2018, **175**:416-428 e413.
This study uses sophisticated modelling to help explain the importance of CD4 T cells in anti-tumor immunity in human populations. The data suggest that mutations influencing antigens able to bind to HLA-II shape tumor evolution.

33. Kreiter S, Vormehr M, van de Roemer N, Diken M, Lower M, Diekmann J, Boegel S, Schrors B, Vascotto F, Castle JC *et al.*: **Mutant MHC class II epitopes drive therapeutic immune responses to cancer**. *Nature* 2015, **520**:692-696.

34. Tran E, Turcotte S, Gros A, Robbins PF, Lu YC, Dudley ME, Wunderlich JR, Somerville RP, Hogan K, Hinrichs CS *et al.*: **Cancer immunotherapy based on mutation-specific CD4+ T cells in a patient with epithelial cancer**. *Science* 2014, **344**:641-645.

35. Platten M, Schilling D, Bunse L, Wick A, Bunse T, Riehl D, Karapanagiotou-Schenkel I, Harting I, Sahm F, Schmitt A *et al.*: **A mutation-specific peptide vaccine targeting IDH1R132H in patients with newly diagnosed malignant astrocytomas: a first-in-man multicenter phase I clinical trial of the German Neurooncology Working Group (NOA-16)**. *J Clin Oncol* 2018, **36** 2001-2001.

36. Abelin JG, Keskin DB, Sarkizova S, Hartigan CR, Zhang W, Sidney J, Stevens J, Lane W, Zhang GL, Eisenhaure TM *et al.*: **Mass spectrometry profiling of HLA-associated peptidomes in mono-allelic cells enables more accurate epitope prediction**. *Immunity* 2017, **46**:315-326.

37. Dutoit V, Herold-Mende C, Hilf N, Schoor O, Beckhove P, Bucher J, Dorsch K, Flohr S, Fritsche J, Lewandrowski P *et al.*: **Exploiting the glioblastoma peptidome to discover novel tumour-associated antigens for immunotherapy**. *Brain* 2012, **135**:1042-1054.

38. Fritsche J, Rakitsch B, Hoffgaard F, Romer M, Schuster H, Kowalewski DJ, Priemer M, Stos-Zweifel V, Horzer H, Satelli A *et al.*: **Translating immunopeptidomics to immunotherapy-decision-making for patient and personalized target selection**. *Proteomics* 2018, **18**:e1700284.

39. Pritchard AL, Burel JG, Neller MA, Hayward NK, Lopez JA, Fatho M, Lennerz V, Wolfel T, Schmidt CW: **Exome sequencing to predict neoantigens in melanoma**. *Cancer Immunol Res* 2015, **3**:992-998.

40. Gee MH, Han A, Lofgren SM, Beausang JF, Mendoza JL, Birnbaum ME, Bethune MT, Fischer S, Yang X, Gomez-Eerland R *et al.*: **Antigen identification for orphan T cell receptors expressed on tumor-infiltrating lymphocytes**. *Cell* 2018, **172**:549-563 e516.

41. Liu XS, Mardis ER: **Applications of immunogenomics to cancer**. *Cell* 2017, **168**:600-612.

42. Yadav M, Jhunjhunwala S, Phung QT, Lupardus P, Tanguay J, Bumbaca S, Franci C, Cheung TK, Fritsche J, Weinschenk T *et al.*: **Predicting immunogenic tumour mutations by combining mass spectrometry and exome sequencing**. *Nature* 2014, **515**:572-576.

43. Pasetto A, Gros A, Robbins PF, Deniger DC, Prickett TD, Matus-Nicodemos R, Douek DC, Howie B, Robins H, Parkhurst MR *et al.*: **Tumor- and neoantigen-reactive T-cell receptors can be identified based on their frequency in fresh tumor**. *Cancer Immunol Res* 2016, **4**:734-743.

44. Stronen E, Toebes M, Kelderman S, van Buuren MM, Yang W, van Rooij N, Donia M, Boschen ML, Lund-Johansen F, Olweus J *et al.*: **Targeting of cancer neoantigens with donor-derived T cell receptor repertoires**. *Science* 2016, **352**:1337-1341.

45. Dash P, Fiore-Gartland AJ, Hertz T, Wang GC, Sharma S, Souquette A, Crawford JC, Clemens EB, Nguyen THO, Kedzierska K *et al.*: **Quantifiable predictive features define epitope-specific T cell receptor repertoires**. *Nature* 2017, **547**:89-93.

46. • Godfrey DI, Le Nours J, Andrews DM, Uldrich AP, Rossjohn J: **Unconventional T cell targets for cancer immunotherapy**. *Immunity* 2018, **48**:453-473.
Review covering the role and therapeutic potential of unconventional T cells (including HLA-E-restricted, but also CD1-restricted and MR1-restricted, as well as $\gamma\delta$ T cells) in tumor immunity.

47. Boegel S, Lower M, Bukur T, Sorn P, Castle JC, Sahin U: **HLA and proteasome expression body map**. *BMC Med Genomics* 2018, **11**:36.

48. Ramalho J, Veiga-Castelli LC, Donadi EA, Mendes-Junior CT, Castelli EC: **HLA-E regulatory and coding region variability and haplotypes in a Brazilian population sample**. *Mol Immunol* 2017, **91**:173-184.

49. • Marijt KA, Doorduijn EM, van Hall T: **TEIPP antigens for T-cell based immunotherapy of immune-edited HLA class I(low) cancers**. *Mol Immunol* 2018. (in press).
Review covering the work of van Hall and others on tumor epitopes associated with antigen processing defects (including Qa-1-restricted T cells and tumor escape mechanisms associated with HLA-I downregulation).

50. Wieten L, Mahaweni NM, Voorter CE, Bos GM, Tilanus MG: **Clinical and immunological significance of HLA-E in stem cell transplantation and cancer**. *Tissue Antigens* 2014, **84**:523-535.

51. Joosten SA, Sullivan LC, Ottenhoff TH: **Characteristics of HLA-E restricted T-cell responses and their role in infectious diseases**. *J Immunol Res* 2016, **2016**:2695396.

52. Oliveira CC, van Veelen PA, Querido B, de Ru A, Sluijter M, Laban S, Drijfhout JW, van der Burg SH, Offringa R, van Hall T: **The nonpolymorphic MHC Qa-1b mediates CD8+ T cell surveillance of antigen-processing defects**. *J Exp Med* 2010, **207**:207-221.

53. • Doorduijn EM, Sluijter M, Querido BJ, Seidel UJE, Oliveira CC, van der Burg SH, van Hall T: **T cells engaging the conserved MHC class Ib molecule Qa-1(b) with TAP-independent peptides are semi-invariant lymphocytes**. *Front Immunol* 2018, **9**:60.
This study highlights that Qa-1(the murine homolog of HLA-E) can present immunogenic self-derived peptides and contribute to the immune surveillance of tumors with antigen processing defects. Also evidenced *in vivo* priming of tumor-reactive Qa-1-restricted CD8 T cells upon prophylactic peptide vaccination.

54. Nagarajan NA, Gonzalez F, Shastri N: **Nonclassical MHC class Ib-restricted cytotoxic T cells monitor antigen processing in the endoplasmic reticulum**. *Nat Immunol* 2012, **13**:579-586.

55. Michaëlsson J, Teixeira de Matos C, Achour A, Lanier LL, Kärre K, Söderström K: **A signal peptide derived from hsp60 binds HLA-E and interferes with CD94/NKG2A recognition**. *J Exp Med* 2002, **196**:1403-1414.

56. Wooden SL, Kalb SR, Cotter RJ, Soloski MJ: **Cutting edge: HLA-E binds a peptide derived from the ATP-binding cassette transporter multidrug resistance-associated protein 7 aSnd inhibits NK cell-mediated lysis**. *J Immunol* 2005, **175**:1383-1387.

57. Lampen MH, Hassan C, Sluijter M, Geluk A, Dijkman K, Tjon JM, de Ru AH, van der Burg SH, van Veelen PA, van Hall T: **Alternative peptide repertoire of HLA-E reveals a binding motif that is strikingly similar to HLA-A2**. *Mol Immunol* 2013, **53**:126-131.

58. Gouttefangeas C, Rammensee HG: **Personalized cancer vaccines: adjuvants are important, too**. *Cancer Immunol Immunother* 2018, **67**:1911-1918.

59. Temizoz B, Kuroda E, Ishii KJ: **Combination and inducible adjuvants targeting nucleic acid sensors**. *Curr Opin Pharmacol* 2018, **41**:104-113.

60. Khong H, Volmari A, Sharma M, Dai Z, Imo CS, Hailemichael Y, Singh M, Moore DT, Xiao Z, Huang XF *et al.*: **Peptide vaccine formulation controls the duration of antigen presentation and magnitude of tumor-specific CD8(+) T cell response**. *J Immunol* 2018, **200**:3464-3474.

61. Hailemichael Y, Dai Z, Jaffarzad N, Ye Y, Medina MA, Huang XF, Dorta-Estremera SM, Greeley NR, Nitti G, Peng W *et al.*: **Persistent antigen at vaccination sites induces tumor-specific CD8(+) T cell sequestration, dysfunction and deletion**. *Nat Med* 2013, **19**:465-472.

62. • Hailemichael Y, Woods A, Fu T, He Q, Nielsen MC, Hasan F, Roszik J, Xiao Z, Vianden C, Khong H *et al.*: **Cancer vaccine formulation dictates synergy with CTLA-4 and PD-L1 checkpoint blockade therapy**. *J Clin Invest* 2018, **128**:1338-1354.

The authors observe a synergistic effect on survival of mice with melanoma upon treatment with a gp100 peptide vaccine in combination with immune checkpoint inhibitors. Of note, the peptide formulation was critical– IFA had a negative impact whereas vaccination with gp100 peptide in saline resulted in better survival.

63. Pfirschke C, Engblom C, Rickelt S, Cortez-Retamozo V, Garris C, Pucci F, Yamazaki T, Poirier-Colame V, Newton A, Redouane Y *et al.*: **Immunogenic chemotherapy sensitizes tumors to checkpoint blockade therapy**. *Immunity* 2016, **44**:343-354.

64. Allen E, Jabouille A, Rivera LB, Lodewijckx I, Missiaen R, Steri V, Feyen K, Tawney J, Hanahan D, Michael IP *et al.*: **Combined antiangiogenic and anti-PD-L1 therapy stimulates tumor immunity through HEV formation**. *Sci Transl Med* 2017, **9**.